Universidade de São Paulo
Instituto de Física

# Máquinas térmicas quânticas em tempo finito

Otavio Augusto Dantas Molitor

Orientador: Prof. Dr. Gabriel Teixeira Landi

Dissertação de mestrado apresentada ao Instituto de Física da Universidade de São Paulo, como requisito parcial para a obtenção do título de Mestre em Ciências.

Banca Examinadora:
Prof. Dr. Gabriel Teixeira Landi - Orientador (Instituto de Física - USP)
Prof. Dr. Lucas Chibebe Céleri (Universidade Federal de Goiás e UPV/EHU – Bilbao)
Prof. Dr. Breno M. G. Teixeira (Universidade Federal do ABC)

São Paulo
2020

University of São Paulo
Physics Institute

# Quantum heat engines in finite-time

Otavio Augusto Dantas Molitor

Supervisor: Prof. Dr. Gabriel Teixeira Landi

Dissertation submitted to the Physics Institute of the University of São Paulo in partial fulfillment of the requirements for the degree of Master of Science.

Examining Committee:
Prof. Dr. Gabriel Teixeira Landi - Supervisor (Physics Institute - USP)
Prof. Dr. Lucas Chibebe Céleri (Federal University of Goiás & UPV/EHU – Bilbao)
Prof. Dr. Breno M. G. Teixeira (Federal University of ABC)

São Paulo
2020

*To my beloved family. . .*

*In memoriam,*
*Helio Molitor (1942-2017)*

# *Agradecimentos*

Longo foi o caminho percorrido até aqui. Passando por incertezas, dificuldades pessoais e adaptações, sinto-me grato por tudo o que ocorreu, pois as experiências pelas quais passei me tornaram mais resiliente e preparado para novos desafios. Além, é claro, da fé em Cristo, a qual é de central importância na minha vida, tive pelo caminho muitos que me ajudaram direta ou indiretamente.

Tudo começa na base. Meus pais, Helio A. Molitor e Rosana A. D. Molitor, sempre incentivaram os meus estudos e os de minha irmã, Isadora D. Molitor, mesmo quando isso significava sacrificar outras coisas. Quanto mais eles vêem o esforço de seus filhos, mais se dedicam em dar a sustentação para as nossas conquistas. Eles são incansáveis, verdadeiros heróis. Nos ensinaram valores essenciais para qualquer indivíduo: honestidade, moralidade, integridade, humildade e bons modos. Fizeram e fazem da nossa casa um lar, onde nos sentimos em paz e harmonia. Além dos meus pais e minha irmã – minha querida amiga e futura internacionalista – expresso aqui meu amor por toda minha família: avô, avós, tios, tias, primos e primas. Quanto eu gostaria que o senhor estivesse aqui vovô Helio!

Expresso também minha gratidão ao meu orientador, Prof. Dr. Gabriel T. Landi. Conheci-o em 2018 ao cursar, na condição de aluno especial, a disciplina "Informação quântica e ruídos quânticos", por ele lecionada. O seu entusiasmo e dinamismo ao tratar dos assuntos apresentados em aula me convenceram de que seria um excelente orientador de Mestrado. Agradeço-o muito por todo o apoio que recebi durante essa parceria, tanto na parte acadêmica, quanto na parte pessoal. Aprendi muito trabalhando ao lado do Gabriel, um pesquisador "fora da curva" e um grande ser humano. Muito obrigado Gabriel! Agradeço também outros docentes que tiveram participação importante neste período: Profa. Dra. Bárbara L. Amaral, Profa. Dra. Valentina Martelli, Prof. Dr. Leandro R. Gasques e Prof. Dr. Antônio D. dos Santos.

O Mestrado não teria sido o mesmo sem os membros do grupo "Quantum Thermodynamics and Quantum Transport ($QT^2$) Group". Os cafés (e os bolos) no Alessandro Volta Bloco C farão muita falta. Cada um dos integrantes, a seu próprio modo, fez deste um grupo muito bom para trabalhar. Agradeço a todos pelos bons momentos no dia a dia e em congressos. Pelos papos diversos envolvendo buracos negros, teoria de campos quânticos e relatividade, agradeço: Naim E. Comar, Marcelo J. B. Pereira e Rodolfo R. Soldati. Quem sabe em breve conseguimos retomar aquela ideia! E por fim agradeço também ao meu ex-companheiro de escritório e amigo, Heitor P. Casagrande. Espero que consiga em algum momento te visitar em Singapura!

Os trabalhos administrativo e operacional de funcionários do Instituto de Física da USP e de funcionários terceirizados hão de ser também lembrados. As secretárias Sandra R. R. Ribeiro e Rosana B. G. Biz, a comissão e a secretaria de pós-graduação do IFUSP, as

faxineiras, os seguranças e os técnicos de laboratório, todos essenciais em suas funções. Agradeço de coração a todos!

Sem o auxílio financeiro proporcionado pelo Conselho Nacional de Desenvolvimento Científico e Tecnológico (CNPq) por meio de bolsa de estudos (Processo:135905/2019-2), muito dificilmente eu conseguiria ir até o final dos meus estudos de Mestrado. Expresso veementemente minha gratidão a este importante órgão de fomento à pesquisa em terras brasileiras, assim como agradeço também ao Ministério da Ciência, Tecnologia e Inovações, gestor do CNPq.

Pelas orientações nos vários momentos de incertezas e dificuldades, agradeço: Maria Rosa C. A. Gomes, Dra. Maria Fernanda Caliani, meu pai espiritual Arquimandrita Dimitrios Attarian (querido abouna!) e todos meus amigos, tanto aqueles de longa data, Pedro R. Vertamatti e Fernando S. Martins, como os que conheço há pouco tempo, meus queridos irmãos de fé.

Por fim, a gratidão maior reservo para Deus. É por Ele que fui criado, é Ele que sustenta a minha vida e é Ele que me permite apreciar a sua Criação de uma forma muito bela. Toda honra e toda glória ao Senhor.

*“How magnified are Thy works, O Lord!*
*In wisdom hast Thou made them all;*
*the earth is filled with Thy creation.”*

— Psalms 103:24

*“Quão magníficas são as Tuas obras, ó Senhor!*
*Em sabedoria Tu fizestes tudo;*
*a terra está repleta da Tua criação.”*

— Salmos 103:24

# *Abstract*

In the last decade, the study of thermodynamic phenomena in ultra-small scales, where quantum mechanics becomes imperative, has gained a lot of attention. The possibility of controlling single quantum states in nowadays experimental setups has encouraged a more intense inquiry over the intersection between thermodynamics and quantum mechanics, which is known as quantum thermodynamics. Particularly relevant in this framework is the study of quantum heat engines, that is, quantum systems undergoing thermodynamic cycles. Thermodynamic cycles contain all the aspects of thermodynamics, thus it's a good testbed for a better comprehension of the thermodynamics of quantum systems. Moreover, modelling quantum heat engines is crucial for the design of future ultra-small engines. Nonetheless, another aspect must be taken into account, finite-time operation. It's very important for the optimization of the output power of the engine. In this dissertation, we present a new model of finite-time quantum heat engines. By making use of collisional models, we construct a model in which a generic quantum chain experiences sequential pure heat and pure work strokes. Dictated by stroboscopic evolution, the engine's state goes through a transient regime until the limit-cycle is reached. After the achievement of the limit-cycle, our results indicate that only the boundary sites of the quantum chain are relevant for the heat currents exchanged with the baths. By means of analytical and numerical methods, we present how the model is useful for optimizing the output power of stroke-based quantum heat engines, without decreasing their respective efficiencies. Lastly, we prove that there is a universal efficiency value, the Otto efficiency, for a whole family of models containing a specific kind of internal interactions. For completeness, other methods from the literature which deal with finite-time quantum heat engines are also presented and discussed.

**Keywords**: Quantum thermodynamics; Quantum heat engines; Open quantum systems; Finite-time thermodynamics; Collisional models.

# *Resumo*

Na última década, o estudo de fenômenos termodinâmicos em escalas ultra-pequenas, onde a mecânica quântica se faz necessária, tem recebido muita atenção. A possibilidade de controlar estados quânticos individuais em plataformas experimentais da atualidade incentivou a intensificação das pesquisas sobre a intersecção entre termodinâmica e mecânica quântica, a qual é conhecida como termodinâmica quântica. Particularmente relevante neste contexto é o estudo de máquinas térmicas quânticas, isto é, sistemas quânticos submetidos a ciclos termodinâmicos. Ciclos termodinâmicos contêm todos os aspectos da termodinâmica, sendo portanto uma boa plataforma para melhor compreensão da termodinâmica de sistemas quânticos. Além disso, a modelagem de máquinas térmicas quânticas é crucial para o projeto de futuras máquinas térmicas ultra-pequenas. Não obstante, outro aspecto deve ser levado em consideração, a operação em tempo finito. Isto é muito importante para a otimização da potência de saída de máquinas térmicas em geral. Nesta dissertação, nós apresentamos um novo modelo de máquinas térmicas quânticas em tempo finito. Por meio do uso de modelos colisionais, nós criamos um modelo no qual uma cadeia quântica genérica passa sequencialmente por processos puramente de troca de calor ou trabalho. Ditado por evolução estroboscópica, o estado da máquina passa por um regime transitório até que o ciclo limite seja alcançado. Após a entrada no ciclo limite, nossos resultados indicam que somente os sítios nas bordas da cadeia quântica são determinantes para as correntes de calor trocadas com os banhos. Lançando mão de métodos analíticos e numéricos, nós apresentamos como o modelo é útil para otimizar a potência de saída de máquinas térmicas quânticas operadas em fases, sem diminuir suas respectivas eficiências. Por fim, nós provamos que há um valor universal de eficiência, a eficiência de Otto, para toda uma família de modelos que contêm um tipo específico de interações internas. Por completeza, outros métodos da literatura que tratam de máquinas térmicas quânticas em tempo finito são apresentados e discutidos.

**Palavras-chave**: Termodinâmica quântica; Máquinas térmicas quânticas; Sistemas quânticos abertos; Termodinâmica em tempo finito; Modelos colisionais.

# List of Symbols & Abbreviations

| | |
|---|---|
| := | Defined as |
| $\dot{}$ | Derivative with respect to $t$ (time) |
| $\oplus$ | Direct sum |
| $\otimes$ | Tensor/Kronecker product |
| $\forall$ | For all |
| $\hat{}$ | Vectorized superoperator |
| $\in$ | Is an element of |
| $\mathbb{N}$ | Set of the Natural numbers |
| $O$ | Big O/Error term |
| $\mathfrak{R}$ | Set of the Real numbers |
| $\mathfrak{R}_{>0}$ | Set of the positive Real numbers |
| tr | Trace |
| $^\dagger$ | Conjugate transpose |
| $^\intercal$ | Transpose |
| $^{th}$ | Thermal |
| GKSL | Gorini-Kossakowski-Sudarshan-Lindblad |
| QED | Quod Erat Demonstrandum |
| QHE | Quantum Heat Engine |
| QHO | Quantum Harmonic Oscillator |
| RHS | Right Hand Side |
| SZE | Szilard Engine |
| vec | Vectorized state |

# List of Figures

# List of Tables

# Contents

# Chapter 1

# Introduction

It's no surprise to anyone that the industrial revolutions happening since the 19$^{th}$ century have shaped the world around us. Despite the clever and ingenious technologies developed during the Antiquity, by people like the Egyptians, Greeks and Romans – to cite a few – and the Middle Ages [1], the disruptive innovations that started to appear roughly two hundred years ago are beyond comparison regarding their good and bad effects to humanity. The power of steam drove the British Empire to its greatest extension during the Victorian era, reinforcing economical and cultural exchanges between distant parts of the globe. Steam was used to move *engines*, as put forward by Watt in the end of the 18$^{th}$ century. The possibility of transforming one kind of energy (heat) into another one (work) boosted the studies of thermodynamics, the branch of physics that deals with the correlations between different kinds of energies and the constraints in converting one type into another.

The technological breakthrough of heat engines came as a practical necessity, while the theoretical background was still incipient. What was then known about thermal processes was learned mainly through observing the phenomena and describing them heuristically. However, this scientific path would not last too long. As soon as optimization and design issues arose, a new scientific strategy grounded on theory would be needed. Indeed, when faced with the question of what was the greatest efficiency an engine could achieve, a mechanical engineer of the French Army, named Sadi Carnot, devised a theoretical model of an engine that had the highest possible efficiency [2]. Without knowing, Sadi Carnot had formulated one possible statement of the 2$^{nd}$ law of thermodynamics[1]. After this remarkable work, a myriad of others followed in that same century, by people like Clausius, Boltzmann and Gibbs. Although thermodynamics became a much broader research field, expanding to statistical mechanics, chemistry and more recently *quantum mechanics*, it is still deeply rooted in the engine's task of converting heat into work. Along the following decades, engines gained more efficiency and applications, once new fuels started to be used, such as coal, oil fuels, gasoline and even steam produced by the heat that is released by nuclear reactors.

Not only the efficiency with which engines convert energy is important, but also the extracted power. In fact it is not only important, it is pivotal for their operation. The analysis of the extracted power, aiming at its optimization, isn't possible within the stan-

[1] This statement is one of many possibilities (e.g. Clausius statement, Kelvin-Planck statement) of describing the 2$^{nd}$ law of thermodynamics.

dard equilibrium thermodynamics framework. This is due to the fact that processes that keep the system in equilibrium at all times are very slow, thus the power tends to zero. Therefore, *finite-time* heat engines must be studied if one wants to take into account the extracted power. This might be done using endoreversible thermodynamics, an approximation of standard thermodynamics for finite-time processes. By doing so, it turns out that there is a trade-off between efficiency and power for (classical) finite-time heat engines [3]. Nevertheless, although not yet established theoretically, physicists and engineers empirically "knew" this trade-off, creating various new and powerful engines, such as gas turbines and internal combustion engines.

However, thermodynamics is far from being totally understood. The great development of this scientific field and the technological innovations related to it, were based on *macroscopic* objects or huge amounts of particles, in the case of statistical mechanics. However, there has been a growing development of experimental control of systems in ultra-small scales, such as trapped-ions [4–6], cavity quantum electrodynamics (cavity QED) [7–9] and semiconductor quantum dots [10–12]. In these experimental setups, the systems are in the quantum regime and phenomena not found in the macro-world start to appear. Hence, questions like how does thermodynamics extend to the quantum scale, or what are the possible implementations of heat engines in the quantum realm, become more relevant than ever. Answering these questions will reinforce knowledge about the foundations of physics, enable better energy management in emergent technologies, such as quantum computers, and bring ideas of future technological applications.

Meant to address these questions, the young research field known as *quantum thermodynamics* treats the interaction of quantum systems with an environment in thermodynamic terms: heat, work and entropy production. Despite the great insight by Scovil and Schulz-Dubois of looking at the maser, a quantum system *per se*, as a heat engine [13], the setting of a solid theory of quantum thermodynamics was only possible after the theory of open quantum systems, an extension of standard quantum mechanics to systems interacting with an environment, was structured. Surprisingly, the first works exploring thermodynamic features of open quantum systems were related to heat engines [14, 15]. It sets a route of research, focusing on heat engines at the quantum scale, or even to a broader topic, *thermodynamic cycles* applied to quantum systems, which is the theoretical basis of the operation of heat engines and other thermodynamic devices (e.g. refrigerators).

In confluence with the development of a theory of thermodynamics in the quantum realm, is another research field known as quantum information theory, which studies aspects of information theory in quantum systems. The relation between information and thermodynamics dates back to the proposition of an apparent paradox by Maxwell. He imagined a box containing a certain gas and divided in two halves by a wall. Then, what if an entity – afterwards nicknamed "demon" – knew[2] the positions and velocities of all gas particles? It could then place the fastest (hottest) in one side of the box and the slowest (coldest) in the other one. The apparent paradox comes when one realizes that this hypothetical situation leads to heat flowing from a cold to a hot body, something that is forbidden by the 2$^{nd}$ law of thermodynamics. Just after many years this problem was solved, mainly by the elucidating works of Landauer [16] and Bennett [17], who showed the intimate relation of information and thermodynamics, or more specifically, the equiv-

[2]The ideas of knowing and not-knowing/ignorance, are the basis of information theory, following the definition of entropy given by Shannon.

alence of Shannon entropy to thermodynamic entropy, apart from a $k_B$ factor, where $k_B$ is the Boltzmann constant ($k_B = 1.380649 \times 10^{-23}\ J/K$). The hint that information could be used as a thermodynamic resource came with the devise of an engine based on Maxwell's paradox by Szilard, in an attempt to solve the then apparent paradox [18]. This idea, together with what was learned from the aforementioned works of Landauer and Bennett, gave birth to the so-called Szilard engine (SZE), which bridges two different research areas, heat engines and information theory. From this point, many of the theoretical tools developed in the studies of quantum information theory can be applied to quantum thermodynamics and Quantum Heat Engines (QHEs).

During the last decade, the amount of scientific papers on quantum heat engines grew considerably, as it can be seen in Fig. 1.1. It shows the number of paper titles matching either "quantum heat engines" or "quantum thermal machines" (occasionally used by some authors) on arXiv.org in the period 2010–2019. From a few papers in the beginning of the decade, the yearly quantity of scientific articles jumped to 33 in 2019 alone. As we enter a new decade, until the 18$^{\text{th}}$ of September 2020, 32 new papers with similar titles had already appeared on arXiv.org, as accessed by the author on that same day. Therefore, there is an increasing trend in the research of quantum heat engines, reflecting the importance that physicists are putting on these studies and justifying the relevance of the present dissertation.

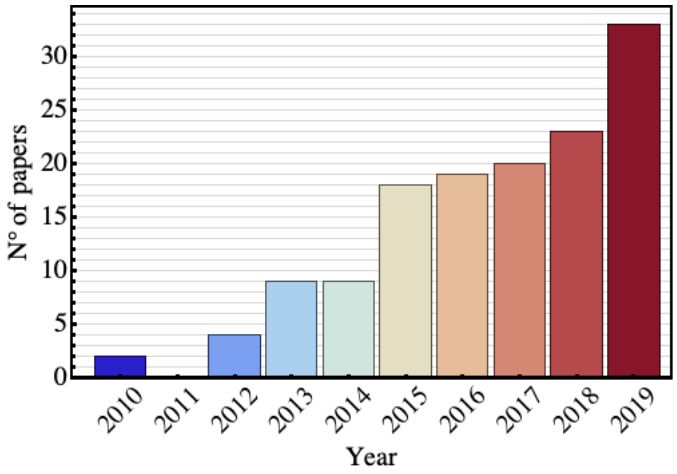


Figure 1.1: Yearly number of arXiv papers containing either "quantum heat engines" or "quantum thermal machines" in their titles, from 2010 to 2019.

Within the context of rapid development of the studies concerning quantum heat engines, this master's dissertation intends to give an original contribution to the specific matter of modelling finite-time QHEs. As it is shown by the historic maturing of classical heat engines, knowing how to optimize the power output without decreasing too much the efficiency is essential. Beyond that, heat engines are implementations of thermodynamic cycles, which contain all the main aspects of thermodynamics and are the cornerstone of this research field since the pioneering work of Sadi Carnot in 1824. Hence, it is expected that, broadening the studies of heat engines to the quantum domain is fundamental for future technologies that need outstanding energy management in ultra-small scales, and also for the theoretical understanding of the real nature of thermodynamics and its relation to quantum mechanics.

The model herein proposed makes use of a theoretical tool, known as *collisional models* [19–27]. This technique is associated with the *Stoßzahlansatz*[3], that appears in Boltzmann's works, which were inspired by previous Maxwell's papers, as a hypothesis of molecular chaos [28]. By applying collisional models, one considers generic quantum systems interacting sequentially with a stream of identical environment units. Each interaction, or "collision", is independent of each other and corresponds to a *quantum dynamical map* connecting the initial state to the final state. It's repeated for an integer number of times, meaning that the time evolution of the system's state is said to follow a *stroboscopic*[4] dynamics [21, 29]. This setup might be connected to quantum master equations, which dictate the *continuous-time* evolution of the state of a system interacting with an environment [30, 31]. This is done by making some approximations regarding the duration of each interaction. Since quantum master equations are the standard way of dealing with the operation of quantum heat engines, collisional models ought be considered even more general. Furthermore, the discrete nature of collisional models allows an easier treatment of the finite-time dynamics of QHEs when compared to other approaches [32–35]. Also, collisional models are flexible when choosing the quantum state of the environment units. Thus, resources stemming from quantum information theory (i.e. entanglement, coherence) can be explored in the context of QHEs [21].

By using the aforementioned technique to model the heat baths [20, 22] and generalizing the SWAP engine [36–40], the *stroboscopic two-stroke QHE* model is conceived. This QHE switches between pure heat and pure work strokes or processes. In the former, the internal interactions of the working fluid – considered as a generic quantum chain – are turned off, and the *boundaries* are connected to the streams of units modelling the cold and hot baths. By choosing the correct kind of interaction with the baths, the energy cost of switching it on and off goes to zero, and as a consequence, all the energy that leaves (enters) the bath enters (leaves) the working fluid in the form of *heat*. On the other hand, in the pure work stroke, the working fluid is disconnected from the baths, and its internal interactions are turned on. The dynamics is then unitary, due to the fact that the working fluid is a closed system and its state evolves according to the von Neumann equation. Differently from the heat stroke case, switching on and off these internal interactions has an energy cost. This in turn is identified as *work*. We show that the state of the system undergoes a stroboscopic evolution, passing from a transient regime and ending in the limit-cycle. When it's reached, solely the boundary sites of the quantum chain are determinant for the heat currents exchanged with the baths. In order to prove the effectiveness of the model, it's applied to two different scenarios. The first considers the working fluid as being made of only two qubits. In this case, an analytical treatment is done, by means of solving a set of difference equations, whose variables are operators of the working fluid. In contrast, the second case, which consists of generic $N$ spin chains, is solved numerically. Finally, the parameter space is explored in both scenarios, aiming at optimizing the output *power*. Interestingly, the efficiency is found to be equal to the Otto efficiency, for whatever choice of parameters. For this reason, we say that there is a family of models, characterized by a specific kind of internal interactions, that share an universal Otto efficiency.

The dissertation is organized as follows: in Chapters 2–5, the main physical con-

[3] "Impulse number approach", in German.

[4] In analogy with the visual effect of seeing a sequence of snapshots of a continuous movement.

cepts and mathematical expressions relevant for the treatment of finite-time QHEs are discussed. Starting with Chapter 2, the concept of thermodynamic cycles is reviewed. Three specific cycles are particularly studied: the Carnot cycle, the Otto cycle and the endoreversible cycle. This chapter aims at discussing qualitatively the cycles and presenting their efficiencies. Moreover, in Chapter 3, the theory of open quantum systems is presented and its relation to thermodynamics is made explicit, originating one formulation of the theory of quantum thermodynamics. Also, in the same chapter, the overlap between (quantum) thermodynamics and (quantum) information theory is explored, by analyzing Landauer's principle and the Szilard engine. Next, in Chapter 4, we introduce what are QHEs and divide them in two categories: continuous-time QHEs and stroke-based QHEs. An example for each kind of QHE is then discussed. Collisional models are then explored in Chapter 5. It starts with the general picture, where the basics of these models are presented. Following it, the particular case of auxiliary systems in a certain thermal state is treated, as well as the correspondent system's steady-state. The chapter ends with the comparison of the aforementioned special case and quantum master equations, showing that the latter is obtained from the former by means of taking the limit of infinitely fast interactions.

The succeeding chapter (Chapter 6) is the most important in the dissertation, where the stroboscopic two-stroke QHE is presented and studied according to what was previously stated. The content of this chapter is based on the preprint recently submitted to arXiv.org [29], which was also recently approved to be published in *Physical Review A*. In order to compare the outcomes of the model therein proposed, in Chapter 7 two other methods for treating finite-time QHEs, namely, shortcut-to-adiabaticity and Lindblad-Floquet theory, are discussed. Finally, in the Conclusion (Chapter 8), the dissertation is briefly reviewed, with emphasis on the stroboscopic two-stroke quantum heat engine (Chapter 6). Also, possible routes for the continuation of this work and experimental implementations are considered. Throughout the dissertation, natural units are employed: $k_B = \hbar = 1$.

# Chapter 2

# Classical thermodynamics: cycles

Classical thermodynamics is deeply rooted in observing thermal processes, such as the heating associated with work applied against friction, or simply how heat flows from hot to cold bodies. The research field arose from the description of thermal phenomena and the formulation of postulates based on the observations, which are known as the four laws of thermodynamics. These laws (by definition) dictate all finite-temperature processes of any macroscopic system. We will not go further into the laws of thermodynamics, for a nice overview, check Chapter 1 of Ref. [41].

Of special interest in this chapter is the concept of *thermodynamic cycle*. This object is the cornerstone of all thermal machines (e.g. heat engines). It consists of a repetitive sequence of processes, namely thermalization with a bath (heat reservoir) and expansion/compression of a gas, arranged in specific ways (e.g. isothermal expansion: a gas is expanded while in contact with a hot bath, maintaining the temperature constant). From the many existing cycles, we now focus on three specifically, the Carnot cycle, the Otto cycle and the endoreversible cycle.

## 2.1 Carnot cycle

In the beginning of the $19^{\text{th}}$ century, Sadi Carnot put forth a theoretical cycle that would be the most efficient possible, that is, with the greatest output-input ratio. He constructed the model from the concept of reversible processes, transformations that occur very slowly and can be done in both ways without any extra energy cost. His result was a turning point in the history of thermodynamics as a scientific subject [42] and paved the way for the many developments in this research field during the last two centuries.

The Carnot cycle is defined by four processes (strokes): (i) isothermal expansion, (ii) adiabatic expansion, (iii) isothermal compression and (iv) adiabatic compression, which are applied to a gas, called generically "working fluid". Adiabatic means that there is no exchange of heat between any of the two baths (one at a cold temperature $T_C$ and the other at a hot temperature $T_H > T_C$) and the working fluid. The state of the working fluid is considered to be always in an equilibrium state (thermal equilibrium is defined by the $0^{\text{th}}$ law of thermodynamics), since all the processes are quasi-static (very slow). The state of the working fluid can be characterized solely by macroscopic quantities, such as internal energy ($E$), volume ($V$) and total number of particles in the working fluid ($N$). These processes are schematically represented in Fig. 2.1a.

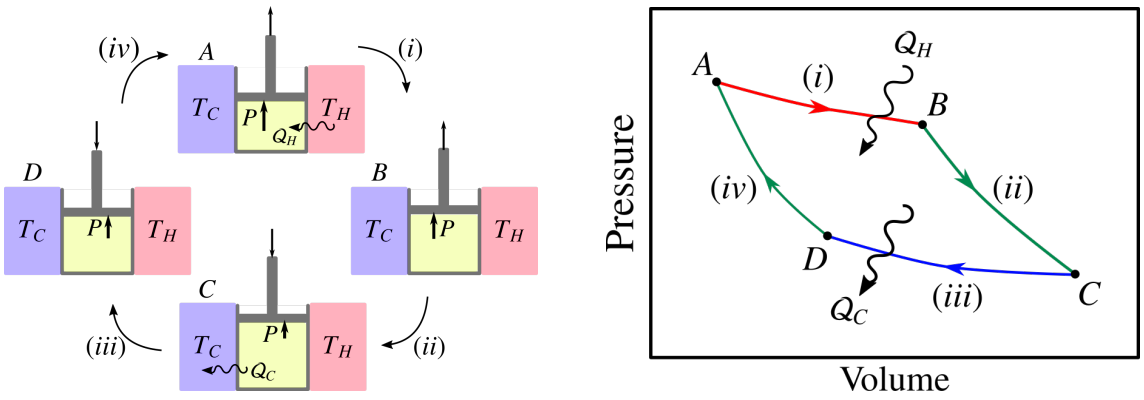


(a) Schematic representation of the Carnot cycle.

(b) Pressure-volume (P-V) diagram.

Figure 2.1: The Carnot cycle represented (a) schematically and (b) diagrammatically.

The pressure-volume (P-V) diagram (Fig. 2.1b) characterizes the state of the working fluid during the transformations. Pressure is defined as minus the derivative of $E$ with respect to $V$, for fixed $S$ (entropy) and $N$ [41]. Heat is only exchanged when the working fluid is put to interact with the hot (i) and cold (iii) baths. In all processes there is work involved, since $V$ is always changing ($\mathcal{W} = -\int P\mathrm{d}V$). According to the 1st law of thermodynamics (energy conservation) and the cyclic property of $E$ ($\oint \mathrm{d}E = 0$), we have that

$$Q_C + Q_H - \mathcal{W} = 0, \tag{2.1}$$

where heat is positive when it enters the working fluid and work is positive when extracted by an external agent.

Furthermore, we might also write the expression quantifying the entropy production, following the 2nd law of thermodynamics and the cyclic property of $S$ ($\oint \mathrm{d}S = 0$),

$$\Sigma = -\frac{Q_C}{T_C} - \frac{Q_H}{T_H} \geqslant 0, \tag{2.2}$$

which in the case of the Carnot cycle is strictly equal to zero (reversible processes). Combining Eqs. (2.1) and (2.2), one might find that the efficiency of the Carnot cycle is expressed by,

$$\eta_C = \frac{\mathcal{W}}{Q_H} \equiv 1 - \frac{T_C}{T_H}. \tag{2.3}$$

Since it saturates the bound given by (2.2), it is the maximum efficiency one can have in cyclic thermal operations.

Other cycles will inherently have lower efficiencies and nonzero entropy production. From the previous equations, the efficiency of any cycle might be written generically as,

$$\eta = \eta_C - \frac{T_C}{Q_H}\Sigma, \tag{2.4}$$

where $Q_H, T_C > 0$ and $\Sigma \geqslant 0$, resulting in $\eta \leqslant \eta_C$, as previously stated. This expression is curious, because it links any other cycle to the Carnot cycle, meaning that these other

cycles may be seen as specific cases of the Carnot cycle, what points to some kind of universality between thermodynamic cycles[1].

Also, it is worth mentioning that the cycle may be operated backwards, whose result is a refrigerator, instead of a heat engine. It means that $\mathcal{W}, Q_H < 0$ and $Q_C > 0$, or in other terms, an external agent applies work to the working fluid in order to transport heat from the cold to the hot bath [41].

## 2.2 Otto cycle

The Otto cycle is of practical importance when it comes to modelling power cycles, being a coarse description of a gasoline combustion engine [41]. This cycle also consists of four strokes: (i) adiabatic compression, (ii) hot isochoric[2], (iii) adiabatic expansion and (iv) cold isochoric, all applied to a working fluid. The transformations (i) and (iii) are (ideally) reversible and do not produce any entropy, on the other hand (ii) and (iv) are inherently irreversible, what results in a nonzero entropy production during the isochorics. This irreversibility can also be explained by the fact that there is only heat being exchanged. Again we can use macroscopic quantities $(E, V, N)$ to describe the state of the working fluid. A schematic depiction of the cycle is shown in Fig. 2.2a.

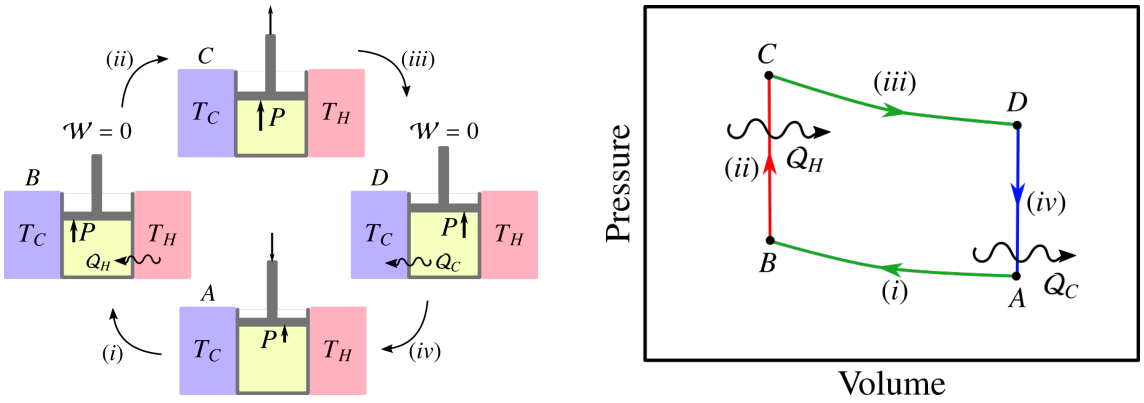


(a) Schematic representation of the Otto cycle.

(b) Pressure-volume (P-V) diagram.

Figure 2.2: The Otto cycle represented (a) schematically and (b) diagrammatically.

Looking at the P-V diagram of the Otto cycle (Fig. 2.2b), we identify the different branches that represent the strokes and see that heat is only exchanged during the isochorics. Furthermore, work in these same two processes is equal to zero, since $V$ is constant. Hence, work is nonzero only during the adiabatic strokes. This is an interesting feature of the Otto cycle, heat and work are decoupled, existing solely in different processes. This separation comes with the cost of producing entropy and decreasing the efficiency compared to the Carnot cycle.

The efficiency of the classical Otto cycle is expressed by [41]:

$$\eta_O = \frac{\mathcal{W}}{Q_H} \equiv 1 - \left(\frac{V_B}{V_A}\right)^{1-\gamma}, \tag{2.5}$$

[1] Until the present moment I have never seen this being discussed in any standard thermodynamics book, but it is a compelling way of looking at how the cycles are related.

[2] Constant volume.

where $V_A, V_B$ are the volumes at points A and B, and $\gamma$ is the specific heat ratio. Combining this with (2.4), one gets

$$\Sigma = \frac{Q_H}{T_C}\left[\eta_C - \left(\frac{V_2}{V_1}\right)^{1-\gamma}\right] > 0, \tag{2.6}$$

which is the entropy produced during one cycle. The Otto cycle will be frequently mentioned throughout the dissertation and will play an important role when talking about quantum heat engines.

## 2.3 Endoreversible cycle

Even though the Carnot cycle presents the greatest achievable efficiency, it has a major problem when it comes to practical applications. It is due to the fact that, since all strokes must be operated quasi-statically, each cycle will take a huge amount of time to be completed, which makes the extracted power tend to zero ($\mathcal{P} = \mathcal{W}/\text{cycle period} \to 0$). Therefore, a compromise between extracted power and efficiency must be taken into account when designing an engine in real life.

In order to treat this issue, the concept of *endoreversible thermodynamics* [3, 43, 44] must be taken into account. It basically consists of considering that the working fluid is at all times in local equilibrium at a different temperature than the bath, and never fully equilibrates with it when they are put to interact. Thus, from the point of view of the bath, the cycle performed by the working fluid is irreversible [44]. This framework matches the consideration that the cycle is completed in finite-time.

A very significant contribution to the theoretical study of finite-time heat engines in the context of endoreversible thermodynamics, was the work done by Curzon and Ahlborn [3]. The authors showed that for a Carnot cycle operated in finite-time, the efficiency at maximum power is

$$\eta_{\text{CA}} = 1 - \sqrt{\frac{T_C}{T_H}}. \tag{2.7}$$

This result is strictly smaller than (2.3), except in the trivial cases $T_C \to 0$, $T_H \to \infty$, $T_C = T_H$. It gives a better estimate of real life efficiencies than the Carnot cycle, as it can be seen in Table 2.1. Although the data therein presented is some decades old, they show how the Curzon-Ahlborn efficiency is close to efficiencies of (then) existing power sources.

| Power source | $T_C$ (°C) | $T_H$ (°C) | $\eta_C$ | $\eta_{\text{CA}}$ | $\eta_{\text{real}}$ |
|---|---|---|---|---|---|
| West Thurrock (U.K.) Coal Fired Steam Plant | 25 | 565 | 64.1% | 40% | 36% |
| CANDU (Canada) PHW Nuclear Reactor | 25 | 300 | 48.0% | 28% | 30% |
| Larderello (Italy) Geothermal Steam Plant | 80 | 250 | 32.3% | 17.5% | 16% |

Table 2.1: Comparison of different real life efficiencies with the Carnot and the Curzon-Ahlborn efficiencies. These data were taken from Ref. [3].

# Chapter 3

# Quantum thermodynamics

Curiously the first proposal for the quantization of energy, the cornerstone of quantum mechanics, occurred when Planck was studying thermal phenomena (radiation) of black bodies [45]. Then it would be argued that the "birth" of quantum mechanics has thus always been intimately related to thermodynamics. However, the early historical development of quantum mechanics happened apart from thermodynamics, because they were seen as entities that lived in radically different size scales, quantum mechanics dealing with atom size objects and thermodynamics an emergent phenomenon of large systems.

Thermodynamics is related to the interaction of a system with its environment. Standard quantum mechanics considers that the system being studied is closed, that is, it doesn't exchange energy and matter with its surroundings. Hence, a formulation of how quantum states evolve under interaction with external systems is crucial to put quantum mechanics and thermodynamics on equal footing. One strategy to solve it is by using the theory of open quantum systems [46].

## 3.1 Open quantum systems

Differently from closed quantum systems, the dynamics of open quantum systems cannot be, in general, described by unitary evolution in time. Consider a quantum system $\mathcal{S}$ surrounded by an environment $\mathcal{E}$ (Fig. 3.1a). Both are subsystems of the global system $\mathcal{S} \oplus \mathcal{E}$, which in turn is considered to be closed, thus evolving according to unitary dynamics [46]. Furthermore, the global Hamiltonian is generically,

$$H_{SE}(t) = H_S + H_E + V_{SE}(t), \tag{3.1}$$

where $H_S$ and $H_E$ live in the Hilbert space of the system ($\mathcal{H}_S$) and of the environment ($\mathcal{H}_E$), respectively. The total Hamiltonian $H_{SE}(t)$ and the interaction $V_{SE}(t)$ live in the tensor product Hilbert space $\mathcal{H}_S \otimes \mathcal{H}_E$, meaning that they act on both system and environment. The time dependence of $V_{SE}(t)$ is not strictly needed, but it was taken for the sake of generality. The double-headed arrows in Fig. 3.1a mean that energy can flow from one subsystem to the other, as a consequence of the interaction Hamiltonian $V_{SE}(t)$.

The time evolution of the state of subsystem $\mathcal{S}$ – also known as the reduced state[1] of $\mathcal{S}$ – in terms of its density operator $\rho_S$ can be done in two different ways [46], as it is shown

[1] This is analogous to marginalized probabilities in statistics.

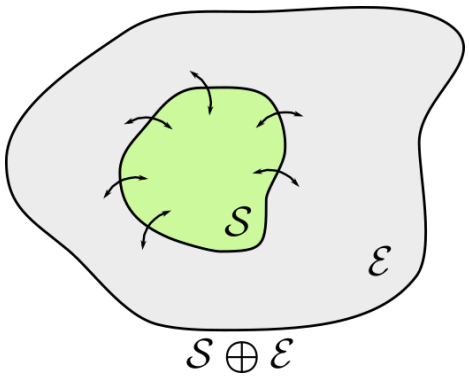


(a) Quantum system ($\mathcal{S}$) and its environment ($\mathcal{E}$).

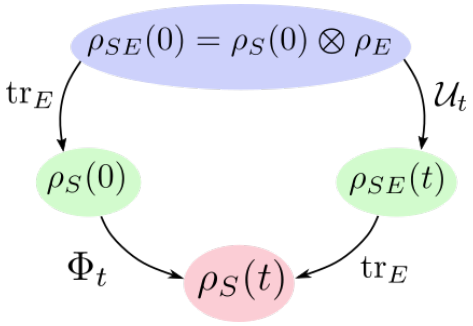


(b) Illustration of the two possible ways of evolving the system's state in time.

Figure 3.1: (a) Basic structure of an open quantum system and (b) schematic time evolution of the state of the quantum system.

in Fig. 3.1b. First, we start with the hypothesis that in the beginning of the dynamics ($t = 0$) the states of the subsystems are not correlated, that is, the global state $\rho_{SE}(0)$ is a product state,

$$\rho_{SE}(0) = \rho_S(0) \otimes \rho_E = \rho_S(0)\rho_E,$$

One way is to evolve unitarily the global state through $\mathcal{U}_t$ and in the end of the evolution trace out the degrees of freedom of the environment – called a partial trace – to obtain the final reduced state of the quantum system. In symbolic terms:

$$\begin{aligned} \rho_S(t) &= \mathrm{tr}_E\{\rho_{SE}(t)\} \\ &= \mathrm{tr}_E\{\mathcal{U}_t[\rho_{SE}(0)]\}, \end{aligned} \tag{3.2}$$

where $\mathcal{U}_t[\rho_{SE}(0)] := U_t \rho_S(0)\rho_E U_t^\dagger$, $U_t = \mathcal{T} e^{-i\int_0^t \mathrm{d}t' H_{SE}(t')}$ and $\mathcal{T}$ is the time-ordering operator. The unitary operator $U_t$ comes from the solution of the von Neumann equation describing the evolution of $\mathcal{S} \oplus \mathcal{E}$:

$$\frac{\mathrm{d}\rho_{SE}}{\mathrm{d}t} = -i[H_{SE}(t), \rho_{SE}]. \tag{3.3}$$

The second way is to define a dynamical map $\Phi_t$, which acts directly on the reduced state $\rho_S$,

$$\rho_S(t) = \Phi_t[\rho_S(0)]. \tag{3.4}$$

The dynamical map $\Phi_t$ is *completely positive and trace preserving* (CPTP),

$$\Phi_t[\rho_S(0)] \geqslant 0, \quad \text{“completely positive”},$$

$$\mathrm{tr}\{\Phi_t[\rho_S(0)]\} = \mathrm{tr}\{\rho_S(0)\} = 1, \quad \text{“trace preserving”}.$$

In the above, $\Phi_t[\rho_S(0)] \geqslant 0$ means the resulting state is a positive semi-definite operator. If the internal correlations of the environment decay at a much faster rate than the time scale of the system dynamics, thanks to the many degrees of freedom of the environment, the family of maps $\{\Phi_t, t \geqslant 0\}$ will usually follow the semigroup property [46]

$$\Phi_{t_1+t_2}(\rho_S) = \Phi_{t_1} \circ \Phi_{t_2}(\rho_S). \tag{3.6}$$

This characteristic is a manifestation of the Markovian dynamics behind $\Phi_t$, which results from the lack of memory effects in the reduced system dynamics[2]. Finally, $\{\Phi_t, t \geqslant 0\}$ is called a quantum dynamical semigroup.

By noting that $\Phi_t$ maps density matrices inside the same space pertaining to $\mathcal{H}_S$, it can be expressed in terms of operators living only in that Hilbert space,

$$\Phi_t(\rho_S) = \sum_i K_i \rho_S K_i^\dagger, \quad \text{with} \quad \sum_i K_i^\dagger K_i = I, \tag{3.7}$$

where $I$ is the identity operator. The operators $\{K_i\}$ that satisfy (3.7) are said to be Kraus operators. Maps following these properties are called quantum operations and they are the most general evolution maps that can exist for a quantum system [46, 47].

Furthermore, given a quantum dynamical semigroup acting on a finite-dimensional Hilbert space, there is a generator of this semigroup $\mathcal{L}$ that satisfies [46]

$$\Phi_t = e^{\mathcal{L}t}, \tag{3.8}$$

which in turn is the solution of a first-order differential equation, known as the Markovian master equation:

$$\frac{\mathrm{d}\rho_S}{\mathrm{d}t} = \mathcal{L}\rho_S. \tag{3.9}$$

In analogy with the Liouville equation in classical physics, the generator $\mathcal{L}$ is called the Liouvillian. The most general form of $\mathcal{L}$ was determined by the works of Gorini, Kossakowski and Sudarshan [30], and Lindblad [48], and reads [46]:

$$\mathcal{L}\rho_S = -i[H_S, \rho_S] + \sum_{k=1}^{N^2-1} \gamma_k \Big( M_k \rho_S M_k^\dagger - \frac{1}{2}\big\{ M_k^\dagger M_k, \rho_S \big\} \Big), \tag{3.10}$$

where $\{M_k\}$ are operators acting on $\mathcal{L}$, $N$ is the dimension of $\mathcal{H}_S$, $\{\cdot,\cdot\}$ is the anti-commutator[3] and $\gamma_k \geqslant 0$ are the relaxation rates, encoding how fast the system exchanges energy with the environment. Combining Eqs. (3.9) and (3.10), one then gets the GKSL master equation:

$$\frac{\mathrm{d}\rho_S}{\mathrm{d}t} = -i[H_S, \rho_S] + \sum_{k=1}^{N^2-1} \gamma_k \Big( M_k \rho_S M_k^\dagger - \frac{1}{2}\big\{ M_k^\dagger M_k, \rho_S \big\} \Big). \tag{3.11}$$

The first term of (3.11) gives rise to the unitary evolution, just as in the case of the von Neumann equation, and the second term is the general form of a dissipator $\mathcal{D}(\rho_S)$, encoding the exchange of information with the environment.

## 3.2 Heat, work and entropy production

Relying on the concepts presented in the last section, we now present how thermodynamic quantities are translated to the quantum realm.

[2] Memory effect is the back-flow of information/energy from the environment into the system. Whenever this happens, we say that the dynamics is non-Markovian.

[3] $\{a, b\} := a\,b + b\,a$.

First, let's start defining what is the equivalent of the classical thermal equilibrium state, called the Gibbs state. The equilibrium state is defined as the one that maximizes the von Neumann entropy ($S(\rho) = -\mathrm{tr}\{\rho \ln \rho\}$), according to the "Principle of Maximum Entropy". Knowing only the dimension of the Hilbert space of a certain system whose density operator is $\rho$, the temperature $T$ of the bath in contact with the system, the system's Hamiltonian $H$ and its energy $E = \mathrm{tr}\{H\rho\}$, it is possible to show that the state that maximizes entropy is equal to [49, 50]:

$$\rho^{th} = \frac{e^{-\beta H}}{Z}, \quad \text{with} \quad Z = \mathrm{tr}\{e^{-\beta H}\}, \tag{3.12}$$

where $\beta = 1/T$ is the inverse temperature. Intuitively, one expects that, when put into contact with a thermal bath whose state is constant and memoryless (Born-Markov approximation), a quantum system should thermalize to (3.12). The next step is to define what is heat and work from the 1st law of thermodynamics (conservation of energy).

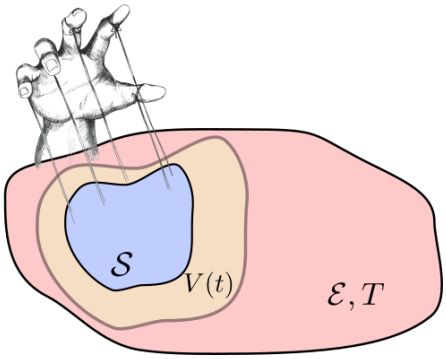


Figure 3.2: Pictorial representation of a quantum system $\mathcal{S}$ interacting with a thermal bath $\mathcal{E}$ through an interaction $V(t)$. The interaction and the system are controlled externally.

We start considering a quantum system $\mathcal{S}$ that is in contact with a thermal bath $\mathcal{E}$ at temperature $T$ and Hamiltonian $H_E$. An external agent (Fig. 3.2) may manipulate the Hamiltonian of the system $\mathcal{S}$ ($H_S(t)$) and the interaction between system $\mathcal{S}$ and bath $\mathcal{E}$ ($V(t)$). The total Hamiltonian is then:

$$H_{SE}(t) = H_S(t) + H_E + V(t),$$

and as it acts on the global system $\mathcal{S} \oplus \mathcal{E}$, which is isolated, the global dynamics is unitary. As a result, any total variation of energy is associated with the work done by the external agent [19, 51]:

$$\dot{\mathcal{W}}(t) := -\frac{\mathrm{d}E_{SE}(t)}{\mathrm{d}t} = -\mathrm{tr}\left\{\frac{\mathrm{d}}{\mathrm{d}t}[H_S(t) + V(t)]\rho_{SE}(t)]\right\}, \tag{3.13}$$

which is positive if work is extracted. On the other hand, looking only at the system $\mathcal{S}$ or the bath, the dynamics is dissipative. The energy that leaves the thermal bath and enters into the system $\mathcal{S}$ is defined as the heat [19, 21, 51]:

$$\dot{\mathcal{Q}}(t) := -\mathrm{tr}\left\{H_E \frac{\mathrm{d}\rho_{SE}(t)}{\mathrm{d}t}\right\}, \tag{3.14}$$

which is defined in such a way that heat is positive when it enters the system. Writing the time derivative of the interaction energy

$$\dot{\mathcal{V}}(t) = \frac{\mathrm{d}}{\mathrm{d}t}\mathrm{tr}\{V(t)\rho_{SE}(t)\}, \tag{3.15}$$

and defining the amount of work extracted from $\mathcal{S}$,

$$\dot{\mathcal{W}}_S(t) := \dot{\mathcal{W}}(t) + \dot{\mathcal{V}}(t), \tag{3.16}$$

the 1st law of thermodynamics is recovered:

$$\frac{\mathrm{d}E_S(t)}{\mathrm{d}t} = \dot{Q}(t) - \dot{\mathcal{W}}_S(t), \tag{3.17}$$

In order to obtain the 2nd law of thermodynamics in this framework, we first define the entropy production as being equal to [52],

$$\Sigma(t) := \Delta S(t) - \beta Q(t), \tag{3.18}$$

where $\Delta S(t)$ is the difference of von Neumann entropy of $\mathcal{S}$ between 0 and $t$, and $Q(t)$ is the Eq. (3.14) integrated with respect to time. The second term on the RHS of Eq. (3.18) is the entropy exchanged between the system $\mathcal{S}$ and the bath, being expressed in the same manner as defined by Clausius [53]. Considering that the initial global state is uncorrelated, $\rho_{SE}(0) = \rho_S \otimes \rho_E^{th} = \rho_S \rho_E^{th}$, it can be shown that Eq. (3.18) may be written in terms of the relative entropy between the joint state at time $t$ and the product of the state of the system $\mathcal{S}$ with the thermal state of the bath [19, 52]:

$$\Sigma(t) = D[\rho_{SE}(t) \| \rho_S(t)\rho_E^{th}] \geq 0, \tag{3.19}$$

with $D[\rho\|\sigma] := \mathrm{tr}\{\rho \ln \rho\} - \mathrm{tr}\{\rho \ln \sigma\} \geqslant 0$ being the quantum relative entropy. It is important to notice, however, that the non-negativity of (3.19) does not imply the non-negativity of the entropy production *rate*, $\dot{\Sigma}$ (see below). Thus, (3.19) is a "weak" expression of the 2nd law of thermodynamics.

What is remarkable about the treatment shown above is that it is independent of the size of the thermal bath, such that the previous results hold even if the bath's size is of the same order of magnitude of the system's size. In such a case, the bath's state is heavily influenced by the system [19]. Another thing that is worth commenting is that the total energy

$$E_{SE}(t) = E_S + E_E(t) + \mathrm{tr}\{V(t)\rho_{SE}(t)\},$$

is not solely the sum of the local energies of the system $\mathcal{S}$ and the bath, but the sum of these local energies and a *non-local* energy due to the interaction $V(t)$ [49]. Here we have a major difference between classical (macroscopic) thermodynamics and quantum thermodynamics, interactions cannot be neglected when accounting for the total energy of a system. Doing so is justified when we have macroscopic objects, whose interaction is by far weaker than the internal energies of the objects. However, in the quantum realm interactions can be of the same order of magnitude of the local energies, and neglecting them is generally a bad approximation. Not only interactions become relevant in the

energy balance, when going down to very small sizes, but also fluctuations (the previous quantities are averages) become important [40, 54–56].

The special case where the interaction energy does not contribute turns out to be associated with the condition

$$[H_S(t) + H_E(t), V(t)] = 0, \qquad \forall t \in \mathfrak{R}, \tag{3.20}$$

known as *strict energy conservation*. It can be shown that this ensures $\mathrm{tr}\{V(t)\rho_{SE}(t)\} = \mathrm{tr}\{V(0)\rho_{SE}(0)\}$, thus $\dot{\mathcal{V}} = 0$ (these calculations can be found in Chapter 5). It means that no energy is trapped in the interaction. The interactions that satisfy Eq. (3.20) are the generators of special quantum operations, called *thermal operations* [21, 57, 58].

For master equations derived from models which either satisfy (3.20) exactly, or at least satisfy it approximately, it's then possible to conveniently write heat and work as

$$\dot{\mathcal{W}}(t) = \mathrm{tr}\left\{\frac{\mathrm{d}H_S(t)}{\mathrm{d}t}\rho_S(t)\right\}, \tag{3.21}$$

$$\begin{aligned}\dot{\mathcal{Q}}(t) &= \mathrm{tr}\left\{H_S(t)\frac{\mathrm{d}\rho_S(t)}{\mathrm{d}t}\right\} \\ &= \mathrm{tr}\{H_S(t)\mathcal{L}\rho_S(t)\} \\ &= \mathrm{tr}\{H_S(t)\mathcal{D}(\rho_S)\}.\end{aligned} \tag{3.22}$$

And also, as a result of applying Spohn's inequality [59], the entropy production rate is found to be greater than or equal to zero,

$$\dot{\Sigma}(t) = \frac{\mathrm{d}S(t)}{\mathrm{d}t} - \beta\dot{\mathcal{Q}}(t) \geqslant 0, \tag{3.23}$$

which is stronger than (3.19). Calculating quantum thermodynamic quantities and modelling quantum heat engines using GKSL master equations is historically at the root of the field of quantum thermodynamics, which dates back to works of Alicki [14] and Kosloff [15].

## 3.3 Information & thermodynamics

In the last sections, we have seen how open quantum systems relate with quantum thermodynamics. In a broader sense, the latter may be associated to another research field, known as *quantum information theory*. This research field, which the reader can get in touch by checking Refs. [47, 60], studies how information theory can be translated to the quantum realm and its possible applications. Thus, we should expect that also thermodynamics is somehow connected to (quantum) information theory, which is not only an important fundamental inquiry [61, 62], but also a cornerstone of future quantum technologies. As a matter of fact, recent works have explored this relation between information and thermodynamics to design quantum engines fueled by information [63–66].

### 3.3.1 Landauer's principle

Information is physical [67]. Far from a mere abstract concept, information needs a physical substrate where it can be encoded, processed and transmitted. The main works that explore this connection gravitate around Landauer's principle [16]. It postulates that erasing information implies a heat dissipation of *at least* $T \ln 2$ for each classical bit, where $T$ is the environment's temperature. This principle already shows the intimate relationship between (quantum) information and thermodynamics, which we shall expose in more detail.

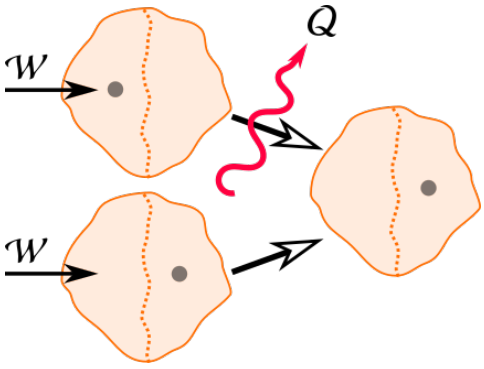


Figure 3.3: Pictorial depiction of the erasure procedure, which culminates at Landauer's principle. $\mathcal{W}$ is the work applied to the particle and $Q$ is the dissipated heat.

In Fig. 3.3, it's shown a simple example of the erasure procedure - in the classical picture - that generates dissipation. A particle may be in the left or in the right partition of a cavity, whose wall dividing the two halves can only be crossed through the action of an external agent. Then, one wants to erase the information of where the particle is by fixing a final state for whatever the initial state of the system was. In order to do so, a work $\mathcal{W}$ must be applied onto the cavity, hence, if the particle was in the left partition, it will move to the right one, and if it was already on the right side, it will continue there.

According to Boltzmann, entropy might be expressed as [42],

$$S = \ln \Omega, \tag{3.24}$$

where $\Omega$ is the number of accessible (micro)states. The erasure procedure has an entropy variation associated with it inside the cavity, for the system starts with 2 accessible states and ends with only 1 possible state. Hence,

$$\begin{aligned} \Delta S &= S_f - S_i \\ &= \ln \Omega_f - \ln \Omega_i \\ &= \cancelto{0}{\ln 1} - \ln 2 \\ &= -\ln 2, \end{aligned} \tag{3.25}$$

which implies that the entropy of the "rest of the world" increases *at least* by $\ln 2$. From the 2$^{\text{nd}}$ law of thermodynamics and assuming that the internal energy of the system cavity-particle is the same before and after the erasure, the work applied to the particle satisfies

$$\mathcal{W} \geqslant \Delta F = -T\Delta S, \tag{3.26}$$

being $F$ the Helmholtz free energy and $T$ the temperature of the environment surrounding the cavity. Finally, by using the 1st law of thermodynamics (heat is positive when flowing to the environment), one finds that

$$Q \geqslant T \ln 2, \tag{3.27}$$

which is exactly what states the Landauer's principle. Its version for a quantum setup, which can be at zero temperature, is done in Ref. [68].

In summary, from simple reasoning one can show the validity of the bound postulated by Landauer. Its universality is expressed by the minimal information it requires to be calculated. This bound has been tested experimentally in microscopic systems [69–72], showing its robustness.

### 3.3.2 Szilard engine

Directly associated to the overlap between information and thermodynamics lies the famous Maxwell's paradox (also known as Maxwell's "demon"). In order to test the limits of the 2nd law of thermodynamics, Maxwell devised a *gedanken*[4] experiment [73]. A hypothetical entity (the demon), possessing information about the positions and velocities of the particles forming a gas, could separate hot (fast) particles from cold (slow) particles, which corresponds to heat flowing from a cold bath to a hot bath, something forbidden the 2nd law of thermodynamics.

In 1929, Szilard[5] came up with a heat engine which makes use of Maxwell's paradox, this machine is called the *Szilard engine* [18]. Together with the idea of using Landauer's principle, conceived by Bennett [17], the Szilard engine (SZE) operation is shown in Fig. 3.4. In the classical framework, we consider a cavity containing a gas particle, in which a wall is inserted (Fig. 3.4a). After placing this barrier, we still don't know where exactly the particle is, so a sneaky entity with a modest memory of one bit measures the position of the particle and registers it (Fig. 3.4b). By knowing where the gas particle is, the wall can be coupled to an external mechanism, such that, by expanding isothermically in contact with a bath at temperature $T$, the particle will deliver a certain amount of work (Fig. 3.4c). Finally, the wall is removed and the memory of the entity is erased, starting all over again the cycle (Fig. 3.4d).

The work extracted from the cavity is equal to [75],

$$\begin{aligned} \mathcal{W}_{extracted} &= T \int_{V/2}^{V} \mathrm{d}V' \frac{1}{V'} \\ &= T \ln 2, \end{aligned} \tag{3.28}$$

where $V$ is the volume of the cavity. However, due to the inherent energy cost of erasing the memory of the entity stemming from Landauer's principle,

$$\mathcal{W}_{erasure} \geqslant T \ln 2, \tag{3.29}$$

[4] "Thought", in German.

[5] Leo Szilard is at the same time very important in scientific history and unknown to many people. He was essential to the Manhattan Project, since he had the original idea of using neutrons to obtain sustained nuclear reactions. Curiously, he had this idea while crossing a street and observing the movement of the cars in London [74].

the net work balance is not positive,

$$\mathcal{W}_{net} = \mathcal{W}_{extracted} - \mathcal{W}_{erasure} \leqslant 0. \tag{3.30}$$

Also, the heat that enters the bath due to the erasure is equal to or greater than the heat absorbed by the particle. Hence, in the end of the cycle, there is no full conversion of heat into work, as one would naively think. As a result, the 2nd law of thermodynamics is saved and the "demon" exorcised [75]. Finally, Landauer's principle guarantees consistency of a thermodynamic cycle containing information theory resources. Just as before, a quantum version of this reasoning is feasible [63].

Far beyond the case of SZEs, the relation between information and thermodynamics is of great relevance for other subjects, such as information processing in ultra-small systems [76]; establishing how and with what efficiency quantum information resources (coherence, entanglement, etc.) can be transformed into work and vice-versa[6] [62, 77–79]; and implementing quantum heat engines operating with engineered reservoirs containing quantum information resources [80–84].

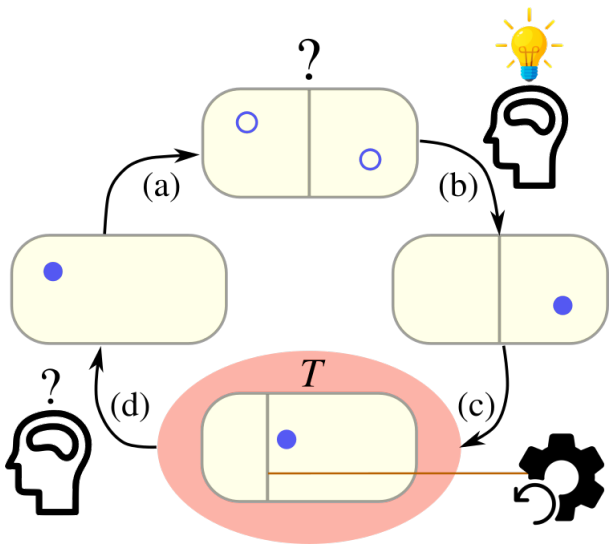


Figure 3.4: Scheme of the Szilard engine. (a) the wall is inserted, (b) the position of the gas particle is measured and registered, (c) work is extracted by means of isothermal expansion, (d) the memory is erased (Landauer's principle) and the wall is removed.

As a last remark, a key problem to *fully* describe (quantum) information and thermodynamics on equal footing is unifying the framework in which they exist, in order to have models and concepts that naturally comprehend both. For the modelling part only, one possibility is to use collisional models, which are studied in Chapter 5 and they are also the building blocks of the quantum heat engine model presented in Chapter 6. Finally, setting a common conceptual ground is a hard quest, since it requires rethinking already established aspects of thermodynamics and information theory, in a coherent and non-contradictory manner. An interesting (and unconventional) approach is known as *constructor theory of thermodynamics* [85], which applies elements introduced by *constructor theory* (e.g. possible/impossible tasks) to hold together thermodynamics and

[6] This is part of a broader research field called *resource theory of thermodynamics*.

information theory. The constructor theory is a kind of "theory of everything", it was created by David Deutsch[7] and it's currently being developed by him, Chiara Marletto and other researchers in the University of Oxford. The curious reader is encouraged to check Ref. [86].

[7]Deutsch is well known for his pioneering works on quantum computation.

# Chapter 4

# Quantum heat engines

Although the research field of quantum heat engines (QHEs) is quite young, some old works have set the ground so that in our days the seed would germinate. Even before the works of Alicki [14] and Kosloff [15], which were very important to start a structured approach of studying QHEs, an older paper dating from the 1950's was the first to envision quantum systems working as heat engines. The short and authentic paper of Scovil and Schulz-Dubois [13] modelled the three-level maser as a heat engine (see Fig. 4.1), giving also experimental reasoning to the model. Therefore, they described a quantum system using thermodynamic arguments.

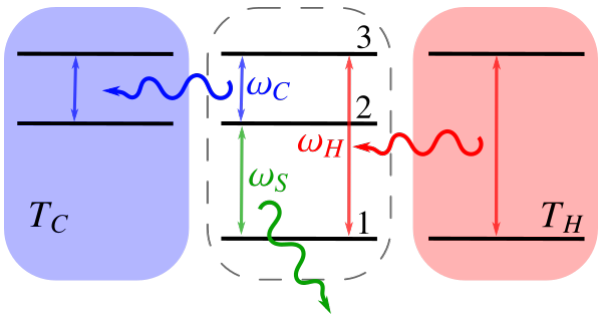


Figure 4.1: Model of the maser as a heat engine [13]. A hot bath at temperature $T_H$ couples with the 1-3 transition (frequency $\omega_H$) of a three-level system, while a cold bath at temperature $T_C$ couples with the 2-3 transition (frequency $\omega_C$). The jump from 2 to 1 at frequency $\omega_S$ is considered to be an extracted signal if population inversion ($p_2 \geqslant p_1$) occurs. The same system may operate as a refrigerator, if run backwards.

The fast miniaturization of devices and the prospect of novel quantum technologies in the near future [87], makes it imperative to understand the relation between quantum mechanics and thermodynamics. Conceiving heat engines in the quantum realm is a promising approach to fill the gaps between the two branches of physics, since they are in the very foundations of classical thermodynamics. The relevance of understanding how to describe quantum and thermodynamic phenomena in a single language lies not only on enlarging the knowledge basis on fundamental physics, but also on providing tools to optimize ultra-small heat engines and to harness quantum effects in thermodynamic processes.

Quantum heat engines come in various flavors, being broadly classified as either

continuous-time QHEs or stroke-based QHEs. The original contributions of this dissertation (Chapter 6) are in the context of the latter. But, for concreteness, in the remainder of this chapter we will discuss both cases, side by side, in order to better appreciate their differences and similarities.

## 4.1 Continuous-time quantum heat engines

As the name suggests, continuous-time QHEs operate continuously in time, that is, all the processes that constitute the engine happen "all at the same time"[1]. As a result, we do not work with integrated quantities, but with currents of heat and work flowing between the parts. Another characteristic of continuous-time QHEs is that they operate in a non-equilibrium steady-state (NESS), meaning that it's a fixed point of the dynamical equation that dictates the time evolution of the working fluid's state, which is also out-of-equilibrium, making it possible to sustain heat and work currents [88]. Continuous-time QHEs can also be formulated in the context of resource theories [57, 58, 89–91]. This framework is intimately related to quantum information theory [90], being suited for determining what are the limits of operation of a certain quantum system, given a set of rules to be obeyed (e.g. global energy conservation). Although very important, this approach to QHEs will not be specifically treated in this dissertation, whose aim is at finite-time operation.

Continuous-time QHEs can be modelled to be autonomous [88, 92]. By autonomous we mean that these QHEs operate by themselves, having all components embedded into them, thus an external agent is not needed [88, 92, 93]. Autonomous QHEs work on the principle of population inversion in quantum systems that are used as working fluids. The simplest quantum system that could be used for autonomous operation is the qutrit (a three-level system) [94], similar to the maser model of Scovil and Schulz-Dubois [13]. However, only considering this model is not enough, as it works close to equilibrium and a dynamical description of the working fluid is desired [88, 92].

The model of autonomous QHEs that is studied in Refs. [95–97] is a generalization of the Scovil-Schulz-Dubois model [13]. This basic model is shown in Fig. 4.2. It shows two qubits, 1 and 2, which have frequencies $\omega_C$ and $\omega_H$ and are thermalized with baths at temperatures $T_C$ and $T_H$ ($T_H > T_C$), respectively. The natural flow of heat from 2 to 1 (from hot to cold) is conditioned to an increase of the energy of a work load, depicted as an infinite ladder with equally spaced energy levels satisfying the resonance condition $\omega_W = \omega_H - \omega_C$. The three entities interact through the Hamiltonian

$$V = \chi(\sigma_H^- \sigma_C^+ a^\dagger + \sigma_H^+ \sigma_C^- a), \tag{4.1}$$

where the $\sigma$'s are Pauli operators[2], which describe the level transitions of the qubits 1 and 2, and $a^\dagger$, $a$ are, respectively, the creation and annihilation operators that act on the ladder, injecting (extracting) one quantum of energy into (from) the work load.

The work load effectively interacts with a virtual qubit [97], which is a two-dimensional subspace of the qubits $\{|g\rangle_C |e\rangle_H, |e\rangle_C |g\rangle_H\}$. This virtual qubit has a transition frequency

[1] In reality, they may be happening at different moments, but their time scales are so short that it seems that they are simultaneous.

[2] For a Hilbert space of dimension 2: $\sigma^+ = \begin{pmatrix} 0 & 1 \\ 0 & 0 \end{pmatrix}$, $\sigma^- = \begin{pmatrix} 0 & 0 \\ 1 & 0 \end{pmatrix}$.

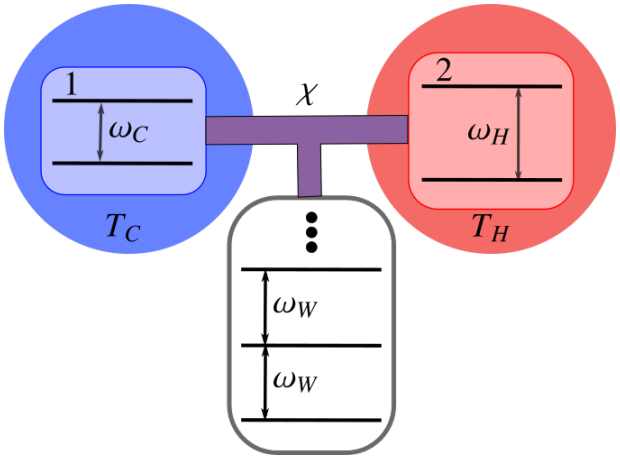


Figure 4.2: Basic model of an autonomous QHE. Two qubits (1 and 2) thermalized with respect to the baths interact with an infinite ladder representing the work load.

equal to $\omega_H - \omega_C$. Now, considering weak interaction and a population ratio between excited (e) and ground (g) states of qubit 1 or 2 being equal to

$$\frac{p_x^{(e)}}{p_x^{(g)}} = e^{-\beta_x \omega_x}, \quad \text{with} \quad x = C, H,$$

the population ratio between the two states of the virtual qubit will be

$$\frac{p_C^{(g)} p_H^{(e)}}{p_C^{(e)} p_H^{(g)}} = e^{-\beta_H \omega_H + \beta_C \omega_C} \equiv e^{-\beta_V \omega_W}. \tag{4.2}$$

The parameter $\beta_V = 1/T_V$ is the inverse *virtual temperature* of the virtual qubit,

$$T_V = \frac{\omega_H - \omega_C}{\beta_H \omega_H - \beta_C \omega_C}. \tag{4.3}$$

This virtual temperature must be less than 0[3], which guarantees that the state $|g\rangle_C |e\rangle_H$ is more likely to be populated than $|e\rangle_C |g\rangle_H$, enabling energy to be transferred to the work load. By doing the proper calculations of the dynamics of the populations of the energy levels of the ladder (as it is done in Ref. [97]), one finds that the ratio between the total energy rate in the work load $\dot{E}_W$ and the heat rate flowing from the hot bath $\dot{Q}_H$ is equal to,

$$\eta = \frac{\dot{E}_W}{\dot{Q}_H} = 1 - \frac{\omega_C}{\omega_H} \leqslant 1 - \frac{T_C}{T_H}. \tag{4.4}$$

By identifying variables of Section 2.2 with the present ones, $V_A \to 1/\omega_C$, $V_B \to 1/\omega_H$ and $\gamma = 0$, we find that (4.4) is the Otto efficiency. The reversed operation of an autonomous QHE generates an *absorption* refrigerator, where the work load drains energy from both qubits 1 and 2.

Nevertheless, when one needs an external power source and/or an intricate feedback control, we say that the continuous-time QHE is driven [92]. By using an external power

[3] Virtual/effective temperatures may be negative.

source, it means that actually the system operates as a refrigerator. One example of driven continuous-time QHE operating as a refrigerator is the maser model of Scovil-Schulz-Dubois run backwards. This can be seen as a simple model of laser cooling [88], a very important technology in experimental condensed matter physics, used, for example, in trapped ion setups to implement quantum algorithms [98]. On the other hand, by also introducing measurements and a feedback loop to regularize the operation of the QHE, the work load attached to the engine becomes a quantum flywheel, which stores in a stable way the energy contained in the load [99].

## 4.2 Stroke-based quantum heat engines

As already discussed in Chapter 2, strokes are thermodynamical processes that can be put into sequence to form a cycle. In the case of stroke-based QHEs, it is not different, transformations of open quantum systems are viewed as strokes and concatenating them gives rise to a quantum thermodynamical cycle. Since each stroke has an explicit length of time associated with it, time is an important parameter to be taken into account, for things to not happen "all at once", as it was the case with continuous-time QHEs, but at specific times. This feature may be explored to optimize the operation of the QHE, in resemblance with the work of Curzon and Ahlborn [35, 92].

In general terms, strokes can be associated to dynamical maps $\mathcal{S}_\alpha$ acting on the state of the working fluid $\rho_t \equiv \rho(t)$,

$$\mathcal{S}_\alpha : \rho_{t_0} \to \rho_{t_0+\tau_\alpha},$$

where the subscript $\alpha$ is a label for the stroke being performed and $\tau_\alpha$ is the time allocated for the process $\alpha$. Furthermore, assuming that these maps form a quantum dynamical semigroup, they can be written as [c.f. Eq. (3.8)],

$$\mathcal{S}_\alpha = e^{\mathcal{L}_\alpha \tau_\alpha}, \tag{4.5}$$

with $\mathcal{L}_\alpha$ being the Liouvillian of stroke $\alpha$. Then, the dynamical map that represents the whole cycle $C$, composed of $k$ strokes, is found by making the composition of all maps,

$$\rho_{t_0+\tau} = C(\rho_{t_0}) = \mathcal{S}_k \circ \cdots \circ \mathcal{S}_1(\rho_{t_0}) = \prod_{\alpha=1}^{k} e^{\mathcal{L}_\alpha \tau_\alpha} \rho_{t_0}, \tag{4.6}$$

in which we define $\tau = \sum_{\alpha=1}^{k} \tau_\alpha$ as the cycle period. In the end, after a certain number $n^*$ of cycles, it's expected that the state of the working fluid will reach a stationary regime, which corresponds to the fixed-point of the cycle's map,

$$\rho^* = C(\rho^*), \tag{4.7}$$

and the system is said to have entered the limit-cycle [100]. Finally, the state of the working fluid after any stroke is found by solving the dynamical equations of motion in (4.6), having in mind the GKSL equation [c.f. Eq.(3.11)], whose dissipator and Hamiltonian depend on the specific characteristics of the working fluid, the thermal baths and the stroke itself.

A simple example of stroke-based QHE is the four-stroke quantum Carnot cycle, which is now presented in the case that the working fluid is a quantum harmonic oscillator

(QHO) with Hamiltonian $H_t = \omega_t(a^\dagger a + 1/2)$, where $\omega_t$ is a time-dependent frequency and $a, a^\dagger$ are the annihilation and creation operators, respectively[4]. Starting with the Carnot cycle, we need the following strokes (see Fig. 4.3a): (a) hot isothermal expansion, (b) isentropic[5] expansion, (c) cold isothermal compression and (d) isentropic compression. The isentropic processes are simply unitary evolution maps. We discuss here the case of quasi-static cycles. Following the adiabatic theorem [101], each isentropic process changes the energy $E$ of the QHO according to,

$$\begin{aligned} E_f = \frac{\omega_f}{\omega_i} E_i &= \omega_f \,\mathrm{tr}\left\{\left(a^\dagger a + \frac{1}{2}\right)\rho_i\right\} \\ &= \frac{\omega_f}{2}\coth\left(\frac{\omega_i}{2T_i}\right), \end{aligned} \tag{4.8}$$

where the indices $i$ and $f$ stand for "initial" and "final", respectively. Then, the frequencies for these strokes are equal to $\omega_i = \omega_2$, $\omega_f = \omega_3$ (expansion) or $\omega_i = \omega_4$, $\omega_f = \omega_1$ (compression), as shown in Fig. 4.3a. The term containing the temperature $T_i$ in (4.8) is explained by the fact that initially the working fluid is in a thermal state of temperature $T_i$, where $T_i = T_H, T_C$ for an isentropic expansion or compression, respectively. Thus, $\langle a^\dagger a\rangle_i = \mathrm{tr}\{a^\dagger a\,\rho_i\} = 1/(e^{\beta_i\omega_i} - 1) = \bar{n}_i$, in which $\bar{n}_i$ is the *Bose-Einstein occupation* with $\beta_i\omega_i = \beta_H\omega_2$ (expansion) or $\beta_i\omega_i = \beta_C\omega_4$ (compression). The extracted work during the isentropic strokes is equal to minus the sum of the energy variations,

$$\begin{aligned} \mathcal{W}_{b,d} &= -(E_f - E_i)^{(b)} - (E_f - E_i)^{(d)} \\ &= -\frac{(\omega_3 - \omega_2)}{2}\coth\left(\frac{\omega_2}{2T_H}\right) - \frac{(\omega_1 - \omega_4)}{2}\coth\left(\frac{\omega_4}{2T_C}\right). \end{aligned} \tag{4.9}$$

Since these strokes are isentropic, there is no exchange of heat with the baths $Q = 0$.

The isentropic strokes are complemented by the hot and cold isothermals. These strokes are more intricate, since one must implement a protocol for both the coupling with the baths and the frequency of the QHO. The final state is calculated by applying the resultant maps – which will follow the form of (3.11) – to the initial state of each stroke. Following the calculations done in Appendix A, one finds that the extracted work during both isothermal strokes is expressed by,

$$\mathcal{W}_{a,c} = -T_H \ln\left[\frac{\sinh(\omega_2/2T_H)}{\sinh(\omega_1/2T_H)}\right] - T_C \ln\left[\frac{\sinh(\omega_4/2T_C)}{\sinh(\omega_3/2T_C)}\right], \tag{4.10}$$

which is followed by a heat exchanged with the hot bath equal to,

$$Q_H = E_2 - E_1 - T_H \ln\left[\frac{\sinh(\omega_2/2T_H)}{\sinh(\omega_1/2T_H)}\right], \tag{4.11}$$

with $E_j = \frac{1}{2}\omega_j \coth(\beta_H\omega_j/2)$ being the energy at the points $j = 1, 2$. Then, the efficiency is given by,

$$\eta = \frac{\mathcal{W}_{a,c} + \mathcal{W}_{b,d}}{Q_H}, \tag{4.12}$$

[4] In this simple case, it's assumed that the QHE is already in the limit-cycle. The general treatment of stroke-based QHEs, as previously presented, is by far more complicated.

[5] Constant entropy.

where the resultant expression comes from the replacement of the terms using Eqs. (4.9)–(4.11). It is readily seen that, in general, this expression is *not* equal to the Carnot efficiency. The explanation is that, although quasi-static, the cycle may not be reversible. It's what happens when at the end of an isentropic stroke (continuous and green branches in Fig. 4.3a), the energy of the QHO doesn't match the initial energy of the subsequent isothermal stroke (red and blue continuous branches in Fig. 4.3a). Whenever it happens, the system will have to thermalize with the bath by exchanging heat irreversibly (red and blue curly arrows in Fig. 4.3a). This in turn will result in entropy production, lowering the efficiency of the QHE. To ensure quasi-static reversibility, we must make the energies at the end of the isentropic strokes match the ones at the beginning of the isothermal strokes (see the dashed branches in Fig. 4.3a). In this case, no extra heat is exchanged with the baths, entropy production is equal to zero and the Carnot efficiency is recovered. By imposing that the energies of the branches match with each other, the following condition is found [35]:

$$\frac{T_C}{T_H} = \frac{\omega_3}{\omega_2} = \frac{\omega_4}{\omega_1}. \tag{4.13}$$

As a result, Eq. (4.12) becomes identically equal to the Carnot efficiency $\eta_C = 1 - T_C/T_H$.

As previously discussed in Chapter 2, the power is asymptotically equal to zero when one has the Carnot efficiency. Lifting this constraint opens the path of exploring finite-time behavior, that is, adjusting the protocols and time allocations to optimize the balance between efficiency and power, while paying the cost of producing entropy. However, the calculations presented in this chapter are restricted to quasi-static strokes. Getting rid of this constraint implies solving much more complicated dynamics (time-dependent GKSL master equations). Hence, one needs to apply approximations [32], or make use of mathematical methods, such as Floquet theory [35] and closed-algebras [102], or introduce the concept of quantum friction [33, 103–105].

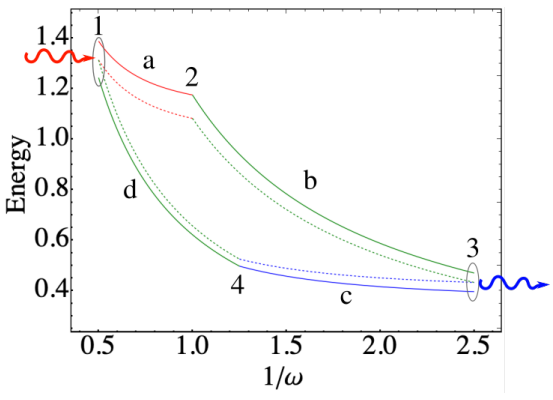


(a) Diagram of the Carnot cycle.

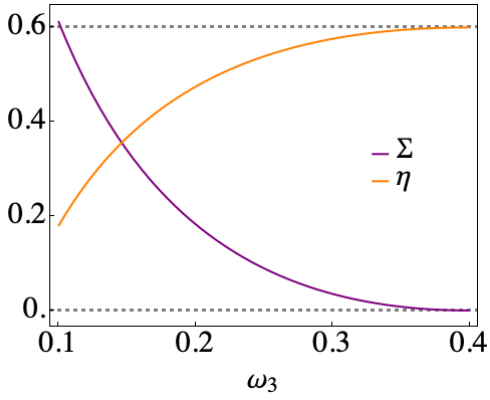


(b) Entropy production and efficiency.

Figure 4.3: Plot of (a) the energy of the working fluid for all strokes, as a function of $1/\omega$ and in the case of reversible (dashed branches) and irreversible (continuous branches) quasi-static cycles. Plot of (b) the entropy production and the efficiency as functions of $\omega_3$. The parameters are equal to: $T_C = 0.4$, $T_H = 1.0$, $\omega_1 = 2.0$, $\omega_2 = 1.0$, $\omega_3 = 0.4$ (except for (b)) and $\omega_4 = 0.8$.

The total entropy production can be found by using Eq. (2.4),

$$\begin{aligned}\Sigma &= \frac{Q_H}{T_C}(\eta_C - \eta) \\ &= \frac{Q_H}{T_C}\left(1 - \frac{T_C}{T_H}\right) - \frac{\mathcal{W}_{a,c} + \mathcal{W}_{b,d}}{T_C},\end{aligned} \tag{4.14}$$

which is plotted together with the efficiency for different values of $\omega_3$ (Fig. 4.3b). Looking at these plots, we reaffirm that entropy production decreases the efficiency. When $\Sigma$ goes to zero, $\eta$ reaches the Carnot efficiency ($T_C = 0.4$, $T_H = 1.0$, $\eta_C = 1 - 0.4/1.0 = 0.6$), as depicted by the gray dashed lines.

By solely using the framework of time-dependent GKSL master equations, one is still limited in studying finite-time behavior, as it was already said. The techniques aforementioned (approximations, closed-algebras, Floquet theory and quantum friction) are valid and have their merits, however it is difficult to know whether the cost-benefit analysis is positive, since all alternatives lead to complicated calculations that, together with a more complex working fluid, makes them prohibitive for the design of real-life QHEs.

Together with these issues, the trade-off between power and efficiency may be problematic for realistic applications. One interesting route is to use the idea of shortcut-to-adiabaticity, which shall be discussed in Chapter 7.

Finally, in the time-dependent GKSL master equations approach, it's hard to embed genuine quantum effects into the QHE model, such as coherence and entanglement. It would be interesting to conceive another route of investigation, which is adapted to quantum effects. Therefore, their relation with thermodynamics would be better understood. On top of that, such an approach to finite-time QHEs must be less complex than the methods aforementioned. Looking for a candidate that fulfills these requirements was a particular motivation of this dissertation. Results that will be presented in Chapter 6 provide an alternative way of modelling finite-time QHEs that doesn't suffer from the same problems as its "competitors".

# Chapter 5

# Collisional models

It is commonly considered that thermal baths are reservoirs containing a large number of constituents. This, together with generally complicated internal interactions, generate a fast decay of their correlations, as already mentioned in Chapter 3. It's the basis on which quantum master equations in the GKSL form are usually obtained. Moreover, these assumptions have another consequence regarding the state of the bath. It is taken for granted that, at all times, the bath's state is a fixed thermal state, meaning constant bath temperature. However, it happens that, for ultra-small systems, the baths may be of comparable size as the working fluid, breaking down the assumption that the bath's state remains unchanged. In addition, trending experimental setups are able to manipulate single quantum states [4–12], and integrating this technological aspect with quantum thermodynamics is a promising way of modelling and testing thermodynamical phenomena in the quantum realm [106–109].

A strategy which has gained a lot of attention in recent years is the application of the so-called collisional models[1] [19–27]. These consist of a set of possible implementations of environments, beyond the standard heat bath [19, 21]. Even more, they may be used in different approaches, such as modelling quantum stochastic systems [27], transport in spin chains [22, 26] and quantum heat engines [20, 29, 38]. Collisional models pave the way for a framework in which information and thermodynamic quantities are mixed together, so that their relation might be better understood. And, in addition, their discretized nature makes them ideal candidates to model finite-time QHEs [29].

## 5.1 The general picture

The basic setup of a collisional model is shown in Fig. 5.1. The environment is seen as a stream of identical units, or *ancillas*[2], in a well-defined state $\rho_E$ and Hamiltonian $H_E$. During a time $\tau$, one ancilla interacts through the Hamiltonian $V$ with a system whose state is $\rho_S^0$ and Hamiltonian $H_S$. It's important to emphasize that, initially, the system and ancilla are uncorrelated (i.e. $\rho_{SE} = \rho_S^0 \rho_E$). After the interaction, the ancilla is discarded and a fresh one is introduced, starting the process again. For simplicity, we assume that the time that it takes for the next interaction to start is negligible. In symbols, the first

[1] Also called "repeated interactions".

[2] Plural of *ancilla*: auxiliary, accessory (in this context).

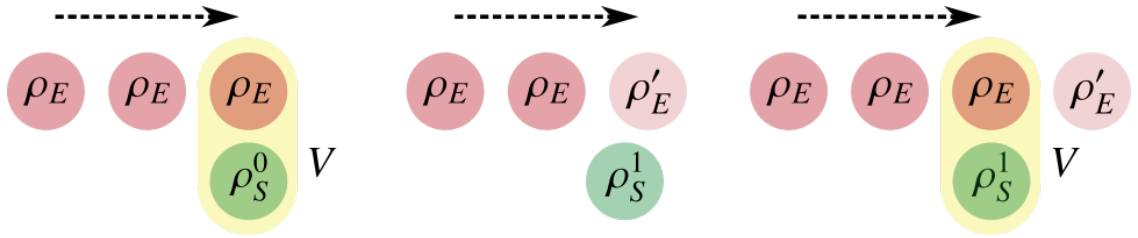


Figure 5.1: Sequential interactions composing a collisional model. The system interacts for a time $\tau$ with an environment ancilla, prepared in a state $\rho_E$, which is then discarded and a fresh new one is introduced.

collision can be summarized by

$$\begin{aligned}\rho_S^1 &= \mathrm{tr}_E\{\rho'_{SE}\} \\ &= \mathrm{tr}_E\{U_{SE}\,\rho_S^0\,\rho_E U_{SE}^\dagger\} \\ &= \mathcal{E}(\rho_S^0),\end{aligned} \tag{5.1}$$

where $U_{SE} = e^{-i(H_S+H_E+V)\tau}$ and $\mathcal{E}$ is the quantum map connecting $\rho_S^0$ to $\rho_S^1$. Likewise, the final state of the ancilla which will be discarded is

$$\begin{aligned}\rho'_E &= \mathrm{tr}_S\{\rho'_{SE}\} \\ &= \mathrm{tr}_S\{U_{SE}\,\rho_S^0\,\rho_E U_{SE}^\dagger\}.\end{aligned} \tag{5.2}$$

Repeating this procedure $n+1$ times then yields the stroboscopic (discrete-time) evolution of the system, in the form

$$\rho_S^{n+1} = \mathcal{E}(\rho_S^n). \tag{5.3}$$

For consistency, the global state $\rho_{SE_n}$ and the state of the environment $\rho_{E_n}$ will also be labelled. It is important to note that the initial state of all ancillas is the same $\{\rho_{E_n} \equiv \rho_E | \forall n \in \mathbb{N}\}$. However, after the interaction that is no longer the case, since each ancilla interacts with the system at a different moment $\{\rho'_{E_n} \neq \rho'_{E_m} | n \neq m\}$. The map $\mathcal{E}$ leads the system to a unique steady-state $\rho_S^*$,

$$\rho_S^* = \mathcal{E}(\rho_S^*), \tag{5.4}$$

which satisfies the Data Processing Inequality (DPI) [19, 31, 46]

$$D[\rho_S^n \| \rho_S^*] > D[\mathcal{E}(\rho_S^n) \| \mathcal{E}(\rho_S^*)] = D[\rho_S^{n+1} \| \rho_S^*], \tag{5.5}$$

where $D[\rho\|\sigma] = \mathrm{tr}\{\rho\ln\rho - \rho\ln\sigma\}$ is the quantum relative entropy. This strict inequality means that $\rho_S^*$ is indeed unique, and also that $D[\mathcal{E}(\rho_S^n)\|\rho_S^*]$ is monotonically decreasing and bounded from below [19].

Moreover, the global evolution of the system plus the environment ancilla is unitary, meaning that the total energy is conserved at any moment, thus

$$\mathrm{tr}\{(H_S + H_E + V)(\rho'_{SE_n} - \rho_S^n\,\rho_{E_n})\} = 0, \qquad \forall n \in \mathbb{Z}. \tag{5.6}$$

This expression may be expanded, so that one obtains,

$$\Delta E_S^n = \mathcal{Q}^n - \mathcal{W}_{\mathrm{on/off}}^n, \tag{5.7}$$

where $\Delta E_S^n = \mathrm{tr}\{H_S(\rho_S^{n+1} - \rho_S^n)\}$, $Q^n := -\Delta E_E^n = -\mathrm{tr}\{H_E(\rho'_{E_n} - \rho_E)\}$ is defined as the heat flowing between the system and the ancilla [19, 110], and $\mathcal{W}^n_{\mathrm{on/off}} = \mathrm{tr}\{V(\rho'_{SE_n} - \rho_S^n \rho_E)\}$. The last term is known as the *on/off work*, which is the cost of switching the interaction on and off [19, 20]. This term may be also justified by looking at the global Hamiltonian as time-dependent,

$$H_{SE}(t) = H_S + H_E + \lambda(t)V,$$

where $\lambda(t)$ is a boxcar function equal to 1 only during the interaction time $\tau$. The work is defined using the standard expression,

$$\mathcal{W}_{\mathrm{on/off}} = -\lim_{\epsilon\to 0}\int_{-\epsilon}^{\tau+\epsilon} \mathrm{d}t\left\langle\frac{\partial H_{SE}(t)}{\partial t}\right\rangle.$$

The only component of the Hamiltonian that is time-dependent is $\lambda(t)$. Its derivative is a pair of anti-parallel Dirac deltas, one at the beginning of the interaction and the other one afterwards. Thus, the result of the integration depends on the initial time, when the interaction is turned on, and on the final time, when the interaction vanishes. After doing the calculations, the result is exactly the same as previously defined for the on/off work.

After tracing out the ancilla, we *loose* information about the correlations created between system and ancilla during the interaction. This loss of information is quantified by the mutual information,

$$\mathcal{I}(\rho'_{SE_n}) = S(\rho_S^{n+1}) + S(\rho'_{E_n}) - S(\rho'_{SE_n}), \tag{5.8}$$

in which $S(\rho) = -\mathrm{tr}\{\rho\ln\rho\}$ is the von Neumann entropy. Also, the change in the state of the environment ancilla must be taken into account, by means of the relative entropy:

$$D[\rho'_{E_n}\|\rho_E] = \mathrm{tr}\{\rho'_{E_n}\ln\rho'_{E_n} - \rho'_{E_n}\ln\rho_E\}. \tag{5.9}$$

Eqs. (5.8) and (5.9) summed together give us how irreversible the process is, quantified by its entropy production [19, 111],

$$\Sigma^n = \mathcal{I}(\rho'_{SE_n}) + D[\rho'_{E_n}\|\rho_E] \geqslant 0. \tag{5.10}$$

These results are very general and do not assume anything about the structure of the states of the system and ancillas. Also, *all* energy sources are identified and well controlled, which is something crucial for a consistent thermodynamic framework. Here lies a core difference from the master equations approach. These describe precisely the *dynamics* of the system's state, but the approximations in the derivation have an impact on tracking all energy sources. This, in turn, has fundamental consequences on the *thermo*dynamics of the system. As it shall be seen, collisional models might be used to obtain quantum master equations, stressing their generality.

## 5.2 Thermal state ancillas

Very relevant to quantum thermodynamics is the case of environments composed of thermal state ancillas. These have a well defined temperature $T = \beta^{-1}$ and are written in the Gibbs state form,

$$\rho_E = \frac{e^{-\beta H_E}}{Z_E}, \tag{5.11}$$

where $Z_E = \mathrm{tr}\{e^{-\beta H_E}\}$ is the partition function of the environment ancilla. Also, the interaction $V$ is chosen such that there is strict energy conservation, that is,

$$[H_S + H_E, V] = 0.$$

Notice that $V$ does not commute with $H_S$ and $H_E$ individually, only with their *sum*. Therefore, the operator $U_{SE}$ will also present this same property. The open dynamics of a system interacting with a thermal environment by means of a strict energy conserving unitary is called a *thermal operation*. [21, 57, 58]. Thermal operations have the special attribute of solely exchanging energy between two parties, without trapping energy in the interaction,

$$\begin{aligned} \mathcal{W}^n_{\text{on/off}} &= \mathrm{tr}\{V(\rho'_{SE_n} - \rho^n_S \rho_E)\} \\ &= \mathrm{tr}\{U^\dagger_{SE} V U_{SE} \rho^n_S \rho_E - V \rho^n_S \rho_E\} \\ &\equiv 0, \end{aligned} \tag{5.12}$$

and

$$\Delta E^n_E = -\Delta E^n_S. \tag{5.13}$$

The minus sign defines the heat as positive when it enters the system,

$$\Delta E^n_S = Q^n. \tag{5.14}$$

Using Eqs. (5.8) and (5.9) in Eq. (5.10), and knowing that the system and the ancilla are uncorrelated in the beginning of the interaction, one gets

$$\begin{aligned} \Sigma^n &= \mathcal{I}(\rho'_{SE_n}) + D[\rho'_{E_n} \| \rho_E] \\ &= \Delta S^n_S + \cancel{S(\rho'_{E_n})} - S(\rho_E) - \cancel{S(\rho'_{E_n})} - \mathrm{tr}\{\rho'_{E_n} \ln \rho_E\} \\ &= \Delta S^n_S + \beta \Delta E^n_E \\ &= \Delta S^n_S - \beta Q^n, \end{aligned} \tag{5.15}$$

where $\Delta S^n_S := S(\rho^{n+1}_S) - S(\rho^n_S)$. Eq. (5.15) is exactly the standard expression for the entropy production in the context of thermodynamics [19, 52]. Then, we can identify the second term on the RHS as the entropy flux between the bath and system.

### 5.2.1 Steady-state

Assuming that the system reaches the steady-state, its *state variables* (energy and entropy) will satisfy

$$\Delta S^*_S = \Delta E^*_S = \Delta E^*_E = 0,$$

which also implies

$$Q^* = \Sigma^* = 0,$$

corroborating the premise that it is a steady-state. By means of thermodynamic arguments, one would say that the system has thermalized with the bath, being now also an equilibrium state with temperature $T = \beta^{-1}$. To confirm this reasoning, suppose that the steady-state of the system is

$$\rho^*_S = \frac{e^{-\beta H_S}}{Z_S}, \tag{5.16}$$

where $Z_S = \mathrm{tr}\{e^{-\beta H_S}\}$ is the partition function. Then, Eq.(5.4) becomes

$$\begin{aligned}\rho_S^* &= \mathrm{tr}_E\{U_{SE}\frac{e^{-\beta H_S}}{Z_S}\frac{e^{-\beta H_E}}{Z_E}U_{SE}^\dagger\}\\ &= \frac{1}{Z_S Z_E}\mathrm{tr}_E\{U_{SE}e^{-\beta(H_S+H_E)}U_{SE}^\dagger\}\\ &= \frac{e^{-\beta H_S}}{Z_S \cancel{Z_E}}\underbrace{\mathrm{tr}_E\{e^{-\beta H_E}\}}_{\cancel{Z_E}}\\ &= \frac{e^{-\beta H_S}}{Z_S}, \qquad \text{QED.}\end{aligned} \tag{5.17}$$

Crucially, we used here the fact that $U_{SE}$ is a thermal operation, so that it commutes with $H_S + H_E$ (but not with each one individually). Therefore, (5.16) is indeed the steady-state of the system. Then, we say that system was thermalized through sequential "collisions" with a stream of thermal ancillas. It appeals to our intuition of thermalization: particles at different temperatures collide until they reach an equilibrium distribution of position and momenta.

## 5.3 Connection to quantum master equations

A powerful trait of collisional models, apart from their versatility and discretized nature, is the possibility of deriving quantum master equations by applying certain approximations [20, 21]. The key idea is to pass from discrete-time to constinuous-time, by means of rescaling the interaction and taking the limit of very fast collisions. Far from being only a mathematical trick, the rescaling procedure has a physical meaning. As already discussed in Chapter 3, the correlations of a (large) thermal bath decay very fast, that is, the characteristic time of the bath is way shorter than the time scale in which the dynamics of the system happens. Therefore, it is reasonable that, in order to "mimic" large baths, one can take the limit of very fast collisions and by doing so, the interaction must be infinitely large to compensate for the short time in which it takes place.

So, let us start with the derivation. First, we rescale the interaction and write the total Hamiltonian as

$$H_{SE} = H_S + H_E + \frac{1}{\sqrt{\tau}}V. \tag{5.18}$$

Hence, by taking $\tau \to 0$, it is guaranteed that a very strong interaction will impose exchange of information/energy between system and bath. The square root will be soon justified. The state of the system after each interaction is given by (5.3) and applying the new rescaled interaction we have,

$$\rho_S^{n+1} = \mathrm{tr}_E\{e^{-i\tau(H_S+H_E+V/\sqrt{\tau})}\rho_S^n\rho_E e^{i\tau(H_S+H_E+V/\sqrt{\tau})}\}. \tag{5.19}$$

Expanding this in a power series yields

$$\begin{aligned}\rho_S^{n+1} &= \mathrm{tr}_E\{\rho_S^n\rho_E - i\tau[H_{SE},\rho_S^n\rho_E] - \frac{\tau^2}{2}[H_{SE},[H_{SE},\rho_S^n\rho_E]] + O(\tau^3)\}\\ &= \rho_S^n - i\tau[H_S,\rho_S^n] - \frac{\tau^2}{2}\mathrm{tr}_E\Big\{[H_{SE},[H_{SE},\rho_S^n\rho_E]] + O(\tau^3)\Big\}.\end{aligned}$$

Dividing it by $\tau$ on both sides, it's written as

$$\frac{\rho_S^{n+1}-\rho_S^n}{\tau} = -i[H_S,\rho_S^n] - \frac{\tau}{2}\mathrm{tr}_E\Big\{[H_{SE},[H_{SE},\rho_S^n\rho_E]] + O(\tau^3)\Big\}. \tag{5.20}$$

When we take the limit $\tau \to 0$, most contributions in the second term of the RHS will vanish. However, the rescaling in $V$ used in (5.18), will now compensate and lead to one term being finite:

$$\begin{aligned}\lim_{\tau\to 0}\frac{\rho_S^{n+1}-\rho_S^n}{\tau} &= -i[H_S,\rho_S^n] - \frac{1}{2}\mathrm{tr}_E\Big\{[V,[V,\rho_S^n\rho_E]]\Big\}\\ \frac{\mathrm{d}\rho_S}{\mathrm{d}t} &= -i[H_S,\rho_S] - \frac{1}{2}\mathrm{tr}_E\Big\{[V,[V,\rho_S\rho_E]]\Big\},\end{aligned} \tag{5.21}$$

justifying the square root in the interaction term, so that it would survive when taking the limit $\tau \to 0$. The expression in (5.21) already looks like a quantum master equation. The first term on the RHS is responsible for the unitary evolution and the second is a kind of "general" dissipator, which applies to any desired interaction,

$$\mathcal{D}(\rho_S) := -\frac{1}{2}\mathrm{tr}_E\Big\{[V,[V,\rho_S\rho_E]]\Big\}. \tag{5.22}$$

In the context of strict energy conservation, the interaction can be generically written in terms of the *eigenoperators* of the system $\{L_k\}$ and bath $\{A_k\}$,

$$V = \sum_k g_k(L_k^\dagger A_k + L_k A_k^\dagger), \tag{5.23}$$

where the eigenoperators satisfy $[H_S, L_k] = -\omega_k L_k$, $[H_E, A_k] = -\omega_k A_k$ and $k$ are the resonant modes between system and bath. The commutators related to the eigenoperators make explicit that only resonant modes are taken into account[3], because these are the modes that mainly drive the interaction. Inserting (5.23) into (5.22), the result is a dissipator in GKSL form [20, 21],

$$\mathcal{D}(\rho_S) = \sum_k \left\{\gamma_k^-\left[L_k\rho_S L_k^\dagger - \frac{1}{2}\Big\{L_k^\dagger L_k,\rho_S\Big\}\right] + \gamma_k^+\left[L_k^\dagger\rho_S L_k - \frac{1}{2}\Big\{L_k L_k^\dagger,\rho_S\Big\}\right]\right\}, \tag{5.24}$$

with $\gamma_k^- := |g_k|^2\,\mathrm{tr}\{A_k A_k^\dagger\rho_E\}$ and $\gamma_k^+ := |g_k|^2\,\mathrm{tr}\{A_k^\dagger A_k\rho_E\}$ being the decay rates modulated by the thermal statistical distribution of the bath.

Using the Baker-Campbell-Hausdorff (BCH) formula[4], together with the fact that $\{A_k\}$ are eigenoperators of $H_E$, one gets

$$e^{\beta H_E}A_k e^{-\beta H_E} = A_k e^{-\beta\omega_k}.$$

Then, the ratio between the decay rates simplifies to a detailed balance relation [46],

$$\begin{aligned}\frac{\gamma_k^+}{\gamma_k^-} &= \frac{\mathrm{tr}\{A_k^\dagger A_k\rho_E\}}{\mathrm{tr}\{A_k A_k^\dagger\rho_E\}}\\ &= \frac{\cancel{\mathrm{tr}\{A_k^\dagger\rho_E A_k\}}e^{-\beta\omega_k}}{\cancel{\mathrm{tr}\{A_k A_k^\dagger\rho_E\}}}\\ &= e^{-\beta\omega_k}.\end{aligned} \tag{5.25}$$

[3] Note that level transitions in both system and bath have an energetic cost of $\omega_k$.

[4] $e^{tA}Be^{-tA} = B + t[A,B] + \frac{t^2}{2!}[A,[A,B]] + \frac{t^3}{3!}[A,[A,[A,B]]] + \ldots$

Finally, joining (5.21) and (5.24) we have a quantum master equation derived from the collisional model,

$$\frac{\mathrm{d}\rho_S}{\mathrm{d}t} = -i[H_S, \rho_S] + \mathcal{D}(\rho_S). \tag{5.26}$$

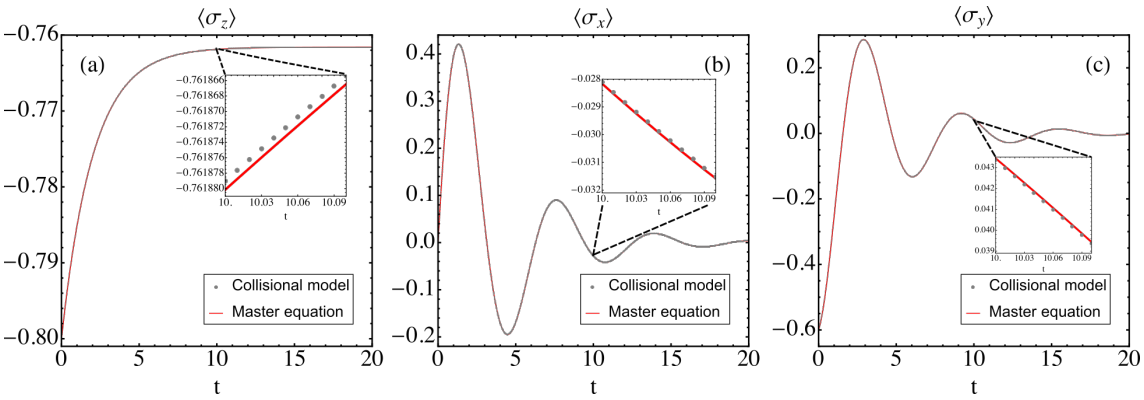


Figure 5.2: Plots of the expectation values of (a) $\sigma_z$, (b) $\sigma_x$ and (c) $\sigma_y$ for both the collisional model and the master equation. The insets show zoomed regions of all three plots. The chosen values of the parameters are: $\omega = 1.0, g = 0.7, T = 0.5, \tau = 0.01$.

In order to check how precise is this approximation, we now compare the outcomes of the collisional model with rescaled interaction and the master equation. Consider the simple case of system ($S$) and bath ($E$) composed of qubits. Their Hamiltonians are then,

$$H_\chi = \frac{\omega}{2}\sigma_z^\chi, \quad \text{with } \chi = S, E, \tag{5.27}$$

where $\sigma_z^\chi$ are Pauli matrices of $S$ and $E$. As it is readily seen, the system and the bath are resonant. The interaction $V$ is chosen according to (5.23),

$$V = g(\sigma_+^S \sigma_-^E + \sigma_-^S \sigma_+^E). \tag{5.28}$$

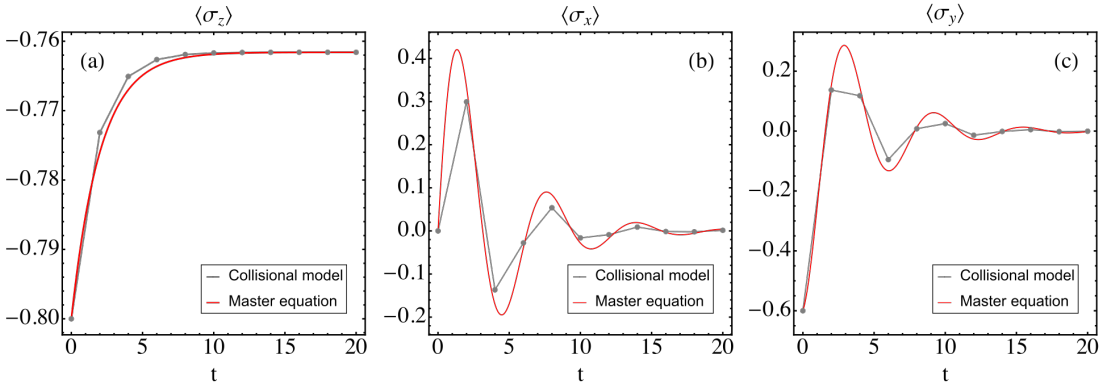


Figure 5.3: Plots of the expectation values of (a) $\sigma_z$, (b) $\sigma_x$ and (c) $\sigma_y$ for both the collisional model and the master equation. Same parameters as in Fig. 5.2, but now $\tau = 2.0$.

To analyze the dynamics, we choose the expectation value of the Pauli matrices $\{\sigma_z, \sigma_x, \sigma_y\}$ for the system. The expectation values are obtained by calculating the trace of the product between each of the Pauli matrices and the state $\rho_S$. The state of the system is given by either (5.19) or (5.26), for the collisional model and the master equation, respectively. Fig. 5.2 shows that, when $\tau$ is small enough, the master equation provides with good precision the time evolution of the system's state. On the other hand, it is not the case when $\tau$ is of the same order as $\omega, g$. As shown in Fig. 5.3, a significant disparity arises in the transient regime. Nevertheless, the stationary values roughly coincide in both situations. The steady-state is diagonal with respect to $\sigma_z$ and its entries depend on $T$, as shown in (5.17).

# Chapter 6

# Stroboscopic two-stroke quantum heat engines

This chapter is the most important of the dissertation, as it summarizes the original contributions of this work. Similar content can be found in the preprint recently submitted to arXiv.org [29], which was also recently accepted for publication in *Physical Review A*.

The proposed model of two-stroke QHEs is herein described. We start by the describing the individual strokes that compose the cycle, the heat and work strokes, in which the relevant thermodynamic variables are defined. Furthermore, it is shown that, depending on the kind of internal interaction established within the working fluid, the QHE has a universal expression for its efficiency. Finally, two applications of the model are discussed, a two-qubit QHE, which is treated analytically, and a spin chain with $N$ sites, that in turn is studied numerically. For both, the influence of the parameter space on the output power and on the number of cycles required to achieve the limit-cycle is explored.

## 6.1 The engine

Inspired by the SWAP engine [36–40] and collisional models [19–27], the stroboscopic two-stroke quantum heat engine is a model meant to treat QHEs operated in finite-time. It's considered to be a toy model, that is, it doesn't take into account all the details of the QHE, but only what is essential to understand the mechanisms behind it. This approach results in a flexible model, which can be adapted for different working fluids and operation protocols, as well as enabling the use of quantum resources (e.g. entanglement, coherence) [21]. For simplicity, "the system" from now on is to be taken as a synonym of "working fluid".

### 6.1.1 Heat stroke

In Fig. 6.1a, a pictorial representation of the heat stroke is presented. The system has $N$ subsystems or sites[1], each with dimension $d_i$ and local Hamiltonian $H_i$. During this stroke, the subsystems do not interact with each other. At the boundaries, the corresponding sites interact with a cold bath ($C$) and a hot bath ($H$). These baths are represented in the

[1] Despite the fact that the system is treated as a chain, all calculations hold for other geometries.

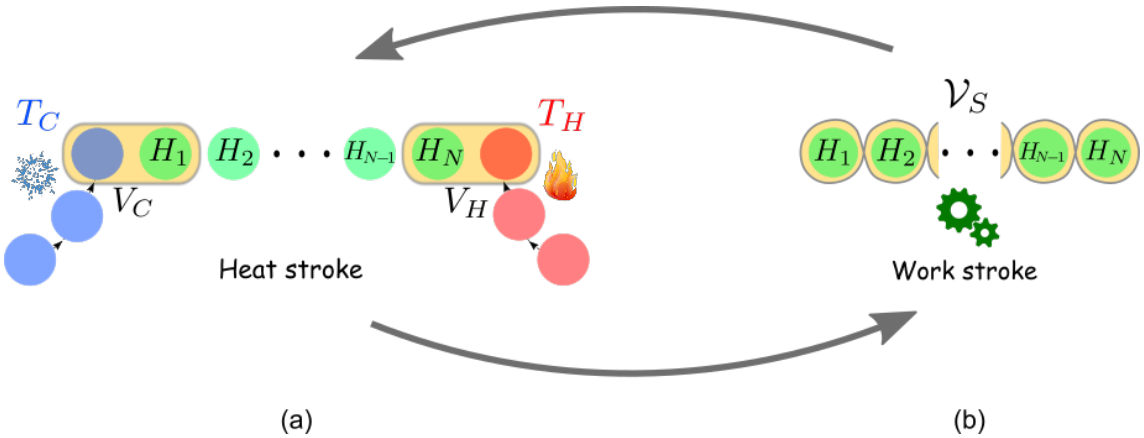


Figure 6.1: The stroboscopic two-stroke quantum heat engine is modelled as having a (a) Heat stroke ($q$) and a (b) Work stroke ($w$). In the heat stroke, the internal interactions between the sites of the system are turned off, while the boundary sites 1 and $N$ interact respectively with a cold bath at temperature $T_C$ and a hot bath at temperature $T_H$ ($T_H > T_C$). On the other hand, during the work stroke the system is disconnected from the baths. The internal interactions are turned on, represented by $\mathcal{V}_S$, putting forth an unitary evolution of the whole system. These strokes are sequentially implemented, in a cyclic fashion, as depicted by the arrows surrounding (a) and (b).

collisional model framework. They consist of streams of identical and independently prepared (iid) ancillas, each with local Hamiltonian $H_x$ and in a thermal (Gibbs) state at temperature $T_x$: $\rho_x = e^{H_x/T_x}/Z_x$ (where $x = C, H$). Obviously, according to the given denomination, the temperatures are such that $T_C < T_H$. The interaction between the bath $C$ and subsystem $S_1$ is called $V_C$, which has support only on these two parties. Likewise, $V_H$ is the interaction between subsystem $S_N$ and bath $H$, which are the two parties on which the interaction has support. Considering that the system is initialized in a random state $\rho_S$, which isn't necessarily a product state, the state of the system in the end of the heat stroke is,

$$\tilde{\rho}_S = \mathrm{tr}_{CH}\{U_q(\rho_C\rho_S\rho_H)U_q^\dagger\} =: \mathcal{E}_q(\rho_S), \tag{6.1}$$

where $U_q = e^{-iH_q\tau_q}$, the total Hamiltonian is $H_q = \sum_{i=1}^N H_i + H_C + H_H + V_C + V_H$ and $\tau_q$ is the time allocated for the heat stroke. As already done in Chapters 3 and 5, heat shall be *defined* as minus the change in energy of the ancillas [19, 21, 110],

$$Q_x := -\mathrm{tr}\{H_x(\tilde{\rho}_x - \rho_x)\}, \quad \text{with } x = C, H. \tag{6.2}$$

The state $\tilde{\rho}_x$ is the final state of the bath $C$ or $H$ after applying,

$$\tilde{\rho}_C = \mathrm{tr}_{SH}\{U_q(\rho_C\rho_S\rho_H)U_q^\dagger\},$$
$$\tilde{\rho}_H = \mathrm{tr}_{CS}\{U_q(\rho_C\rho_S\rho_H)U_q^\dagger\}.$$

The quantity in (6.2) is not in general the change in energy of the system, due to the fact that there is an inherent energy cost of turning the interactions on and off, called "*on/off work*" [20]. This quantity was discussed in Chapter 5 and according to energy

conservation, it is written as,

$$\mathcal{W}_C^{\text{on/off}} := -\mathcal{Q}_C + \text{tr}\{H_1(\tilde{\rho}_S - \rho_S)\} = -\Delta V_C, \tag{6.3}$$
$$\mathcal{W}_H^{\text{on/off}} := -\mathcal{Q}_H + \text{tr}\{H_N(\tilde{\rho}_S - \rho_S)\} = -\Delta V_H, \tag{6.4}$$

where $\Delta V_x := \text{tr}\{V_x(\tilde{\rho}_{CSH} - \rho_C\rho_S\rho_H)\}$. This definition stresses the fact that part of the energy may get stuck in the interactions. To circumvent this issue, one has to ensure *strict energy conservation*, expressed by,

$$[V_C, H_1 + H_C] = [V_H, H_N + H_H] = 0. \tag{6.5}$$

This condition implies that the map (6.1) is the concatenation of two thermal operations [57, 58, 77, 79] acting at the boundaries of the system. Once strict energy conservation is ensured, then

$$\mathcal{Q}_C := \text{tr}\{H_1(\tilde{\rho}_S - \rho_S)\}, \tag{6.6}$$
$$\mathcal{Q}_H := \text{tr}\{H_N(\tilde{\rho}_S - \rho_S)\}, \tag{6.7}$$

where, according to the adopted convention, heat is *positive* when it *enters* the system. After the interaction, the bath ancillas are thrown away, giving room for a fresh one to interact in the next heat stroke. Thus, any kind of measurement applied on the ancillas does not introduce possible measurement backreaction [56].

### 6.1.2 Work stroke

The work stroke is depicted in Fig. 6.1b. The system is now disconnected from the baths and the internal interaction Hamiltonian $\mathcal{V}_S = \sum_{i,i+1}$, where $V_{i,i+1}$ are next-neighbour interactions, is turned on. The map dictating the time evolution of the system's state is simply given by an unitary evolution,

$$\rho_S' = U_w\tilde{\rho}_S U_w^\dagger =: \mathcal{E}_w(\tilde{\rho}_S), \tag{6.8}$$

where $U_w = e^{-iH_w\tau_w}$, the total Hamiltonian during the work stroke is $H_w = \sum_{i=1}^N H_i + \mathcal{V}_S$ and $\tau_w$ is the time duration of the work stroke.

Mediated by the internal interaction, energy currents will flow through the sites, "scrambling" the change in energy at the boundaries, caused by the heat stroke. This in turn has an energy cost associated with the on/off work of switching $\mathcal{V}_S$. Work is then defined as,

$$\mathcal{W} := -\sum_{i=1}^N \text{tr}\{H_i(\rho_S' - \tilde{\rho}_S)\} = \text{tr}\{\mathcal{V}_S(\rho_S' - \tilde{\rho}_S)\}, \tag{6.9}$$

which is *positive* when there is a *decrease* of energy in the system; that is, when work is *extracted*. This definition of work is analogous to what is done in Chapter 5. In it, a boxcar function multiplies the internal interaction Hamiltonian and, since work is the integral of the rate of change of the total Hamiltonian, the result of doing this calculation is equal to (6.9).

### 6.1.3 Stroboscopic dynamics

Applying sequentially the two strokes previously described gives rise to a cycle with period $\tau = \tau_q + \tau_w$. In Fig. 6.1, the cyclic operation is depicted by the arrows surrounding the strokes. To track the state of the system after an arbitrary number of cycles, we introduce the notation $\rho_S^n$ as the state of the system after the $n^{\text{th}}$ cycle. This state, as well as the intermediate state of the system – that is, after the heat stroke and before the work stroke – $\tilde{\rho}_S^n$, will evolve according to,

$$\tilde{\rho}_S^n = \mathcal{E}_q(\rho_S^n), \tag{6.10}$$

$$\rho_S^{n+1} = \mathcal{E}_w(\tilde{\rho}_S^n) = \mathcal{E}_w \circ \mathcal{E}_q(\rho_S^n), \tag{6.11}$$

valid for $n \in \mathbb{N}$.

In a similar manner, the heat and work will inherit an upper index $n$, $\mathcal{Q}_x^n$ and $\mathcal{W}^n$. Combining Eqs. (6.6) and (6.9), the 1st law of thermodynamics for the system reads,

$$\Delta E_n = \mathcal{Q}_C^n + \mathcal{Q}_H^n - \mathcal{W}^n, \tag{6.12}$$

in which $\Delta E_n := \text{tr}\{(\sum_i H_i)(\rho_S^{n+1} - \rho_S^n)\}$ measures how much energy has entered/left the system. In agreement with what is known from classical thermodynamics, the energy of the system is a *state variable/function of state*, enabling one to write $\Delta E_n$ as a difference of average energies at consecutive strokes. However, heat and work cannot be written likewise, as they are not functions of state.

Since it corresponds to a unitary evolution, the work stroke produces no entropy. On the other hand, the heat stroke is intimately related to entropy production. Hence, using a similar expression than the one presented in Chapter 5, the entropy production is

$$\Sigma^n = \Delta S_n - \frac{\mathcal{Q}_C^n}{T_C} - \frac{\mathcal{Q}_H^n}{T_H} \geqslant 0, \tag{6.13}$$

where $\Delta S_n := S(\rho_S^{n+1}) - S(\rho_S^n)$ and $S(\rho_S^n) = -\text{tr}\{\rho_S^n \ln \rho_S^n\}$ is the von Neumann entropy of the system after $n$ cycles. The positivity of (6.13) is obtained from writing it as a sum of the mutual information generated between system and bath ancilla, with the relative entropy between the final and initial states of the ancilla [52, 68][c.f. Eq. (5.15)]. Thus, the 2nd law of thermodynamics is ensured to hold in this QHE model.

### 6.1.4 Limit-cycle

Owing to the dissipative dynamics of the system during the heat strokes, the system is expected to reach a *limit-cycle*, characterized by the states $\rho_S^*$ and $\tilde{\rho}_S^*$,

$$\rho_S^* = \mathcal{E}_w \circ \mathcal{E}_q(\rho_S^*), \tag{6.14}$$

$$\tilde{\rho}_S^* = \mathcal{E}_q(\rho_S^*). \tag{6.15}$$

The state $\rho_S^*$, which is a fixed point of the joint map $\mathcal{E}_w \circ \mathcal{E}_q$, together with its complement $\tilde{\rho}_S^*$, form the stroboscopic analog of a non-equilibrium steady-state (NESS). Illustrating the evolution of the initial state $\rho_S^0$ to the limit-cycle, Fig. 6.2 shows that, once the limit-cycle is achieved, the state of the system is constrained to the states $\rho_S^*$ and $\tilde{\rho}_S^*$.

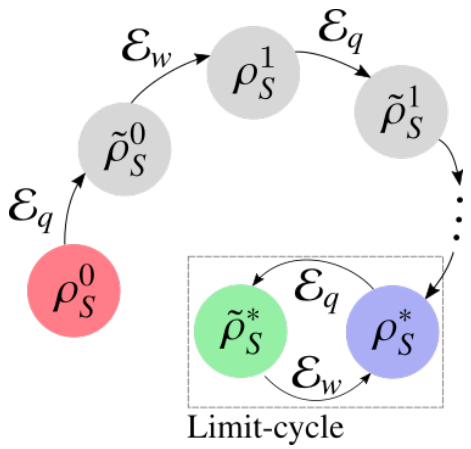


Figure 6.2: Evolution of the state of the system from its initial state $\rho_S^0$ to the limit-cycle, comprised of $\rho_S^*$ and $\tilde{\rho}_S^*$. As it is shown, the state of the system evolves stroboscopically.

The limit-cycle implies that all functions of state are $\tau$-periodic. Therefore, $\Delta E^* = \Delta S^* = 0$, meaning that the 1st and 2nd laws of thermodynamics simplify to

$$\mathcal{W}^* = Q_C^* + Q_H^*, \tag{6.16}$$

$$\Sigma^* = -\frac{Q_C^*}{T_C} - \frac{Q_H^*}{T_H}, \tag{6.17}$$

where the first equation indicates that the net heat flux in the system is converted into work. The second equation contains only terms associated with the flow of entropy at the boundaries, showing that all entropy produced by the system will flow to the environment.

Moreover, the explicit expressions for the heat and work in the limit-cycle are,

$$Q_C^* = \mathrm{tr}\{H_1(\tilde{\rho}_S^* - \rho_S^*)\}, \tag{6.18}$$

$$Q_H^* = \mathrm{tr}\{H_N(\tilde{\rho}_S^* - \rho_S^*)\}, \tag{6.19}$$

$$\mathcal{W}^* = -\sum_{i=1}^{N} \mathrm{tr}\{H_i(\rho_S^* - \tilde{\rho}_S^*)\}, \tag{6.20}$$

$$= \mathrm{tr}\{\mathcal{V}_S(\rho_S^* - \tilde{\rho}_S^*)\}. \tag{6.21}$$

During the heat stroke, the energies of the internal sites ($i = 2, \ldots, N-1$) do not change. In the limit-cycle, we find that the energy of the internal sites must remain the same also during the work stroke,

$$\mathrm{tr}\{H_i(\rho_S^* - \tilde{\rho}_S^*)\} = 0, \qquad i = 2, \ldots, N-1. \tag{6.22}$$

Therefore, in the limit-cycle, the energies of the internal subsystems become constant and all the thermodynamic quantities are determined by the subsystems at the boundaries. This characteristic of our QHE model is quite peculiar and non-intuitive.

### 6.1.5 Universal Otto efficiency

It is known that SWAP engines [36–40] always have the same Otto efficiency. Nevertheless, based on our model, we now show that this is actually more general, embracing a

broad class of problems. In fact, we prove that if the internal interaction Hamiltonian has the form,

$$\mathcal{V}_S = \sum_{i=1}^{N-1} g_{i,i+1}(L_i^\dagger L_{i+1} + L_i L_{i+1}^\dagger), \tag{6.23}$$

a two-stroke QHE will present Otto efficiency, provided the $\{L_i\}$ are eigenoperators of the local Hamiltonians and have support only on their respective subsystems. That is, $[H_i, L_i] = -\omega_i L_i$, where the transition frequency $\omega_i$ can be chosen freely for each site. However, a constraint must be applied. There must be only *one* jump operator per site, otherwise the following calculations are void.

The proof of universality of the Otto efficiency for QHEs whose internal interaction Hamiltonians are written like (6.23), goes as follows. Looking only at the work stroke, the time-evolution of the average of each local site Hamiltonian is given by Heisenberg's equation,

$$\frac{\mathrm{d}\langle H_i\rangle}{\mathrm{d}t} = i\omega_i g_{i-1,i}\langle L_{i-1}^\dagger L_i - L_{i-1}L_i^\dagger\rangle - i\omega_i g_{i,i+1}\langle L_i^\dagger L_{i+1} - L_i L_{i+1}^\dagger\rangle. \tag{6.24}$$

Which, by means of integrating in the time range $[0, \tau_w]$, when the QHE has already reached the limit-cycle, gives

$$\mathrm{tr}\{H_i(\rho_S^* - \tilde{\rho}_S^*)\} = \omega_i(J_{i-1,i} - J_{i,i+1}), \tag{6.25}$$

with:

$$J_{i,i+1} = i g_{i,i+1}\int_0^{\tau_w} \mathrm{d}t\, \langle L_i^\dagger L_{i+1} - L_i L_{i+1}^\dagger\rangle.$$

The last expressions is, in principle, applicable only to the internal sites $i = 2, \ldots, N-1$. Nonetheless, if one defines $J_{0,1} = J_{N,N+1} = 0$, then the validity is extended to all sites from 1 to $N$. A relation between the $J$'s is established when Eq. (6.22) is invoked:

$$J_{1,2} = J_{2,3} = \cdots = J_{N-1,N} \tag{6.26}$$

Using Eqs. (6.18) and (6.19), it follows that

$$Q_C^* = \omega_1 J_{1,2} = \omega_1 J_{N-1,N} = -\frac{\omega_1}{\omega_N} Q_H^*, \tag{6.27}$$

which determines that the ratio of the heat exchanged with the cold bath to the heat exchanged with the hot bath is proportional to the ratio of the characteristic energies of the sites at the boundaries.

Together with the 1st law of thermodynamics (6.16), the efficiency might be written as

$$\eta := \frac{\mathcal{W}^*}{Q_H^*} = 1 + \frac{Q_C^*}{Q_H^*}, \tag{6.28}$$

and, by applying the heat relation expressed by (6.27), one gets

$$\eta = 1 - \frac{\omega_1}{\omega_N}, \tag{6.29}$$

which is precisely the Otto efficiency [41] and our proof is finished. It is worth mentioning that this result is a direct consequence of the specific $\omega_i$'s selected by the $\mathcal{V}_S$ in (6.23).

Thus, even though the local Hamiltonians $H_i$ generally have more than one possible level transition, the filtering of a specific frequency done by $\mathcal{V}_S$ is enough to secure a universal Otto efficiency. Also, the efficiency (6.29) is *independent* of the time allocated for the strokes and, consequently, independent of the cycle period $\tau$. It is an important feature for finite-time QHEs, because optimizing power by adjusting $\tau$ will not lead to a decrease in the efficiency.

The relation (6.27) can also be applied to the entropy production (6.17),

$$\Sigma^* = \left(\frac{\omega_1}{T_C} - \frac{\omega_N}{T_H}\right)\frac{\mathcal{Q}_H^*}{\omega_N} \tag{6.30}$$

The positivity of the entropy production ($\Sigma^* \geqslant 0$) implies that $\mathcal{Q}_H^*$ must have the same sign as the term preceding it. Physically, it means that the difference of $\omega_1/T_C$ and $\omega_N/T_H$ (the "gradient of $\omega/T$") dictates the direction in which the heat flows. It differs from the Clausius statement, saying that the gradient of $1/T$ determines the heat flow ("from hot to cold"). It is explained by the fact that in our QHE model there is work involved, while in Clausius' case there was only heat. It generalizes previous results, in which the difference of occupation numbers (Bose-Einstein for bosonic chains and Fermi-Dirac for fermionic chains) is determinant for the heat flow [20, 112].

Finally, the framework just presented is viewed as a generalization of the SWAP engine [36–40]. This kind of QHE considers a system composed of solely two non-resonant qubits, thus restricting the number of sites to $N = 2$ and the global Hilbert space dimension to $d = 4$. Furthermore, it employs only full thermalization and full SWAP strokes. The former means that, while in contact with the baths, the qubits 1 and 2 thermalize to $T_C$ and $T_H$, respectively. The latter implies that the states of the qubits are swapped by the unitary $U_{\text{SWAP}} = \frac{1}{2}(1 + \sigma_x^1\sigma_x^2 + \sigma_y^1\sigma_y^2 + \sigma_z^1\sigma_z^2)$. Nevertheless, the proposed stroboscopic two-stroke QHE is more versatile. It includes systems with arbitrary $N$, as well as different geometries, and arbitrary Hilbert space dimensions of the subsystems and ancillas. Furthermore, a wide class of unitaries can be employed, enabling partial thermalization and the study of finite-time features.

## 6.2 Applications and examples

All the previous results are very general and hold for a wide class of problems. Two of them are now considered for further investigation. We start by studying the case in which the system is made of two *non-resonant* qubits. In this situation, analytical solutions are found by solving a set of difference equations for some relevant observables of the system. Second, we treat numerically systems composed of generic XYZ chains. The analysis in both situations is focused at quantifying how the output power and the number of cycles needed to converge to the limit-cycle are influenced by the parameter space.

### 6.2.1 Partial SWAP engine

Just as the SWAP engine [36–40], we consider a system composed of two non-resonant qubits, each with local Hamiltonian

$$H_i = \frac{\omega_i}{2}\sigma_z^i, \qquad i = 1, 2. \tag{6.31}$$

Furthermore, each bath is resonant with the subsystem it is interacting with,

$$H_C = \frac{\omega_C}{2}\sigma_z^C, \quad \omega_C = \omega_1. \tag{6.32}$$

$$H_H = \frac{\omega_H}{2}\sigma_z^H, \quad \omega_H = \omega_N. \tag{6.33}$$

And, since the baths are modelled as qubits, their thermal state is equal to

$$\rho_x = \begin{pmatrix} f_x & 0 \\ 0 & 1 - f_x \end{pmatrix}, \qquad x = C, H, \tag{6.34}$$

where $f_x = 1/(e^{\beta_x \omega_x} + 1)$ is the Fermi-Dirac population. For future use, we define $f_1 \equiv f_C$ and $f_2 \equiv f_H$. The interactions are all of the form (6.23), so to represent all of them compactly, we introduce the notation

$$\vartheta_{\mu,\nu} := g_{\mu,\nu}(\sigma_+^\mu \sigma_-^\nu + \sigma_-^\mu \sigma_+^\nu). \tag{6.35}$$

It means that $\mathcal{V}_S = \vartheta_{1,2}$, $V_C = \vartheta_{1,C}$ and $V_H = \vartheta_{2,H}$. By imposing the resonance conditions (6.32) and (6.33), and writing the interaction of the subsystems with the baths in the form (6.35), it is guaranteed that there is no work cost of turning on and off the interactions with the baths. However, the *non-resonance* of the qubits ($\omega_1 \neq \omega_2$) implies that during the work stroke there will be an associated work cost.

As previously stated, we shall handle this case analytically. Therefore, instead of applying the full map (4.6), we show that a closed set of difference equations for a few number of observables of the system is achievable. These observables are the $c$-number variables,

$$Z_i^n = \langle \sigma_z^n \rangle_n, \qquad i = 1, 2, \tag{6.36}$$

$$S^n = \langle \sigma_+^1 \sigma_-^2 + \sigma_-^1 \sigma_+^2 \rangle_n, \tag{6.37}$$

$$A^n = i\langle \sigma_+^1 \sigma_-^2 - \sigma_-^1 \sigma_+^2 \rangle_n. \tag{6.38}$$

where $\langle \dots \rangle_n := \mathrm{tr}\{\dots \rho_S^n\}$. The variables $Z_i^n$ correspond to the *spin component* of qubits 1 and 2, and $S^n$, $A^n$ are the correlations between them. Using these $c$-numbers, the heat and work are readily found,

$$Q_C^n = \frac{\omega_1}{2}(\tilde{Z}_1^n - Z_1^n), \tag{6.39}$$

$$Q_H^n = \frac{\omega_2}{2}(\tilde{Z}_2^n - Z_2^n), \tag{6.40}$$

$$\mathcal{W}^n = -\sum_{i=1,2} \frac{\omega_i}{2}(Z_i^{n+1} - \tilde{Z}_i^n). \tag{6.41}$$

Due to the restricted Hilbert space of the system, it's simply found that, by applying map (6.1), the $c$-number variables will evolve during the heat stroke according to

$$\tilde{Z}_i^n = (1 - \lambda)Z_i^n + \lambda Z_i^{\mathrm{th}}, \qquad i = (1, 2), \tag{6.42}$$

$$\tilde{S}^n = (1 - \lambda)[\sqrt{p}S^n + \sqrt{1 - p}A^n], \tag{6.43}$$

$$\tilde{A}^n = (1 - \lambda)[\sqrt{p}A^n - \sqrt{1 - p}S^n], \tag{6.44}$$

where $Z_i^{\text{th}} = \omega_i(2f_i - 1)/2$ is the equilibrium spin component of qubit $i$ ($i = 1, 2$) in the temperature of the bath connected to it. Moreover, other parameters were also introduced, $p = \cos^2[(\omega_1 - \omega_2)\tau_q]$ and $\lambda = [1 - \cos(2g_{CH}\tau_q)]/2$, being $g_{CH} = g_{1,C} = g_{2,H}$ the interaction strength for both baths. The parameter $\lambda$ modulates the system-bath interactions, which are *partial* SWAPs. When $\lambda = 1$, each qubit thermalizes with its respective bath ($\tilde{Z}_i^n = Z_i^{\text{th}}$). Meanwhile, the parameter $p$ quantifies how far from resonance the qubits are and "mixes" the variables $S^n$, $A^n$. Moreover, if $S^n = A^n = 0$, then also $\tilde{S}^n = \tilde{A}^n = 0$, meaning that, during the heat stroke, correlations cannot be created, only *destroyed*. This feature of the heat stroke is associated with the absence of internal interaction between the qubits.

Doing the same procedure to the work stroke, which evolves according to the map (6.8), and setting $g = g_{1,2}$, one gets

$$Z_1^{n+1} = (1 - \eta)\tilde{Z}_1^n + \eta\tilde{Z}_2^n + 2\eta\tan(\theta)\tilde{S}^n - 2\xi\tilde{A}^n, \tag{6.45}$$

$$Z_2^{n+1} = (1 - \eta)\tilde{Z}_2^n + \eta\tilde{Z}_1^n - 2\eta\tan(\theta)\tilde{S}^n + 2\xi\tilde{A}^n, \tag{6.46}$$

$$S^{n+1} = \eta\tan(\theta)(\tilde{Z}_1^n - \tilde{Z}_2^n) + (1 - 2\eta\tan^2\theta)\tilde{S}^n + 2\xi\tan(\theta)\tilde{A}^n, \tag{6.47}$$

$$A^{n+1} = \xi(\tilde{Z}_1^n - \tilde{Z}_2^n) - 2\xi\tan(\theta)\tilde{S}^n + (1 - 2\eta\sec^2\theta)\tilde{A}^n, \tag{6.48}$$

where $\eta = (2g^2/\omega_r^2)[1 - \cos(\omega_r\tau_w)]$, $\xi = (g/\omega_r)\sin(\omega_r\tau_w)$ and $\tan(\theta) = (\omega_1 - \omega_2)/2g$ (not to confuse $\eta$ with the efficiency). Furthermore, $\omega_r := \sqrt{4g^2 + (\omega_1 - \omega_2)^2}$ is the Rabi frequency which drives the time-evolution of the *dressed states* of the system. The three parameters are related by $\xi^2 = \eta(1 - \eta\sec^2\theta)$.

We note in Eqs. (6.45) and (6.46) that the parameter $\eta$ implements a partial SWAP onto the qubits. Differently from $\lambda$ in the heat stroke, this can never be a full SWAP, that is, we can never achieve $\eta = 1$. This is attested by the fact that, using the aforementioned relation between the parameters, $\eta < \cos^2\theta$. It is a consequence of the fact that the qubits are non-resonant. If they were resonant, the parameter $\eta$ would then be allowed to be equal to 1, since $\omega_r = 2g$ for resonant qubits ($\omega_1 = \omega_2$). Nevertheless, the QHE would also stop working, because the lack of resonance between the qubits is what enables the extraction of power. Like $p$, the parameter $\theta$ is related to the frequency mismatch of the qubits. One difference though, is that $\theta$ is independent of the interaction time.

Interestingly, one also notes by looking at Eqs. (6.45)–(6.48) that the local populations ($Z_i^n$) and correlations ($S^n$, $A^n$) are mixed during the work stroke. This is caused by the parameters $\theta$ and $\xi$ in a rather intricate way. Related to the previous statement on the resonance of the qubits, even in the case that $\theta = 0$, that is, resonant qubits, the blending persists, since $\xi \neq 0$.

Casting the $c$-number variables into a vector,

$$\boldsymbol{x}_n = \begin{pmatrix} Z_1^n \\ Z_2^n \\ S^n \\ A^n \end{pmatrix},$$

we can write a set of *vector difference equations* with respect to $\boldsymbol{x}_n$, using Eqs. (6.42)–(6.44) and Eqs. (6.45)–(6.48). The result is

$$\tilde{\boldsymbol{x}}_n = J\boldsymbol{x}_n + S, \tag{6.49}$$

$$\boldsymbol{x}_{n+1} = D\tilde{\boldsymbol{x}}_n = DJ\boldsymbol{x}_n + DS. \tag{6.50}$$

The entries of the $4 \times 4$ matrices $J$ and $D$, and the vector $S$ are combinations of the set of parameters previously presented, determined by Eqs. (6.42)–(6.44) and Eqs. (6.45)–(6.48). The entries of the vector $S$ are simply given by Eq. (6.42),

$$S = \lambda \begin{pmatrix} 2f_C - 1 \\ 2f_H - 1 \\ 0 \\ 0 \end{pmatrix}.$$

Furthermore, the matrices $J$ and $D$ are given by,

$$J = (1-\lambda) \begin{pmatrix} 1 & 0 & 0 & 0 \\ 0 & 1 & 0 & 0 \\ 0 & 0 & \sqrt{p} & \sqrt{1-p} \\ 0 & 0 & -\sqrt{1-p} & \sqrt{p} \end{pmatrix},$$

$$D = \begin{pmatrix} 1-\eta & \eta & 2\eta\tan(\theta) & -2\xi \\ \eta & 1-\eta & -2\eta\tan(\theta) & 2\xi \\ \eta\tan(\theta) & -\eta\tan(\theta) & 1-2\eta\tan^2\theta & 2\xi\tan(\theta) \\ \xi & -\xi & -2\xi\tan(\theta) & 1-2\eta\sec^2\theta \end{pmatrix}.$$

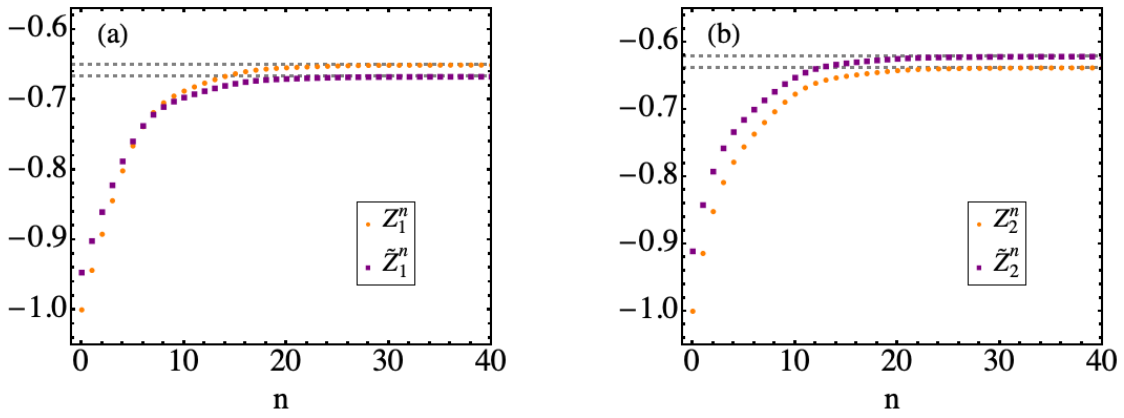


Figure 6.3: Plots of the local populations (a) $Z_1^n$, $\tilde{Z}_1^n$ and (b) $Z_2^n$, $\tilde{Z}_2^n$ with respect to the number $n$ of performed cycles. The gray dashed lines represent the stationary values $Z_i^*$, $\tilde{Z}_i^*$. The values of the parameters used to obtain these plots are: $\lambda = 0.2$, $p = 0.99$, $T_C = 0.4$, $T_H = 0.8$, $\omega_1 = 0.75$, $\omega_2 = 1.0$, $g = 0.3$ and times $\tau_q = \tau_w = 1.0$ fixed. The system is initially in a product state of the qubits, each one in its own ground state.

The general solution of $\boldsymbol{x}_n$ in (6.50) is equal to [113]

$$\boldsymbol{x}_n = (DJ)^n \boldsymbol{x}_0 + \sum_{r=0}^{n-1} (DJ)^{n-r-1} (DS). \tag{6.51}$$

The first term on the RHS of (6.51) is directly related to the transient regime, although not the only one responsible for it. On the other hand, the second term on the RHS of the same equation is the only one that survives in the stationary regime. We also see that the matrix $DJ$ is present in both terms, hence being the main object responsible for the

dynamics of $\boldsymbol{x}_n$. The steady-state value of $\boldsymbol{x}_n$ is found by imposing $\boldsymbol{x}_{n+1} = \boldsymbol{x}_n = \boldsymbol{x}^*$ in (6.50), whose result is

$$\boldsymbol{x}^* = (I_4 - DJ)^{-1} DS, \tag{6.52}$$

where $I_4$ is the $4 \times 4$ identity matrix. The explicit expression of $\boldsymbol{x}^*$ is quite clumsy, but easily obtained using, for example, *mathematica*.

In Figs. 6.3 and 6.4, plots of the evolution of the $c$-number variables, for specific values of the parameters, are presented. First, in Fig. 6.3, one finds the plots of the local populations $Z_i^n$ and $\tilde{Z}_i^n$. Clearly they depart from an initial value at $n = 0$ and converge to steady-state values, alternating between $Z_i^*$ and $\tilde{Z}_i^*$. Then, in Fig. 6.4, the plots of the correlations $S^n$, $\tilde{S}^n$, $A^n$ and $\tilde{A}^*$ are shown. Since the initial state was chosen to be a product state, there are no correlations at $n = 0$, which can be seen in both plots. Like the populations, the correlations also converge to steady-state values, which constrain the time-evolution to only two values. The bouncing back and forth between two values of the $c$-number variables is a signature of the limit-cycle (Fig. 6.2). This behavior can be, at a certain extent, viewed as an analogy of the up and down movement of an engine piston.

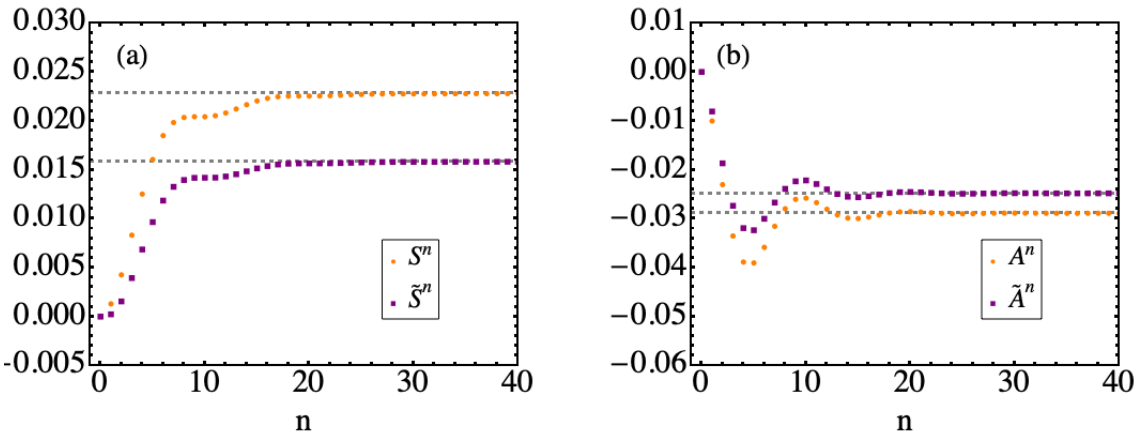


Figure 6.4: Plots of the correlations (a) $S^n$, $\tilde{S}^n$ and (b) $A^n$, $\tilde{A}^n$ with respect to the number $n$ of performed cycles. The gray dashed lines represent the stationary values $S^*$, $\tilde{S}^*$, $A^*$, $\tilde{A}^*$. The values of the parameters used to obtain these plots and the initial state of the system are the same as in Fig. 6.3.

Having obtained the evolution of all the entries of $\boldsymbol{x}_n$ and $\tilde{\boldsymbol{x}}_n$, the heat and work are calculated using Eqs. (6.39)–(6.41). These quantities are plotted in Fig. 6.5. As it can be seen, the heat and work converge to non-zero values, attested by the values put alongside the plots in the stationary regime. The steady-state value of the work is positive, which, in our convention, means that work is *extracted* and thus, the system is indeed working as a heat engine. There is a deep contrast between the transient and stationary regimes. In the beginning of the QHE operation, the work is quite small, while the heat exchanged with the baths is much larger. Then, after a few cycles, the work attains a value even higher than its steady-state value, and the heat decreases considerably. And finally, after that all internal energies have accommodated, the system enters the limit-cycle.

Noting that the QHE takes a certain number of cycles to attain the limit-cycle, we now proceed to quantify this number, which is proportional to the *relaxation time*. As already shown, the matrix $DJ$ dictates the dynamics of $\boldsymbol{x}_n$. Therefore, the relaxation time

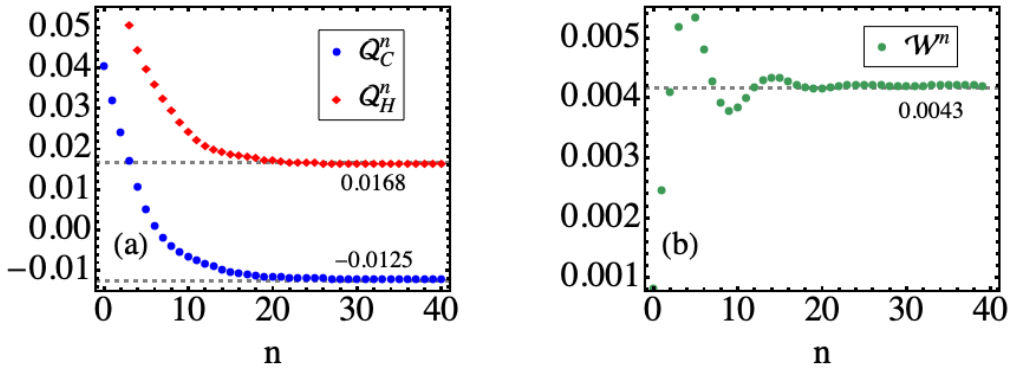


Figure 6.5: Values of (a) $Q_C^n$, $Q_H^n$ and (b) $\mathcal{W}^n$ as functions of the number of cycles $n$. The parameters are considered to have the same values as in Fig. 6.3. The steady-state value of each quantity is depicted by the numbers present in the plot.

is associated with the eigenvalues of $DJ$. This matrix appears in powers in (6.51), which imposes the condition that all eigenvalues of $DJ$ must have magnitude smaller than one, for the sake of stability. Then, large eigenvalues persist for much more time than small ones, due to the fact that they appear in powers of $n$. The closer an eigenvalue is from having magnitude equal to one, the longer it will take for the system to relax to the limit-cycle. As a consequence, the relaxation time is determined by the largest eigenvalue of $DJ$,

$$\mu := \max|\text{eigs}(DJ)|. \tag{6.53}$$

The matrix $DJ/(1-\lambda)$ can be verified to have an eigenvalue 1. Since all other eigenvalues must be smaller than one, we conclude that the maximum eigenvalue is $\mu = 1-\lambda$. It means that the heat stroke determines how long the QHE takes to attain the limit-cycle. It would be expected from the dissipative nature of the heat stroke, that is, by exchanging energy with an environment, the internal energies are able to relax to a certain value, as seen in Chapter 5.

Lastly, now we deal with the output power,

$$\mathcal{P}^* = \frac{\mathcal{W}^*}{\tau_q + \tau_w}, \tag{6.54}$$

whose dependence on $\tau_q$ and $\tau_w$ is not only in its denominator, but also in $\mathcal{W}^*$ itself. Manipulating the previous difference equations, one finds an explicit expression for $\mathcal{W}^*$,

$$\mathcal{W}^* = \frac{2\eta(2-\lambda)\lambda(f_C - f_H)(\omega_1 - \omega_2)}{\lambda^2 + 2(1-\lambda)\Big\{(1+\eta) - \sqrt{p}[1-\eta(\tan^2\theta + \sec^2\theta)] + 2\sqrt{1-p}\,\xi\tan\theta\Big\}}. \tag{6.55}$$

The numerator of (6.55) makes it evident when the work vanishes: (i) $\lambda = 0$, that is, the coupling with the baths vanish; (ii) $\eta = 0$, meaning that the internal couplings of the system go to zero; (iii) $\omega_1 = \omega_2$, that is, the qubits are resonant; and (iv) $f_H = f_C$, which is equivalent to $\omega_1/\omega_2 = T_C/T_H$. Furthermore, the sign of (6.55) is determined by the product $(f_C - f_H)(\omega_1 - \omega_2)$. Fixing the temperatures $T_C < T_H$ and knowing that $f_x$ is monotonically decreasing with respect to $\omega_x/T_x$, the product is positive if, and only if,

$f_C < f_H$ and $\omega_1 < \omega_2$. These two inequalities define the range for the system to work as an engine,

$$\frac{T_C}{T_H} \leqslant \frac{\omega_1}{\omega_2} \leqslant 1. \tag{6.56}$$

Below the lower bound the machine works as a refrigerator ($Q_C^* > 0$, $Q_H^* < 0$, $\mathcal{W}^* < 0$) and above the upper bound it operates as an oven/heat accelerator ($Q_C^* < 0$, $Q_H^* > 0$, $\mathcal{W}^* < 0$) [20]. One more interesting feature about (6.55) is that, when there is full thermalization ($\lambda = 1$), the expression reduces to

$$\mathcal{W}^* = 2\eta(f_C - f_H)(\omega_1 - \omega_2),$$

which turns out to be very similar to the work delivered by the SWAP engine [36–40]. The difference, though, is that SWAP engines implement full SWAPs, otherwise saying $\eta = 1$. This limit, as discussed before, is not achievable in our model, which comports partial SWAPs ($0 < \eta < 1$).

Finally, by plugging Eq. (6.55) into Eq. (6.54), we plot $\mathcal{P}^*$ as a function of the times $\tau_q$ and $\tau_w$ in Fig. 6.6. The result is quite curious, presenting two patterns almost symmetric with respect to $\tau_w = 10$. The lower pattern distinguishes itself by having a higher peak. The behaviour shown in the plot of the output power is related to the oscillatory dependence of $\lambda$, $\eta$ and $p$ on the interaction times $\tau_q$ and $\tau_w$. Very important to this analysis is the fact that, as this model of partial SWAP engine falls into the condition presented in Section 6.1.5, its efficiency will always be equal to the Otto efficiency, regardless of the values of $\tau_q$, $\tau_w$ or any other parameter. It constitutes an advantage of the model, enabling one to optimize the QHEs output power, without affecting the the efficiencies.

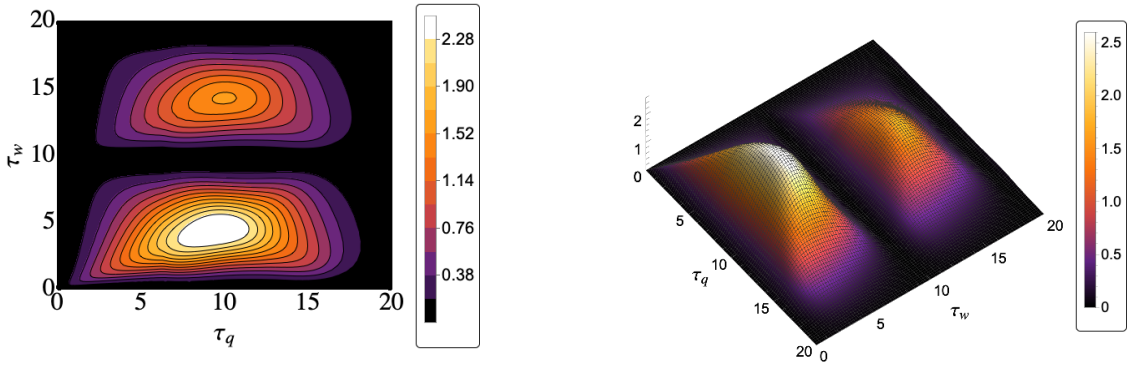


Figure 6.6: Plots of the output power $\mathcal{P}^*$ as a function of the interaction times $\tau_q$ and $\tau_w$. It is presented both as a contour plot (left) and as a 3D plot (right). The plots are scaled by $10^3$. The parameters assume the values: $\omega_1 = 0.75$, $\omega_2 = 1.0$, $T_C = 0.4$, $T_H = 0.8$, $g = g_{CH} = 0.3$.

### 6.2.2 Generic XYZ chain

In this section we study a QHE having as working fluid a spin chain of $N$ sites. Each spin has a local Hamiltonian $H_i = \frac{1}{2}\omega_i\sigma_i^z$. The baths are modelled as before, that is,

single spins with Hamiltonian $H_b = \frac{1}{2}\omega_b\sigma_b^z$ ($b = C, H$) interacting sequentially with the boundary subsystems. The baths are resonant with their respective spins ($\omega_C = \omega_1$, $\omega_H = \omega_N$) and the system-bath interactions ($1C$, $NH$) are of the same form as (6.35). These two factors imply that there is no energy cost of switching the interactions with the baths, namely $\mathcal{W}_{\text{on/off}} = 0$. Nevertheless, the internal interaction Hamiltonian of the system assumes the generic form

$$\mathcal{V}_S = \sum_{i=1}^{N-1}\left\{J_x\sigma_i^x\sigma_{i+1}^x + J_y\sigma_i^y\sigma_{i+1}^y + J_z\sigma_i^z\sigma_{i+1}^z\right\}. \tag{6.57}$$

This generic interaction, combined with the size of the spin chain, add more layers of complexity to the endeavour of solving the dynamical equations that dictate the stroboscopic evolution of the system. Thus, we shall treat the problem numerically, since trying to find a set of difference equations in these more complex cases is unbearable.

The analysis of this QHE will focus on two cases: (i) the XX model ($J_x = J_y = J$, $J_z = 0$) and (ii) the XXZ chain ($J_x = J_y = J$, $J_z = J\Delta$). We consider chains with size $N < 6$, such that exact diagonalization can be achieved. The plots of $\mathcal{Q}_x^n$ and $\mathcal{W}^n$ as functions of $n$, and the plot of $\mathcal{P}^*$ with respect to $\lambda$ – which itself is a function of $\tau_q$ – for the XX model and the XXZ chain are shown in Figs. 6.7 and 6.8, respectively.

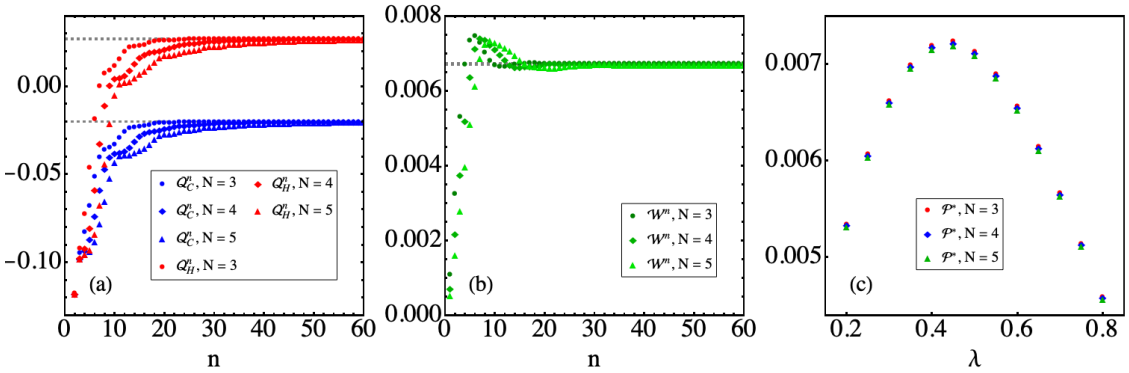


Figure 6.7: XX model. Plots of (a) $\mathcal{Q}_x^n$, (b) $\mathcal{W}^n$ with respect to $n$, and (c) $\mathcal{P}^*$ as a function of $\lambda$ (which is itself a function of $\tau_q$). The plots (a) and (b) show the convergence of the heat and the work toward their respective steady-state values. On the other hand, the plot (c) depicts how the parameter $\lambda$ influences the value of $\mathcal{P}^*$. In all three cases, the values are obtained for $N = 3, 4, 5$. The local frequencies $\omega_i$ were chosen to interpolate linearly between $\omega_1 = 1.5$ and $\omega_N = 2.0$, $J_x = J_y = 0.8$, $J_z = 0$, $T_C = 0.2$, $T_H = 0.8$ and $\tau_w = 0.25$.

Starting with the XX model (Fig. 6.7), we note that, both $\mathcal{Q}_x^n$ (Fig. 6.7a) and $\mathcal{W}^n$ (Fig. 6.7b) present the same steady-state values, independently of the chain size. However, the transient dynamics differs for each value of $N$. By changing $\lambda$, the output power $\mathcal{P}^*$ (Fig. 6.7c) suffers a feeble disturbance, as well as the $\lambda$ for which $\mathcal{P}^*$ is maximum. These results are explained by a symmetry property of the XX model. By changing the variables $\sigma_x \to \sigma_+ + \sigma_-$ and $\sigma_y \to -i(\sigma_+ - \sigma_-)$, it turns out that $\mathcal{V}_S$ is of the same form as Eq. 6.35. Thus, for whatever size of the chain, it would be expected that similar results than $N = 2$ would hold, due to this symmetry of the internal interaction Hamiltonian.

On the other hand, the XXZ chain (Fig. 6.8) presents a different behaviour when compared to the XX model. For increasing $N$, the heat intake from the hot bath ($\mathcal{Q}_H^n$) is

slightly decreased (Fig. 6.8a). Furthermore, the extracted work $\mathcal{W}^n$ gets lower for larger chains (Fig. 6.8b). And finally, the output power $\mathcal{P}^*$ (Fig. 6.8c) is inversely proportional to $N$, hence larger chains deliver less power. The $\lambda$ for which the output power is maximum also changes, as $N$ increases, it's weakly shifted to greater values.

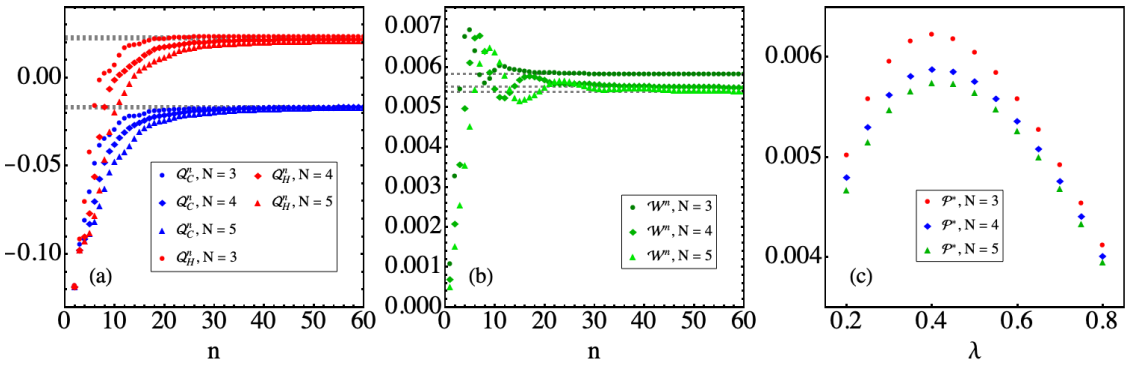


Figure 6.8: XXZ chain. Plots of (a) $\mathcal{Q}_x^n$, (b) $\mathcal{W}^n$ with respect to $n$, and (c) $\mathcal{P}^*$ as a function of $\lambda$ (which is itself a function of $\tau_q$). The plots (a) and (b) show the convergence of the heat and the work toward their respective steady-state values. On the other hand, the plot (c) depicts how the parameter $\lambda$ influences the value of $\mathcal{P}^*$. In all three cases, the values are obtained for $N = 3, 4, 5$. The local frequencies $\omega_i$ were chosen to interpolate linearly between $\omega_1 = 1.5$ and $\omega_N = 2.0$, $J_x = J_y = 0.8$, $J_z = 0.7$, $T_C = 0.2$, $T_H = 0.8$ and $\tau_w = 0.25$.

## 6.3 Continuous-time limit

Following the appropriate approximations and criteria, the stroboscopic two-stroke QHE can be shown to be equivalent to a continuous-time QHE, whose dynamics is dictated by Local Master Equations (LME)[2] [20]. The proof, which relies on coarse-graining the time scale $\tau$, is similar to what is done in Chapter 5, but containing two baths instead of one. Hence,

$$\lim_{\tau\to 0}\frac{\rho_S^{n+1}-\rho_S^n}{\tau} = \frac{\mathrm{d}\rho_S}{\mathrm{d}t} = -i[H_w,\rho_S] + \mathcal{D}_C(\rho_S) + \mathcal{D}_H(\rho_S), \tag{6.58}$$

where $H_w = \sum_i H_i + \mathcal{V}_S$ and the $\mathcal{D}_x$ ($x = C, H$) are dissipators in Lindblad form considering only one resonant mode ($k = 1$) for the sake of simplicity,

$$\mathcal{D}_C(\rho_S) = \gamma_C^-\left[L_1\rho_S L_1^\dagger - \frac{1}{2}\left\{L_1^\dagger L_1,\rho_S\right\}\right] + \gamma_C^+\left[L_1^\dagger\rho_S L_1 - \frac{1}{2}\left\{L_1 L_1^\dagger,\rho_S\right\}\right],$$
$$\mathcal{D}_H(\rho_S) = \gamma_H^-\left[L_N\rho_S L_N^\dagger - \frac{1}{2}\left\{L_N^\dagger L_N,\rho_S\right\}\right] + \gamma_H^+\left[L_1^\dagger\rho_S L_N - \frac{1}{2}\left\{L_N L_N^\dagger,\rho_S\right\}\right],$$

with $\gamma_x^- := |g_{CH}|^2\,\mathrm{tr}\{A_x A_x^\dagger\rho_x\}$ and $\gamma_x^+ := |g_{CH}|^2\,\mathrm{tr}\{A_x^\dagger A_x\rho_x\}$ being the decay rates modulated by the baths and their eigenoperators $[H_x, A_x] = -\omega_x A_x$. The system-bath coupling

[2] These are also known as "boundary driven master equations".

strength $g_{CH}$ is considered to be the same for both baths. Taking, as an example, the case in which the system and the baths are composed of qubits, we have that: $L_i \to \sigma^i_-$, $L_i^\dagger \to \sigma^i_+$ $(i = 1, \ldots, N)$, $\gamma^-_x \to |g_{CH}|^2 (1 - f_x)$ and $\gamma^+_x \to |g_{CH}|^2 f_x$. Thus, one sees that the dissipators act only *locally* at the boundaries, such that (6.58) is said to be a LME.

Although LMEs were previously thought to violate the 2nd law of thermodynamics [112], it is shown in Ref. [20] that (6.58) fixes this issue, making the reconciliation of LMEs and thermodynamics. This is done by studying whether local or/and global detailed balance hold. For the system-bath interactions we have

$$[H_1 + H_C, V_C] = [H_N + H_H, V_H] = 0,$$

because we impose strict energy conservation. Therefore, local detailed balance holds. However, when we look at the whole QHE, it follows that, in general,

$$[\sum_i H_i + \mathcal{V}_S + H_C + H_H, V_C + V_H] = [\mathcal{V}_S, V_C + V_H] \neq 0.$$

It means that global detailed balance *doesn't* hold. Consequently, there is a work cost associated with the fact that the internal interactions don't commute with the system-bath interactions. Therefore, if one finds that heat is flowing from the cold bath to the hot bath, it is due to a work input and the 2nd law is saved.

From (6.58), it can be shown that the heat rate and the work rate are given by [20]

$$\dot{Q}_C = \omega_1 \Big( \gamma^+_C \langle L_1 L_1^\dagger \rangle - \gamma^-_C \langle L_1^\dagger L_1 \rangle \Big), \tag{6.59}$$

$$\dot{Q}_H = \omega_N \Big( \gamma^+_H \langle L_N L_N^\dagger \rangle - \gamma^-_H \langle L_N^\dagger L_N \rangle \Big), \tag{6.60}$$

$$\begin{aligned} \dot{\mathcal{W}} = -\frac{1}{2} \Big\{ & \gamma^-_C \, \langle L_1^\dagger F_1 + F_1^\dagger L_1 \rangle - \gamma^+_C \langle F_1 L_1^\dagger + L_1 F_1^\dagger \rangle \\ & + \gamma^-_H \, \langle L_N^\dagger F_N + F_N^\dagger L_N \rangle - \gamma^+_H \langle F_N L_N^\dagger + L_N F_N^\dagger \rangle \Big\}, \end{aligned} \tag{6.61}$$

where $F_i := [\mathcal{V}_S, L_i]$, attesting that the work depends directly on the internal interaction. For both cases of system composed of qubits and quantum harmonic oscillators, it is found that Eqs. (6.59)–(6.61) establish three possible operation modes for the model, as shown in Tab. 6.1. The condition required for operating in the engine mode is the same as in Eq. (6.56). On top of that, the refrigerator and the oven/heat accelerator regimes are consistent with what was stated below Eq. (6.56).

| **Operation mode** | $\dot{Q}_C$ | $\dot{Q}_H$ | $\dot{\mathcal{W}}$ | Conditions |
|---|---|---|---|---|
| **Refrigerator** | $> 0$ | $< 0$ | $< 0$ | $\frac{\omega_1}{\omega_N} < \frac{T_C}{T_H}$ |
| **Engine** | $< 0$ | $> 0$ | $> 0$ | $\frac{T_C}{T_H} \leqslant \frac{\omega_1}{\omega_N} \leqslant 1$ |
| **Oven/Heat accelerator** | $< 0$ | $> 0$ | $< 0$ | $\omega_1 > \omega_N$ |

Table 6.1: Different operation modes of the continuous-time limit of the stroboscopic QHE, whose dynamics is dictated by a Local Master Equation (LME).

The continuous-time limit is analogous to when one watches a process repeated at a rate faster than the persistence of vision [3]. As a consequence, the frames arriving at one's

[3] The interval of time in which an image continues to be seen by the human eye after the external source has been turned off.

eyes cannot been distinguished and then the movement will be perceived as being smooth. For example, car engines are stroke-based. However, they happen so fast that we cannot distinguish between the strokes. In this coarse-grained time scale, the car engine is seen as a continuous-time engine. In conclusion, it is worth mentioning that the equivalence of stroke-based QHEs and continuous-time QHEs is not always just a matter of time scale, as it is in our case. Sometimes other considerations must be taken into account. In Ref. [114], the authors demonstrate that if quantum coherence is erased by dephasing from one cycle to the other, the equivalence isn't possible.

# Chapter 7

# Other approaches to finite-time quantum heat engines

## 7.1 Shortcut-to-adiabaticity

Energy efficiency is a very important aspect to be addressed for present and future technologies. Its relevance lies on the fact that natural resources are finite, thus finding a wiser way to allocate them is imperative for sustained development. Energy efficiency can be translated to delivering more energy output for the same energy input, or decreasing the energy input without losing energy output. Both ways of thinking about energy efficiency are complementary and serve the same purpose.

When dealing with finite-time (quantum) heat engines, one must also keep in mind the trade-off between efficiency and power output, since increasing the latter could mean decreasing significantly the former. One possible alternative to tackle this issue is by using techniques generically known as shortcuts-to-adiabaticity [34, 115, 116]. The result of applying these methods is that the final state of evolution of a finite-time nonadiabatic process mimics the final state of a slow adiabatic process, raising the efficiency of the engine.

### 7.1.1 Concept

To get a grasp of the basic idea behind shortcuts to adiabaticity, consider a system with $n$ nondegenerate eigenstates, as shown in Fig. 7.1. At time $t = 0$ the system is in a given state $|\psi(0)\rangle = \sum_n c_n(0)\,|n(0)\rangle$, such that the populations of its energy levels are equal to $p_n(0) = |c_n(0)|^2$. Then, the Hamiltonian of the system $H_0(t)$, which satisfies

$$H_0(t)\,|n(t)\rangle = E_n(t)\,|n(t)\rangle\,, \tag{7.1}$$

drives the system to a final state $|\psi(t)\rangle = \sum_n c_n(t)\,|n(t)\rangle$, with new populations $p_n(t) = |c_n(t)|^2$. In general,

$$p_n(t) \neq p_n(0), \qquad \forall t \in \mathfrak{R}_{>0},$$

which means that transitions may take place between energy levels, a situation which evidences nonadiabaticity. The adiabatic theorem [101] then presents an approximation

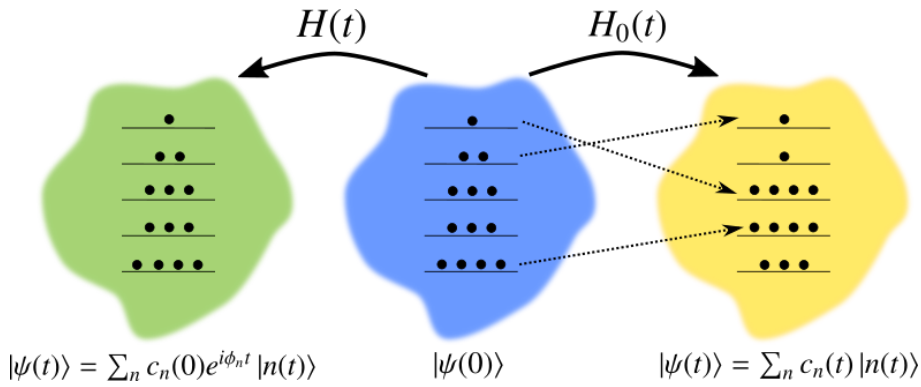


Figure 7.1: Time evolution of the state $|\psi(t)\rangle$ of a system in two situations: (right) Nonadiabatic driving and (left) Transitionless driving, with $\phi_n = \theta_n + \gamma_n$.

for slow driving,

$$|\psi(t)\rangle \to \sum_n c_n(0) e^{i\theta_n t} e^{i\gamma_n t} |n(t)\rangle = \sum_n c_n(0) |\psi_n(t)\rangle\,, \tag{7.2}$$

$$\theta_n = -\int_0^t dt' E_n(t'), \tag{7.3}$$

$$\gamma_n = i\int_0^t dt' \langle n(t')|\dot{n}(t')\rangle\,, \tag{7.4}$$

such that the populations are constant at any time, since the states pick up only a phase $\phi_n = \theta_n + \gamma_n$, where $\theta_n$ is the dynamic phase factor and $\gamma_n$ is the geometric phase[1],

$$p_n(t) = |c_n(0)e^{i\theta_n t} e^{i\gamma_n t}|^2 = |c_n(0)|^2 \equiv p_n(0).$$

What if the drive is inherently nonadiabatic, discarding the possibility of making approximations? In Ref. [115] an alternative was proposed. It starts asking what Hamiltonian $H(t)$ drives exactly the result of the adiabatic theorem,

$$H(t)\,|\psi_n(t)\rangle = i\frac{\mathrm{d}}{\mathrm{d}t}\,|\psi_n(t)\rangle\,, \tag{7.5}$$

ensuring that the eigenstates of $H_0(t)$ pick up only phases and the populations are unchanged (Fig. 7.1). The unitary operator $U(t)$ that describes the dynamics of $H(t)$ must fulfill

$$H(t)U(t) = i\frac{\mathrm{d}}{\mathrm{d}t}U(t). \tag{7.6}$$

A possible choice of $U(t)$ is equal to,

$$U(t) = \sum_n e^{i\theta_n t} e^{i\gamma_n t} |n(t)\rangle\langle n(0)|\,, \tag{7.7}$$

what leads to the Hamiltonian,

$$\begin{aligned} H(t) &= \sum_n E_n(t)\,|n(t)\rangle\langle n(t)| + i\sum_n (|\dot{n}(t)\rangle\langle n(t)| - \langle n(t)|\dot{n}(t)\rangle\,|n(t)\rangle\langle n(t)|) \\ &= \sum_n E_n(t)\,|n(t)\rangle\langle n(t)| + i\sum_{m\neq n}\sum_n \frac{|m(t)\rangle\langle m(t)|\,\dot{H}_0(t)\,|n(t)\rangle\langle n(t)|}{E_n(t) - E_m(t)}. \end{aligned} \tag{7.8}$$

[1] Also known as Berry phase.

By making the identifications,

$$H_0(t) = \sum_n E_n(t)\,|n(t)\rangle\langle n(t)| \tag{7.9}$$

$$H_{CD}(t) := i\sum_{m\neq n}\sum_n \frac{|m(t)\rangle\langle m(t)|\,\dot{H}_0(t)\,|n(t)\rangle\langle n(t)|}{E_n(t)-E_m(t)}, \tag{7.10}$$

we note that, in order to make a system with a certain nonadiabatic Hamiltonian $H_0(t)$ preserve its populations and effectively evolve adiabatically, one has to add a Hamiltonian $H_{CD}(t)$, where "CD" means "counterdiabatic" [34], for it is one of the possible shortcut methods.

### 7.1.2 Example: quantum Otto heat engine

An example of application of the procedure shown above is the quantum version of the Otto cycle (Section 2.2). In this section, we discuss in detail the studies of Ref. [34]. We consider a time-dependent quantum harmonic oscillator as the working fluid,

$$H_0(t) = \frac{p^2}{2m} + \frac{1}{2}m\Omega_t^2 q^2, \tag{7.11}$$

where $m$ is the mass term, $\Omega_t \equiv \Omega(t)$ is the driving frequency and $p$, $q$ are the momentum and position operators, respectively[2]. Note that when $\Omega_t$ is time-dependent, some subtleties arise in recasting Eq. (7.11) in terms of bosonic operators. This is discussed in Appendix B.

Similar to the classical Otto cycle, four strokes are implemented: (a) isentropic expansion, (b) cold isochoric, (c) isentropic compression and (d) hot isochoric. The working fluid starts with a driving frequency $\Omega_1$ and follows, during a time $\tau_a$, a certain protocol with final driving frequency $\Omega_2$. Afterwards, it is put in contact with a cold bath at temperature $T_C$ during a time interval $\tau_b$, without changing the driving frequency. Then, in a time $\tau_c$, the driving frequency is brought back to $\Omega_1$. And finally, the working fluid interacts with a hot bath at temperature $T_H$ during a time $\tau_d$, remaining constant the driving frequency. As it is common in the literature [104, 117], the isochoric processes are assumed to be much faster than the isentropic ones, that is, $\tau_b, \tau_d \ll \tau_a, \tau_c$, and we shall also set $\tau_a = \tau_c = \tau$. Therefore, the time period of the cycle is equal to $\tau_{\text{cycle}} = 2\tau$.

During the isentropic processes, no heat is exchanged with the baths, and hence energy variations are identified as work. In the beginning of these strokes, the working fluid is thermalized with respect to the baths, so that it is in a thermal equilibrium state and its energy becomes

$$E_1 = \frac{\Omega_1}{2}\coth\left(\frac{\Omega_1}{2T_H}\right), \tag{7.12}$$

$$E_2 = \frac{\Omega_2}{2}\coth\left(\frac{\Omega_2}{2T_C}\right). \tag{7.13}$$

By defining an adiabaticity parameter $\Gamma$ as the ratio between the energy in the end of the isentropic stroke and the corresponding equilibrium energy [118], the extracted work in

[2] As quadrature operators, they satisfy $[q, p] = i$.

each stroke is written as [119],

$$\mathcal{W}_a = \frac{1}{2}(\Omega_1 - \Omega_2\Gamma_a)\coth\left(\frac{\Omega_1}{2T_H}\right), \tag{7.14}$$

$$\mathcal{W}_c = \frac{1}{2}(\Omega_2 - \Omega_1\Gamma_c)\coth\left(\frac{\Omega_2}{2T_C}\right), \tag{7.15}$$

such that it is positive (negative) when it increases (decreases) the energy of the working fluid. In a similar manner, the heat exchanged during the hot and cold isochores are equal to,

$$Q_H = \frac{\Omega_1}{2}\left[\coth\left(\frac{\Omega_1}{2T_H}\right) - \Gamma_c\coth\left(\frac{\Omega_2}{2T_C}\right)\right], \tag{7.16}$$

$$Q_C = \frac{\Omega_2}{2}\left[\coth\left(\frac{\Omega_2}{2T_C}\right) - \Gamma_a\coth\left(\frac{\Omega_1}{2T_H}\right)\right], \tag{7.17}$$

and they are positive (negative) for heat intake (output). The indices in $\Gamma$ are simply labels to identify whether it's an isentropic expansion ("a") or an isentropic compression ("c").

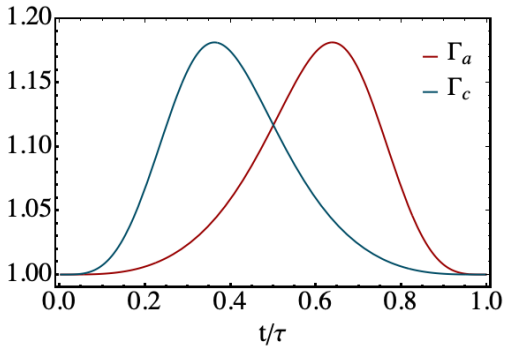


Figure 7.2: Adiabaticity parameters of the isentropic expansion ($\Gamma_a$) and the isentropic compression ($\Gamma_c$), with respect to the normalized time $t/\tau$. Plot for $\Omega_1 = 2.5$, $\Omega_2 = 1.3$, $\tau = 0.7$.

Now we implement the shortcut-to-adiabaticity technique. Following the result shown in Eq. (7.8), we must add a Hamiltonian $H_{CD}(t)$ that will prevent the populations of the energy levels from changing during the isentropic strokes. A possible choice of $H_{CD}(t)$ is [120],

$$H_{CD}(t) = -\frac{\dot{\Omega}_t}{4\Omega_t}(xp + px), \tag{7.18}$$

and then the total Hamiltonian reads,

$$\begin{aligned} H(t) &= H_0(t) + H_{CD}(t) \\ &= \frac{p^2}{2m} + \frac{1}{2}m\Omega_t^2 q^2 - \frac{\dot{\Omega}_t}{4\Omega_t}(xp + px). \end{aligned} \tag{7.19}$$

It can then be shown that the adiabaticity parameter $\Gamma$ becomes [121],

$$\Gamma = \left(1 - \frac{\dot{\Omega}_t^2}{4\Omega_t^4}\right)^{-\frac{1}{2}} \tag{7.20}$$

Considering a frequency protocol given by [122],

$$\Omega_t = \Omega_i + 10(\Omega_f - \Omega_i)\left(\frac{t}{\tau}\right)^3 - 15(\Omega_f - \Omega_i)\left(\frac{t}{\tau}\right)^4 + 6(\Omega_f - \Omega_i)\left(\frac{t}{\tau}\right)^5, \tag{7.21}$$

where $\Omega_i = \Omega_1$, $\Omega_f = \Omega_2$ for the isentropic expansion and vice-versa for the isentropic compression. This in turn defines the index of $\Gamma$. In Fig. 7.2 the adiabaticity parameter for both strokes is plotted as a function of the ratio between time ($t$) and the stroke's time duration ($\tau$).

Having obtained the adiabaticity parameter, the next step is to calculate the extracted power and the efficiency. First, the extracted power is found by noting that the work is the same as in the adiabatic case, that is, $\Gamma_a = \Gamma_c = 1$ for $t = \tau$. Therefore,

$$\mathcal{P} = \frac{\frac{1}{2}(\Omega_1 - \Omega_2)\left[\coth\left(\frac{\Omega_1}{2T_H}\right) - \coth\left(\frac{\Omega_2}{2T_C}\right)\right]}{2\tau}. \tag{7.22}$$

The efficiency, on the other hand, must take into account the energy cost of implementing the counterdiabatic Hamiltonian. This energy cost can be shown to be equal to [34],

$$E_{CD} = \frac{1}{\tau}\int_0^\tau \mathrm{d}t\left[\frac{\Omega_t^a}{\Omega_1}(\Gamma_a - 1)E_1\right] + \frac{1}{\tau}\int_0^\tau \mathrm{d}t\left[\frac{\Omega_t^c}{\Omega_2}(\Gamma_c - 1)E_2\right], \tag{7.23}$$

where the upper indices on $\Omega_t$ are simply to indicate what are the initial and final frequencies of Eq. (7.21). Then, the efficiency is expressed by,

$$\eta_{CD} = \frac{\mathcal{W}_a + \mathcal{W}_c}{Q_H + E_{CD}}, \tag{7.24}$$

in which the same reasoning applied to the power holds for $Q_H$.

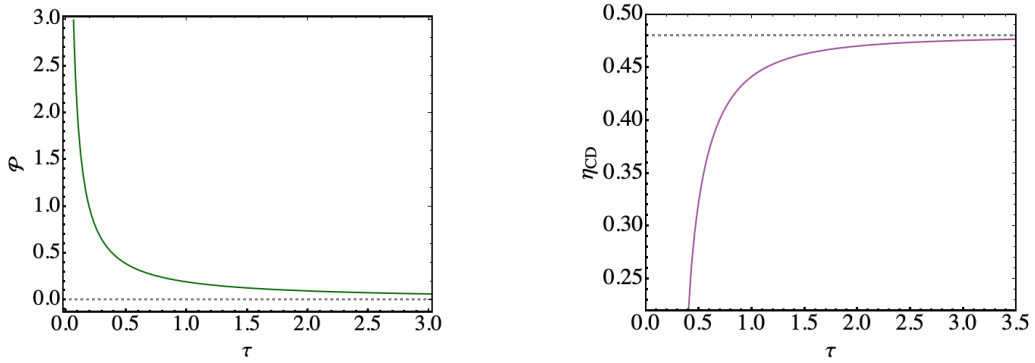


(a) Extracted power.

(b) Efficiency.

Figure 7.3: Plots of the (a) extracted power $\mathcal{P}$ and the (b) efficiency $\eta_{CD}$, as functions of the driving time $\tau$. The dashed line of (b) corresponds to the quasi-static Otto efficiency, $\eta_O = 1 - \Omega_2/\Omega_1 = 0.48$. The values of the parameters are: $\Omega_1 = 2.5$, $\Omega_2 = 1.3$, $T_H = 2.0$, $T_C = 0.5$.

The extracted power Eq. (7.22) and the efficiency Eq. (7.24) are plotted with respect to the driving time $\tau$ of each isentropic stroke in Fig. 7.3. The extracted power (Fig. 7.3a)

clearly converges to zero for very long $\tau$, which is the main problem of quasi-static engines. Moreover, the efficiency (Fig. 7.3b) tends asymptotically to the quasi-static Otto efficiency $\eta_O = 1 - \Omega_2/\Omega_1$ for increasing $\tau$, as it should be expected. Finally, these plots show that the trade-off between extracted power and efficiency still exists, but now it is not as dramatic as before. One can choose an operation point with nonzero extracted power and efficiency not too distant from the quasi-static value. Nevertheless, the divergent power for vanishing $\tau$ is yet an issue to be tackled. The assumption that, for brief isochoric strokes, full thermalization is attained, may not be very realistic, since it depends a lot on the system being studied.

## 7.2 Lindblad-Floquet approach to quantum heat engines

Another way to treat finite-time QHEs is by applying the Lindblad-Floquet framework. This technique, developed in Ref. [35], combines the Lindblad dynamics generated by a Liouvillian encompassing *all* strokes, and Floquet's theory, which is suited for periodically driven systems, in order to obtain the state of the working fluid in the limit-cycle.

### 7.2.1 Lindblad-Floquet theory

We start with a working fluid, whose Hilbert space has dimension $N$, undergoing a random thermodynamic cycle, not specifying if it is Otto, Carnot, etc. This QHE is periodic, with period $\tau$. Differently from what is commonly done for stroke-based QHEs, we'll define a Liouvillian $\mathcal{L}_t$ that drives the whole cycle, that is, it encapsulates all the strokes, independently of their nature. The periodicity manifests itself in the Liouvillian, which must satisfy $\mathcal{L}_{t+\tau} = \mathcal{L}_t$. The state of the working fluid $\rho_t$ then evolves according to,

$$\frac{\mathrm{d}\rho_t}{\mathrm{d}t} = \mathcal{L}_t \rho_t. \tag{7.25}$$

It is convenient to rewrite this expression in *vectorized* form, which is equivalent to the Choi-Jamiołkowski isomorphism [123, 124]. Following the vectorization procedure (see Appendix C), the state of the system is written as a vector of size $N^2$ and any other superoperator, such as $\mathcal{L}_t$, becomes an $N^2 \times N^2$ matrix. Eq. (7.25) is then rewritten as,

$$\frac{\mathrm{d}}{\mathrm{d}t}\mathrm{vec}(\rho_t) = \hat{\mathcal{L}}_t\, \mathrm{vec}(\rho_t), \tag{7.26}$$

where $\mathrm{vec}(\rho_t)$ and $\hat{\mathcal{L}}_t$ are the vectorized forms of $\rho_t$ and $\mathcal{L}_t$, respectively.

With this on hands, now we apply Floquet's theory. The first step is to change our frame from Schrödinger's to a generic rotating frame, defined by

$$\mathrm{vec}(\rho'_t) = \hat{\mathcal{S}}_t\, \mathrm{vec}(\rho_t),$$

with $\hat{\mathcal{S}}_t$ being a superoperator whose time period is the same as the cycle $\hat{\mathcal{S}}_{t+\tau} = \hat{\mathcal{S}}_t$. Inserting the previous equation in (7.26), we find that the state $\mathrm{vec}(\rho'_t)$ in the rotating frame will satisfy another master equation,

$$\frac{\mathrm{d}}{\mathrm{d}t}\mathrm{vec}(\rho'_t) = \hat{\mathcal{L}}'_t\, \mathrm{vec}(\rho'_t), \tag{7.27}$$

in which a new Liouvillian is introduced:

$$\hat{\mathcal{L}}'_t = \hat{\mathcal{S}}_t\,\hat{\mathcal{L}}_t\,\hat{\mathcal{S}}_t^{-1} + \frac{\mathrm{d}\hat{\mathcal{S}}_t}{\mathrm{d}t}\,\hat{\mathcal{S}}_t^{-1}. \tag{7.28}$$

Then, we want the Liouvillian $\hat{\mathcal{L}}'_t$ to be time-independent $\hat{\mathcal{L}}'_t \to \hat{\mathcal{L}}'$, so that the solution simplifies dramatically. Doing so is possible by just choosing the right $\hat{\mathcal{S}}_t$. Thus, the solution of Eq. (7.27) is,

$$\mathrm{vec}(\rho'_t) = e^{\hat{\mathcal{L}}'(t-t_0)}\,\mathrm{vec}(\rho'_{t_0}). \tag{7.29}$$

So far, so good, but this is not the actual state of the working fluid. To find it, we must come back to Schrödinger's picture by using the superoperator $\hat{\mathcal{S}}_t$,

$$\begin{aligned}\mathrm{vec}(\rho_t) &= \hat{\mathcal{S}}_t^{\,-1}\,\mathrm{vec}(\rho'_t)\\ &= \hat{\mathcal{S}}_t^{\,-1}\,e^{\hat{\mathcal{L}}'(t-t_0)}\,\mathrm{vec}(\rho'_{t_0})\\ &= \hat{\mathcal{K}}_{t,t_0}\,e^{(t-t_0)\hat{\mathcal{L}}_F(t_0)}\,\mathrm{vec}(\rho_{t_0}),\end{aligned} \tag{7.30}$$

where we defined the micromotion superoperator $\hat{\mathcal{K}}_{t,t_0}$ and the Floquet Liouvillian $\hat{\mathcal{L}}_F(t_0)$ as [35]:

$$\hat{\mathcal{K}}_{t,t_0} := \hat{\mathcal{S}}_t^{-1}\,\hat{\mathcal{S}}_{t_0}, \tag{7.31}$$

$$\hat{\mathcal{L}}_F(t_0) := \hat{\mathcal{S}}_{t_0}^{-1}\,\hat{\mathcal{L}}'\,\hat{\mathcal{S}}_{t_0}, \tag{7.32}$$

Note that the Floquet Liouvillian is also periodic with period $\tau$. The micromotion superoperator satisfies $\hat{\mathcal{K}}_{t_0,t_0} = \hat{\mathcal{K}}_{t_0+n\tau,t_0} = 1$ and, as a result, if we choose to track the state of the working fluid after $n \in \mathbb{N}$ cycles, we get the *stroboscopic* evolution as

$$\mathrm{vec}(\rho_{t_0+n\tau}) = e^{n\tau\hat{\mathcal{L}}_F(t_0)}\,\mathrm{vec}(\rho_{t_0}). \tag{7.33}$$

This result tells us an interesting feature of the Floquet Liouvillian. If it has no eigenvalues containing a positive real component, then the limit-cycle is guaranteed to exist, since Eq. (7.33) will always converge. Furthermore, as the Floquet Liouvillian is connected to the time-independent Liouvillian of the generic rotating frame through a similarity transformation [c.f. Eq. (7.32)], they have the same eigenvalues, which are time-independent.

After that a certain amount of time has passed, such that all terms containing eigenvalues with negative real parts vanish, the QHE will attain the limit-cycle. Assuming that a unique nonequilibrium steady-state (NESS) exists, it corresponds to the zero eigenstate of the Floquet Liouvillian, that is,

$$\hat{\mathcal{L}}_F(t_0)\,\mathrm{vec}(\rho_F(t_0)) = 0 \Rightarrow e^{n\tau\hat{\mathcal{L}}_F(t_0)}\,\mathrm{vec}(\rho_F(t_0)) = \mathrm{vec}(\rho_F(t_0)), \quad \forall n, \tau, t_0.$$

Combining Eq. (7.30) with the zero eigenstate of the Floquet Liouvillian, we find that

$$\mathrm{vec}(\rho_t) = \hat{\mathcal{K}}_{t,t_0}\,\mathrm{vec}(\rho_F(t_0)), \tag{7.34}$$

which together with the periodic property of the micromotion superoperator aforementioned, gives:

$$\mathrm{vec}(\rho_t) \equiv \mathrm{vec}(\rho_F(t)), \tag{7.35}$$

meaning that it is indeed the state of the working fluid in the limit-cycle and $t$ is a parameter, rather than a time-dependency [35].

This is shortly what the Lindblad-Floquet technique consists of. In deriving the previous results, we considered the Liouvillian as given and hence swept under the rug the problematic in obtaining it. As shown in Ref. [125], deriving the Floquet Liouvillian is not always guaranteed to preserve complete positivity. For this reason, one must proceed with caution when dealing with the Lindblad-Floquet framework.

### 7.2.2 Example: simplified quantum harmonic oscillator

Now we proceed to apply the Lindblad-Floquet framework to a working fluid composed of a quantum harmonic oscillator whose Hamiltonian is time-dependent,

$$H_t = \omega_t \left( a^\dagger a + \frac{1}{2} \right), \tag{7.36}$$

with $a, a^\dagger$ being the annihilation and creation operators, respectively. For the sake of simplicity, we didn't take into account squeezing-like terms, such as $a^\dagger a^\dagger$ and $aa$.

Considering that the working fluid is in contact with resonant[3] and Gaussian preserving bosonic baths, the dissipators that appear in the Liouvillian will be,

$$\mathcal{D}_1(\rho_t) = \gamma_t (n_t + 1) \left( a \rho_t a^\dagger - \frac{1}{2} \{ a^\dagger a, \rho_t \} \right), \tag{7.37}$$

$$\mathcal{D}_2(\rho_t) = \gamma_t n_t \left( a^\dagger \rho_t a - \frac{1}{2} \{ a a^\dagger, \rho_t \} \right), \tag{7.38}$$

where $n_t = 1/(e^{\beta_t \omega_t} - 1)$ is the Bose-Einstein occupation number of the bath at inverse temperature $\beta_t$, and $\gamma_t$ is the relaxation rate between bath and working fluid. Adding up the unitary term $\mathcal{U}_t(\rho_t) = -i[H_t, \rho_t]$, the Liouvillian at a time $t$ is found to be equal to

$$\mathcal{L}_t = \mathcal{U}_t + \mathcal{D}_t, \tag{7.39}$$

with $\mathcal{D}_t$ being defined as the sum of the two dissipators presented in Eqs. (7.37) and (7.38). It is worth mentioning that this particular case does not have the risk of suffering from the complete positivity issue, since $\{[\mathcal{U}_t, \mathcal{D}_{1,2}] = 0 \,|\, \forall t \in \Re\}$ [35]. Furthermore, the Liouvillian has a time period $\tau$.

Next, we apply the aforementioned vectorization technique, leading to $\mathcal{L}_t \to \hat{\mathcal{L}}_t$, $\mathcal{U}_t \to \hat{\mathcal{U}}_t$ and $\mathcal{D}_t \to \hat{\mathcal{D}}_t$. By means of switching to a generic rotating frame, according to (7.28), and redefining the terms, likewise done in Eqs. (7.31) and (7.32), then one gets the Floquet Liouvillian. The technical parts of these (long) calculations are detailed in the Appendices of Ref. [35]. The final result looks like

$$\hat{\mathcal{L}}_F(t) = \frac{\bar{\omega}}{\omega_t} \hat{\mathcal{U}}_t + \bar{\gamma}(n_F(t) + 1) \hat{\mathcal{D}}_1 + \bar{\gamma} n_F(t) \hat{\mathcal{D}}_2, \tag{7.40}$$

[3] Only the modes of the baths that satisfy $\omega_k = \omega_t$ are deemed relevant.

where $\hat{\mathcal{D}}_1, \hat{\mathcal{D}}_2$ are the vectorized forms of the previous dissipators and

$$\bar{\omega} := \frac{1}{\tau}\int_0^\tau \mathrm{d}t\, \omega_t, \tag{7.41}$$

$$\bar{\gamma} := \frac{1}{\tau}\int_0^\tau \mathrm{d}t\, \gamma_t, \tag{7.42}$$

$$\dot{n}_F + \gamma_t n_F = \gamma_t n_t. \tag{7.43}$$

On top of that, by finding the zero eigenstate of the Floquet Liouvillian and using it to carry out the calculations of the time evolution of the average number of quanta ($\langle a^\dagger a\rangle_t = \mathrm{tr}\{a^\dagger a \rho_F(t)\}$), the working fluid's energy is expressed by,

$$\begin{aligned} E_t &= \omega_t\left(\langle a^\dagger a\rangle_t + \frac{1}{2}\right) \\ &= \omega_t\left(n_F(t) + \frac{1}{2}\right), \end{aligned} \tag{7.44}$$

which is a simplified result, requiring only the solution of Eq. (7.43). In more general scenarios, considering squeezing for instance, the calculations are much more intricate. Finally, after defining a protocol for $\omega_t$, $\gamma_t$ and $\beta_t$, a thermodynamic cycle operating in finite-time is achieved, and all the relevant thermodynamic quantities can be obtained.

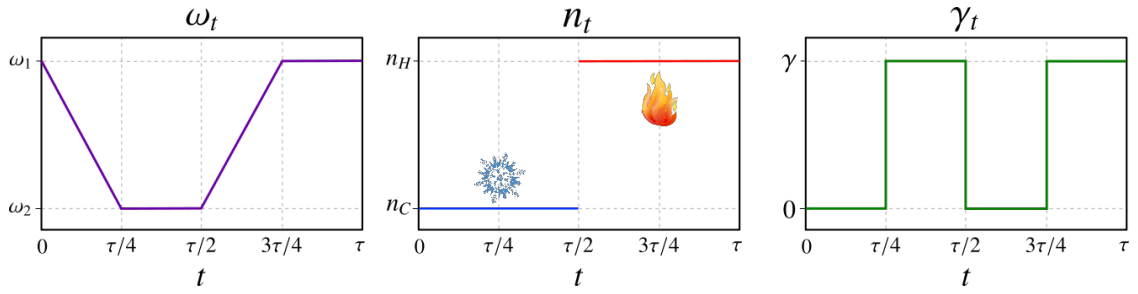


Figure 7.4: Depiction of the protocol implementing the Otto cycle. The protocol is characterized by (left) the working fluid's frequency $\omega_t$, (middle) the bath's occupation number $n_t$ and (right) the relaxation rate $\gamma_t$, all as functions of the time $t$. The four strokes last for a time $\tau/4$ each one.

As an example, the Otto cycle may be implemented by the protocol shown in Fig. 7.4. Since we are in the Floquet picture, the QHE is considered to be already in the limit-cycle. Starting at a random time $t = 0$, the working fluid undergoes an isentropic expansion from $\omega_1$ to $\omega_2$ in a linear fashion for a time $\tau/4$. During this time, the working fluid is disconnected from any of the baths, showed by the fact that $\gamma_t = 0$, which in its turn makes the value of $n_t$ irrelevant during this stroke. Then, from $\tau/4$ until $\tau/2$ the working fluid enters in contact with the cold bath, characterized by $n_C = \frac{1}{2}\coth(\beta_C\omega_2/2)$. The relaxation rate is constant and equal to $\gamma$. The other half of the cycle is the dual of the previous two strokes, that is, the working fluid instead of being expanded, is compressed from $\omega_2$ to $\omega_1$ and finally it enters in contact with the hot bath, identified by $n_H = \frac{1}{2}\coth(\beta_H\omega_1/2)$.

To obtain the energy of the working fluid at any time $t$, the quantity $n_F(t)$ is then calculated, according to Eq. (7.44). It is done by solving Eq. (7.43), which, in this case,

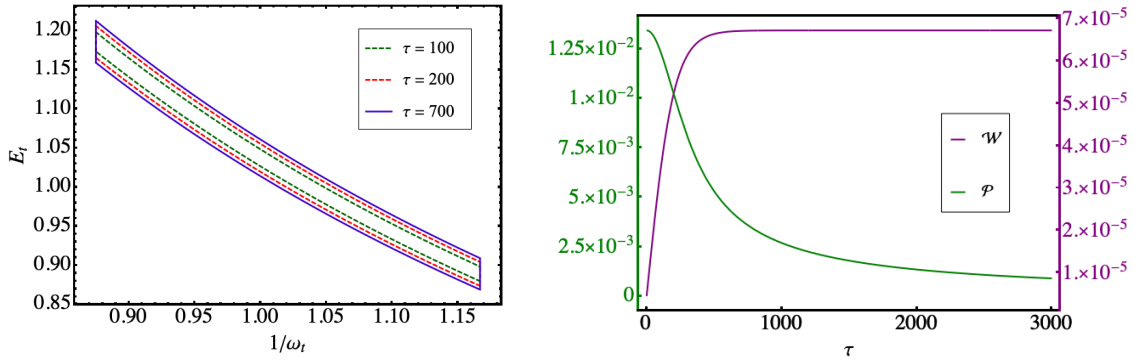


(a) Frequency$^{-1}$ vs. energy diagram.

(b) Cycle period vs. work/power.

Figure 7.5: Characterization of the finite-time QHE undergoing an Otto cycle, within the Lindblad-Floquet theory. (a) Shows the diagram frequency$^{-1}$ vs. energy ($\omega_t^{-1}$ vs. $E_t$) for different cycle durations ($\tau = 100, 200, 700$) and (b) is the plot of the extracted work ($\mathcal{W}$) and the power ($\mathcal{P} = \mathcal{W}/\tau$). The other physical parameters are equal to: $\omega_1 = 1.143$, $\omega_2 = 0.857$, $\gamma = 0.04$, $\beta_C^{-1} = 0.4$, $\beta_H^{-1} = 0.8$.

can be done separately for each stroke and the solutions are sewed together by adjusting the integration constants. The result is

$$n_F(t) = \begin{cases} \dfrac{e^{\gamma\tau/4}\coth(\beta_H\omega_1) + \coth(\beta_C\omega_2)}{2 + 2e^{\gamma\tau/4}}, & \text{for } 0 \leqslant t < \tau/4 \\ \dfrac{e^{-\gamma t}[\coth(\beta_H\omega_1) - \coth(\beta_C\omega_2)]}{2 + 2e^{-\gamma\tau/4}} + \dfrac{\coth(\beta_C\omega_2)}{2}, & \text{for } \tau/4 \leqslant t < \tau/2 \\ \dfrac{\coth(\beta_H\omega_1) + e^{\gamma\tau/4}\coth(\beta_C\omega_2)}{2 + 2e^{\gamma\tau/4}}, & \text{for } \tau/2 \leqslant t < 3\tau/4 \\ \dfrac{e^{-\gamma t}[\coth(\beta_C\omega_2) - \coth(\beta_H\omega_1)]}{2 + 2e^{-\gamma\tau/4}} + \dfrac{\coth(\beta_H\omega_1)}{2}, & \text{for } 3\tau/4 \leqslant t < \tau \end{cases} \tag{7.45}$$

which, together with the frequency modulation, gives us the energy $E_t$.

In Fig. 7.5a, a frequency$^{-1}$ vs. energy diagram, parameterized by $t$, is plotted. It shows a remarkable similarity with the P-V diagram of the Otto cycle seen in Fig. 2.2, reinforcing that the inverse frequency may be seen as a "volume". Coming back to the quantum case, three different cycle periods are presented. The cycle with the shortest period ($\tau = 100$) is identified with the innermost curve (green dashed line); the next curve surrounding it (red dashed line) corresponds to a larger cycle period ($\tau = 200$); and finally, the outermost curve (purple line) represents the cycle with the longest time period ($\tau = 700$).

Looking at the curves of Fig. 7.5a, we immediately see that the area inside the curves increases, reaching a maximum area that remains the same if we continue to increase the cycle period. What explains this saturation behavior can be learned from Fig. 7.5b. This figure shows the extracted work and power as functions of the cycle period $\tau$. Starting with the extracted work, we note that it increases for longer cycle periods until a moment in which it reaches a plateau around $\tau \sim 700$. This is directly linked to the saturation which was previously seen. Hence, we are drawn to the conclusion that the area inside the curves of a $\omega_t^{-1}$ vs. $E_t$ diagram is proportional to the work extracted from the QHE[4]. On

[4]This could be expected from the classical expression of work, $\mathcal{W} = -\int P\mathrm{d}V$.

the other hand, the power monotonically decreases for increasing $\tau$, vanishing eventually for $\tau \to \infty$. This is in accordance with the fact that, for infinitely slow cycles, the evolution is quasi-static and then, from what we already know, the power must be equal to zero.

Nevertheless, it may be argued that it is strange to have the maximum power for $\tau \to 0$, since the extracted work goes to zero for vanishing $\tau$, and obviously it would make the power also have the same fate. A mathematical explanation of the finite value of the power, lies on how the ratio between work and period behaves when $\tau \to 0$,

$$\begin{aligned} \mathcal{P} &= \frac{\mathcal{W}}{\tau} \propto \frac{\tanh(\gamma\tau/8)}{\tau}, \\ \lim_{\tau\to 0} \frac{\mathcal{W}}{\tau} &\propto \frac{\gamma\cancel{\tau}}{8\cancel{\tau}} = \text{constant}. \end{aligned} \tag{7.46}$$

Thus, both numerator and denominator approach the origin at the same speed. But, it isn't satisfactory yet, because the *physical* explanation is missing. In a realistic scenario, there should be a power peak for nonzero $\tau$. A hypothesis of why we failed to observe it in Fig.7.5b, is that our model is too simplified, discarding completely degrees of freedom that may affect considerably the dynamics of the working fluid. By making account of these, a more reasonable result is obtained in Ref. [35].

Lastly, the efficiency of the finite-time QHE can also be calculated. Surprisingly, one finds that

$$\begin{aligned} \eta &= \frac{\mathcal{W}}{Q_H} \\ &\equiv 1 - \frac{\omega_2}{\omega_1} = \eta_O, \end{aligned} \tag{7.47}$$

that is, for the applied protocol and for whatever physical parameters, the efficiency is *always* equal to Otto's efficiency. This result is in agreement with the general ideas put forth in Chapter 6, even though the scenario here is in continuous time.

# Chapter 8

# Conclusion

Within the context of quantum thermodynamics, this dissertation introduced an original way of modelling finite-time quantum heat engines. It consists of alternating between two different strokes. The first, called *heat stroke*, acts locally on the boundaries of the working fluid. The baths, modelled within the collisional model approach [19–27], interact with the working fluid in such a way that every energy change is associated with heat. In this process the internal subsystems of the working fluid don't interact. On the other hand, the second is known as *work stroke*. The baths are disconnected from the boundaries of the working fluid, while its internal interactions are turned on. The system evolves unitarily, thus, any energy variation during this stroke is identified with work. The cyclic operation of these strokes leads to a stroboscopic (discrete-time) evolution of the working fluid's state. This discretized behaviour enables the analysis of the transient regime, which the engine goes through before reaching the limit-cycle, and also the optimization of the output work, by manipulating the parameter space of the system. Furthermore, for a broad class of interactions, it was shown that the engine has a universal Otto efficiency. This *stroboscopic two-stroke quantum heat engine* [29] is a generalization of the SWAP engine [36–40], for it encompasses partial thermalization, partial SWAP unitaries and working fluids with arbitrary number of subsystems, each with a Hilbert space of arbitrary dimension.

As a benchmark, the framework was used to model two specific cases. The first was the generalization of the two-qubit SWAP engine, and the second was a spin chain of $N$ sites, which was considered to be either a XX chain or a XXZ chain. While the spin chains were treated numerically, the two-qubit engine was solved analytically. In both cases results were consistent and appointed to combinations of the parameter space that enhanced the output power. Moreover, the system was found to admit different operation modes beyond the engine one. These operation modes were: refrigerator and oven/heat accelerator. Therefore, the stroboscopic two-stroke quantum heat engine (QHE), for its relative simplicity and discretized structure, poses itself as a powerful tool to grasp the finite-time dynamics of QHEs and optimize the power extracted from the engines. These, in turn, are of great importance for a better understanding of thermodynamic phenomena in the quantum realm and for the design of energy-efficient future technologies (e.g. quantum computers, ultra-small engines).

To set the ground to present the stroboscopic QHE, the dissertation reviewed important topics related to finite-time quantum thermodynamics. It started by briefly discussing

what are cycles in a classical thermodynamics context (Chapter 2). Three cycles were presented: the Carnot cycle, the Otto cycle and the endoreversible cycle. The first two were described within the equilibrium thermodynamics framework, while the last one was related to the Curzon-Ahlborn efficiency [3], which considers finite-time thermodynamics. In Chapter 3 the main concepts of quantum thermodynamics were discussed. Open quantum systems theory was introduced as the forefather of quantum thermodynamics, and how to define heat, work and entropy production, within this context, was examined. As a complement, the strong link between information theory and thermodynamics, through the concept of entropy, was indicated. This relation was made explicit by Landauer's principle [16] and the Szilard engine [18], both were studied and interpreted.

After that, the two main categories of QHEs were discussed in Chapter 4. The first kind, continuous-time QHEs [13, 88, 92], was described as operating in non-equilibrium steady-states (NESS), where one identifies heat and work currents. Some of these engines are said to be autonomous [95–97], that is, self-contained engines that have population inversion between energy levels. The other type of QHEs, called stroke-based QHEs [32, 35, 38, 92], was shown to be made of sequential thermodynamic processes, in clear analogy with classical thermodynamics cycles. The strokes were modelled as quantum dynamical maps, which were explained in Chapter 3. These maps allow one to allocate time intervals for each stroke, which in turn enables the possibility of studying finite-time effects in QHEs.

Following the analysis of the different kinds of QHEs in Chapter 4, the reader was presented with the two main chapters of the dissertation. In Chapter 5, the concept of collisional models [19–27] was introduced. Then, its thermodynamic variables were defined in the general case, as well as when the ancillas are in thermal states. The intimate relation between collisional models and quantum master equations was shown by coarse-graining the time scale. Moreover, in Chapter 6 the stroboscopic two-stroke QHE [29] was presented and discussed, as already mentioned in the first two paragraphs. These results are the core of the dissertation, for their originality and their consistency with the current scientific literature on QHEs. Also, the content of Chapter 6 is part of the preprint recently submitted to arXiv.org [29], and that was also accepted for publication in *Physical Review A*.

Furthermore, in Chapter 7 two other approaches to finite-time QHEs were studied. The first was the technique known as shortcut-to-adiabaticity [34, 115, 116]. It consisted of adding a counterdiabatic [34] term to the Hamiltonian of the working fluid of a QHE, whose task was to inhibit transitions between energy levels during isentropic strokes for whatever time duration. This, in turn, lead a system driven in finite-time to the same final state as if it was quasi-statically driven. Taking into account the energetic cost of implementing the shortcut-to-adiabaticity, the analysis of the trade-off between output power and efficiency was done for a quantum Otto engine. The other approach was the implementation of the Lindblad-Floquet theory to QHEs [35]. It was achieved by combining the Liouvillian containing the Lindblad dynamics of the whole finite-time cycle, with Floquet's theory, which applies to periodically driven systems. The result was a new generator of the dynamics, called the Floquet Liouvillian. Its zero eigenstate was the non-equilibrium steady-state that corresponded to the limit-cycle. One then could calculate the energy of the working fluid at any part of the limit-cycle, and as a consequence the output power could be obtained. This framework was applied to a simplified quantum

harmonic oscillator (i.e. cannot be squeezed). Remarkably, the efficiency of this QHE in the Lindblad-Floquet picture was found to be always equal to the Otto efficiency, for any time duration of the cycle.

Finally, future work can be done using the QHE model herein presented. First, different kinds of internal interactions can be tested, such as long range interactions, with the aim of comparing the output power and the efficiency, and then maybe find a class of optimal interactions. Second, resources pertaining to quantum information theory, like coherence and entanglement, can be readily implemented by choosing different bath ancillas other than "pure" thermal states. A starting point for this study could be Ref. [21]. And third, from the standpoint of experimental physics, the stroboscopic two-stroke QHE, or any other implementation based on it, can in principle be tested in experimental setups that are already well established. For instance, trapped ions are a good candidate, because the electronic and motional degrees of freedom are well controlled, and each ion can be directly addressed using photons from a laser, which in turn can mimic a thermal bath.

Overall, the stroboscopic two-stroke QHE model, for its suitability in treating finite-time features of QHEs and its flexibility in choosing the working fluid and/or bath ancillas, is a very promising approach to go deeper in the relation between quantum mechanics and thermodynamics, as well as to provide a good platform for the design of future quantum technologies.

# Appendix A

# Work and heat in isothermal strokes

As the name suggests, isothermal processes are those in which the working fluid stays thermalized with the thermal bath at all times. It means that one drives the stroke very slowly compared to the time it takes for the working fluid to thermalize.

Consider, for instance, a working fluid consisting of a quantum harmonic oscillator (QHO), whose Hamiltonian in bosonic form is

$$H_t = \omega_t \left( a^\dagger a + \frac{1}{2} \right), \tag{A.1}$$

where $\omega_t$ is the time-dependent frequency of the QHO, and $a, a^\dagger$ are the annihilation and creation operators, respectively. The QHO is driven from $\omega_i$ at $t = t_0$ to $\omega_f$ at $t$. If it's always thermalized at temperature $T = \beta^{-1}$, its density operator can be written in Gibbs form:

$$\rho_t = \frac{e^{-\beta H_t}}{Z}, \tag{A.2}$$

where $Z = \mathrm{tr}\{e^{-\beta H_t}\}$ is the partition function. Hence, the energy of the working fluid is equal to

$$\begin{aligned} E_t &= \langle H_t \rangle \\ &= \mathrm{tr}\{H_t \rho_t\} \\ &= \frac{1}{2}\omega_t \coth\left(\frac{\omega_t}{2T}\right). \end{aligned} \tag{A.3}$$

Therefore, the energy difference during the process is equal to

$$\begin{aligned} \Delta E &= E_t - E_{t_0} \\ &= \frac{1}{2}\omega_t \coth\left(\frac{\omega_t}{2T}\right) - \frac{1}{2}\omega_{t_0} \coth\left(\frac{\omega_{t_0}}{2T}\right). \end{aligned} \tag{A.4}$$

The work extracted in the transformation is given by the integral,

$$\begin{aligned} \mathcal{W} &= -\int_{t_0}^{t} \mathrm{d}t' \left\langle \frac{\partial H_{t'}}{\partial t'} \right\rangle \\ &= -\int_{t_0}^{t} \mathrm{d}t' \, \frac{\dot{\omega}_{t'}}{2} \coth\left(\frac{\omega_{t'}}{2T}\right) \\ &= -T \ln\left[ \frac{\sinh(\omega_t/2T)}{\sinh(\omega_{t_0}/2T)} \right], \end{aligned} \tag{A.5}$$

which is written in such a way that work is positive when extracted from the system. The heat exchanged with the thermal bath is obtained by evoking the 1st law of thermodynamics,

$$\begin{aligned} Q &= \Delta E + \mathcal{W} \\ &= \frac{1}{2}\omega_t \coth\left(\frac{\omega_t}{2T}\right) - \frac{1}{2}\omega_{t_0} \coth\left(\frac{\omega_{t_0}}{2T}\right) - T \ln\left[\frac{\sinh(\omega_t/2T)}{\sinh(\omega_{t_0}/2T)}\right], \end{aligned} \tag{A.6}$$

which is positive if the system absorbs heat from the bath.

# Appendix B

# Bosonic vs. mechanical picture

Consider the following bosonic Hamiltonian of a time-dependent quantum harmonic oscillator (QHO),

$$H_t = \omega_t\left(a^\dagger a + \frac{1}{2}\right) + \frac{\lambda_t}{2}aa + \frac{\lambda_t^*}{2}a^\dagger a^\dagger, \tag{B.1}$$

where $\omega_t$ is the time-dependent frequency of the QHO, $\lambda_t$ is a squeezing parameter, and $a, a^\dagger$ are the annihilation and creation operators, respectively. For time-dependent quantum QHOs, the transformation between the bosonic and mechanical pictures must be done with care. If one just uses the common transformation,

$$a = \frac{1}{\sqrt{2}}(q + ip),$$
$$a^\dagger = \frac{1}{\sqrt{2}}(q - ip),$$

the quadrature operators $p, q$ become time-dependent. Thus, it becomes a rather complicated Hamiltonian to be treated, since it does not commute in different times. An alternative route is to consider the transformations

$$a = \frac{1}{\sqrt{2}}\left(\sqrt{\eta}q + \frac{i}{\sqrt{\eta}}p\right), \tag{B.2}$$

$$a^\dagger = \frac{1}{\sqrt{2}}\left(\sqrt{\eta}q - \frac{i}{\sqrt{\eta}}p\right), \tag{B.3}$$

with $\eta$ being a random frequency scale, which determines the units of the quadrature operators [35]. Then, by substituting Eqs. (B.2) and (B.3) in (B.1), one gets

$$H_t = \frac{(\omega_t - \lambda_t)}{2\eta}p^2 + \frac{\eta(\omega_t + \lambda_t)}{2}q^2. \tag{B.4}$$

Hence, we see that it is almost a Hamiltonian of a QHO in which only the frequency is time-dependent. To conclude the calculations, we define

$$\eta := m(\omega_t - \lambda_t), \tag{B.5}$$

where $m$ is the "mass" term of the QHO. Therefore, the Hamiltonian assumes its final form,

$$H_t = \frac{p^2}{2m} + \frac{1}{2}m\Omega_t^2 q^2, \tag{B.6}$$

in which we define $\Omega_t^2 := \omega_t^2 - \lambda_t^2$.

# Appendix C

# Vectorization

The vectorization or Choi-Jamiołkowski isomorphism [123, 124] maps a Hilbert space $\mathcal{H}$ with $\dim\mathcal{H} = N$ to another Hilbert space $\mathcal{H}'$ with $\dim\mathcal{H}' = N^2$. Therefore, an outer product transforms like

$$|i\rangle\langle j| \rightarrow |j\rangle \otimes |i\rangle\,. \tag{C.1}$$

In practical terms, if applied to a matrix the procedure stacks its columns, for instance,

$$\mathrm{vec}\begin{pmatrix} a & b \\ c & d \end{pmatrix} = \begin{pmatrix} a \\ c \\ b \\ d \end{pmatrix}.$$

Furthermore, the analog of the "bra-ket" inner product $\langle\psi|\phi\rangle$ in $\mathcal{H}'$ is given by the *Hilbert-Schmidt inner product*,

$$\mathrm{tr}\{X^\dagger Y\} = \mathrm{vec}(X)^\dagger \mathrm{vec}(Y). \tag{C.2}$$

Another useful relation comes from vectorizing a product of three matrices $XYZ$,

$$\mathrm{vec}(XYZ) = (Z^\intercal \otimes X)\mathrm{vec}(Y). \tag{C.3}$$

This framework may then be applied to density operators and superoperators. First, the density operators transform according to,

$$\begin{aligned} \mathrm{vec}(\rho) &= \mathrm{vec}\Big(\sum_{i,j} \rho_{i,j}\,|i\rangle\langle j|\Big) \\ &= \sum_{i,j} \rho_{i,j}\,|j\rangle \otimes |i\rangle\,, \end{aligned} \tag{C.4}$$

whose normalization is conserved,

$$\begin{aligned} \mathrm{tr}\{\rho\} &= \mathrm{tr}\{I\rho\} \\ &= \mathrm{vec}(I)^\dagger \mathrm{vec}(\rho) \\ &= \Big(\sum_i \langle i| \otimes \langle i|\Big)\Big(\sum_{i',j} \rho_{i',j}\,|j\rangle \otimes |i'\rangle\Big) \\ &= \sum_i \rho_{i,i} \\ &= 1, \end{aligned} \tag{C.5}$$

where $I$ is the identity operator.

Regarding the superoperators, a good example is the Liouvillian [c.f. Eq. (3.11)]. Starting with the unitary term [47],

$$\begin{aligned}\mathrm{vec}(-i[H,\rho]) &= -i[\mathrm{vec}(H\rho I) - \mathrm{vec}(I\rho H)] \\ &= -i[I\otimes H - H^{\intercal}\otimes I]\mathrm{vec}(\rho) \\ &= \hat{\mathcal{U}}\mathrm{vec}(\rho). \end{aligned} \tag{C.6}$$

And then the dissipator [47],

$$\begin{aligned}\mathrm{vec}[\mathcal{D}(\rho)] &= \sum_k \gamma_k \,\mathrm{vec}\Big(M_k\rho M_k^{\dagger} - \frac{1}{2}\{M_k^{\dagger}M_k,\rho\}\Big) \\ &= \sum_k \gamma_k\Big[M_k^{*}\otimes M_k - \frac{1}{2}I\otimes M_k^{\dagger}M_k - \frac{1}{2}(M_k^{\dagger}M_k)^{\intercal}\otimes I\Big]\mathrm{vec}(\rho) \\ &= \hat{\mathcal{D}}\,\mathrm{vec}(\rho). \end{aligned} \tag{C.7}$$

Finally, the vectorized Liouvillian is

$$\hat{\mathcal{L}} = \hat{\mathcal{U}} + \hat{\mathcal{D}}, \tag{C.8}$$

and the master equation becomes

$$\frac{\mathrm{d}}{\mathrm{d}t}\mathrm{vec}(\rho) = \hat{\mathcal{L}}\,\mathrm{vec}(\rho). \tag{C.9}$$

The solution of this vectorized master equation is equal to

$$\mathrm{vec}(\rho_t) = e^{\hat{\mathcal{L}}t}\,\mathrm{vec}(\rho_0), \tag{C.10}$$

thus, one clearly sees that the *steady-state* $\rho^*$ of the Liouvillian corresponds to the zero eigenstate of the vectorized Liouvillian $\hat{\mathcal{L}}\,\mathrm{vec}(\rho^*) = 0$, such that

$$\begin{aligned}\mathrm{vec}(\rho_t) &= e^{\hat{\mathcal{L}}t}\,\mathrm{vec}(\rho^*) \\ &= \mathrm{vec}(\rho^*), \qquad \forall t \in \mathfrak{R}_{>0}. \end{aligned} \tag{C.11}$$

# Bibliography


[1] J. Gimpel, *La révolution industrielle au Moyen Âge*. Éditions du Seuil/Éditions Points (2002), 1975.

[2] S. Carnot, *Réflexions sur la puissance motrice du feu et sur les machines propres à développer cette puissance*. Bachelier (Paris), 1824.

[3] F. L. Curzon and B. Ahlborn, "Efficiency of a Carnot engine at maximum power output," *Am. J. Phys.*, vol. 43, no. 1, pp. 22–24, 1975. DOI: 10.1119/1.10023.

[4] J. I. Cirac and P. Zoller, "Quantum computations with cold trapped ions," *Phys. Rev. Lett.*, vol. 74, pp. 4091–4094, 20 1995. DOI: 10.1103/PhysRevLett.74.4091.

[5] D. Leibfried, R. Blatt, C. Monroe, and D. Wineland, "Quantum dynamics of single trapped ions," *Rev. Mod. Phys.*, vol. 75, pp. 281–324, 1 2003. DOI: 10.1103/RevModPhys.75.281.

[6] R. Blatt and C. F. Roos, "Quantum simulations with trapped ions," *Nature Phys*, vol. 8, pp. 277–284, 2012. DOI: 10.1038/nphys2252.

[7] A. Imamog¯lu, D. D. Awschalom, G. Burkard, D. P. DiVincenzo, D. Loss, M. Sherwin, and A. Small, "Quantum information processing using quantum dot spins and cavity qed," *Phys. Rev. Lett.*, vol. 83, pp. 4204–4207, 20 1999. DOI: 10.1103/PhysRevLett.83.4204.

[8] S.-B. Zheng and G.-C. Guo, "Efficient scheme for two-atom entanglement and quantum information processing in cavity qed," *Phys. Rev. Lett.*, vol. 85, pp. 2392–2395, 11 2000. DOI: 10.1103/PhysRevLett.85.2392.

[9] "Cavity QED with a Bose–Einstein condensate," *Nature*, vol. 450, no. 7167, pp. 268–271, 2007. DOI: 10.1038/nature06120.

[10] L. Bányai and S. W. Koch, *Semiconductor Quantum Dots*. WORLD SCIENTIFIC, 1993. DOI: 10.1142/2019.

[11] A. P. Alivisatos, "Semiconductor clusters, nanocrystals, and quantum dots," *Science*, vol. 271, no. 5251, pp. 933–937, 1996. DOI: 10.1126/science.271.5251.933.

[12] D. Loss and D. P. DiVincenzo, "Quantum computation with quantum dots," *Phys. Rev. A*, vol. 57, pp. 120–126, 1 1998. DOI: 10.1103/PhysRevA.57.120.

[13] H. E. Scovil and E. O. Schulz-Dubois, "Three-level masers as heat engines," *Phys. Rev. Lett.*, vol. 2, pp. 262–263, 6 1959. DOI: 10.1103/PhysRevLett.2.262.

[14] R. Alicki, "The quantum open system as a model of the heat engine," *Journal of Physics A: Mathematical and General*, vol. 12, no. 5, pp. L103–L107, 1979. DOI: 10.1088/0305-4470/12/5/007.

[15] R. Kosloff, "A quantum mechanical open system as a model of a heat engine," *The Journal of Chemical Physics*, vol. 80, no. 4, pp. 1625–1631, 1984. DOI: 10.1063/1.446862.

[16] R. Landauer, "Irreversibility and heat generation in the computing process," *IBM Journal of Research and Development*, vol. 5, no. 3, pp. 183–191, 1961.

[17] C. H. Bennett, "The thermodynamics of computation—a review," *International Journal of Theoretical Physics*, vol. 21, no. 12, pp. 905–940, 1982. DOI: 10.1007/BF02084158.

[18] L. Szilard, "über die Entropieverminderung in einem thermodynamischen System bei Eingriffen intelligenter Wesen," *Zeitschrift für Physik*, vol. 53, no. 11, pp. 840–856, 1929. DOI: 10.1007/BF01341281.

[19] P. Strasberg, G. Schaller, T. Brandes, and M. Esposito, "Quantum and information thermodynamics: A unifying framework based on repeated interactions," *Phys. Rev. X*, vol. 7, p. 021 003, 2 2017. DOI: 10.1103/PhysRevX.7.021003.

[20] G. De Chiara, G. Landi, A. Hewgill, B. Reid, A. Ferraro, A. J. Roncaglia, and M. Antezza, "Reconciliation of quantum local master equations with thermodynamics," *New Journal of Physics*, vol. 20, no. 11, p. 113 024, 2018. DOI: 10.1088/1367-2630/aaecee.

[21] F. L. S. Rodrigues, G. De Chiara, M. Paternostro, and G. T. Landi, "Thermodynamics of Weakly Coherent Collisional Models," *Phys. Rev. Lett.*, vol. 123, no. 14, p. 140 601, 2019. DOI: 10.1103/physrevlett.123.140601.

[22] G. T. Landi, E. Novais, M. J. De Oliveira, and D. Karevski, "Flux rectification in the quantum *XXZ* chain," *Phys. Rev. E*, vol. 90, p. 042 142, 4 2014. DOI: 10.1103/PhysRevE.90.042142.

[23] F. Ciccarello, "Collision models in quantum optics," *Quantum Measurements and Quantum Metrology*, vol. 4, no. 1, pp. 53–63, 2017. DOI: https://doi.org/10.1515/qmetro-2017-0007.

[24] V. Giovannetti and G. M. Palma, "Master equations for correlated quantum channels," *Phys. Rev. Lett.*, vol. 108, p. 040 401, 4 2012. DOI: 10.1103/PhysRevLett.108.040401.

[25] M. Ziman, P. Štelmachovi č, V. Bu žek, M. Hillery, V. Scarani, and N. Gisin, "Diluting quantum information: An analysis of information transfer in system-reservoir interactions," *Phys. Rev. A*, vol. 65, p. 042 105, 4 2002. DOI: 10.1103/PhysRevA.65.042105.

[26] E. Pereira, "Heat, work, and energy currents in the boundary-driven *xxz* spin chain," *Phys. Rev. E*, vol. 97, p. 022 115, 2 2018. DOI: 10.1103/PhysRevE.97.022115.

[27] P. Strasberg, "Repeated Interactions and Quantum Stochastic Thermodynamics at Strong Coupling," *Phys. Rev. Lett.*, vol. 123, no. 18, p. 180 604, 2019. DOI: 10.1103/PhysRevLett.123.180604.

[28] L. Boltzmann, *Wissenschaftliche Abhandlungen*, F. Hasenöhrl, Ed. Leipzig: Barth, 1909, vol. I, II and III, reissued New York: Chelsea, 1969.

[29] O. A. D. Molitor and G. T. Landi, "Stroboscopic two-stroke quantum heat engines," 2020. arXiv: 2008.07512.

[30] V. Gorini, A. Kossakowski, and E. C. G. Sudarshan, "Completely positive dynamical semigroups of n-level systems," *Journal of Mathematical Physics*, vol. 17, no. 5, pp. 821–825, 1976. DOI: 10.1063/1.522979.

[31] G. Lindblad, "Completely positive maps and entropy inequalities," *Communications in Mathematical Physics*, vol. 40, no. 2, pp. 147–151, 1975. DOI: 10.1007/BF01609396.

[32] E. Geva and R. Kosloff, "A quantum-mechanical heat engine operating in finite time. a model consisting of spin-1/2 systems as the working fluid," *The Journal of Chemical Physics*, vol. 96, no. 4, pp. 3054–3067, 1992. DOI: 10.1063/1.461951.

[33] T. Feldmann and R. Kosloff, "Performance of discrete heat engines and heat pumps in finite time," *Phys. Revi. E*, vol. 61, pp. 4774–4790, 5 2000. DOI: 10.1103/PhysRevE.61.4774.

[34] O. Abah and E. Lutz, "Performance of shortcut-to-adiabaticity quantum engines," *Phys. Rev. E*, vol. 98, p. 032 121, 3 2018. DOI: 10.1103/PhysRevE.98.032121.

[35] S. Scopa, G. T. Landi, and D. Karevski, "Lindblad-Floquet description of finite-time quantum heat engines," *Phys. Rev. A*, vol. 97, p. 062 121, 6 2018. DOI: 10.1103/PhysRevA.97.062121.

[36] A. E. Allahverdyan, K. Hovhannisyan, and G. Mahler, "Optimal refrigerator," *Phys. Rev. E*, vol. 81, p. 051 129, 5 2010. DOI: 10.1103/PhysRevE.81.051129.

[37] M. Campisi, "Fluctuation relation for quantum heat engines and refrigerators," *Journal of Physics A: Mathematical and Theoretical*, vol. 47, no. 24, p. 245 001, 2014. DOI: 10.1088/1751-8113/47/24/245001.

[38] R. Uzdin and R. Kosloff, "The multilevel four-stroke swap engine and its environment," *New Journal of Physics*, vol. 16, p. 095 003, 2014. DOI: 10.1088/1367-2630/16/9/095003.

[39] M. Campisi, J. Pekola, and R. Fazio, "Nonequilibrium fluctuations in quantum heat engines: Theory, example, and possible solid state experiments," *New Journal of Physics*, vol. 17, no. 3, p. 035 012, 2015. DOI: 10.1088/1367-2630/17/3/035012.

[40] A. M. Timpanaro, G. Guarnieri, J. Goold, and G. T. Landi, "Thermodynamic Uncertainty Relations from Exchange Fluctuation Theorems," *Phys. Rev. Lett.*, vol. 123, no. 9, p. 090 604, 2019. DOI: 10.1103/PhysRevLett.123.090604.

[41] H. B. Callen, *Thermodynamics and an introduction to thermostatistics; 2nd ed.* New York, NY: Wiley, 1985.

[42] P. Perrot, *A to Z of thermodynamics*. Oxford Univ. Press, 1998, ISBN: 0198565569.

[43] K. H. Hoffmann, J. M. Burzler, and S. Schubert, "Endoreversible thermodynamics," *Journal of Non-Equilibrium Thermodynamics*, vol. 22, no. 4, pp. 311–355, 1997. DOI: https://doi.org/10.1515/jnet.1997.22.4.311.

[44] S. Deffner, "Efficiency of harmonic quantum otto engines at maximal power," *Entropy*, vol. 20, no. 11, p. 875, 2018. DOI: 10.3390/e20110875.

[45] M. Planck, "Ueber das gesetz der energieverteilung im normalspectrum," *Annalen der Physik*, vol. 309, no. 3, pp. 553–563, 1901. DOI: 10.1002/andp.19013090310.

[46] H. P. Breuer and F. Petruccione, *The theory of open quantum systems*. Oxford Univ. Press, 2002.

[47] G. T. Landi, *Lecture notes on quantum information & quantum noise*, 2018. [Online]. Available: http://www.fmt.if.usp.br/~gtlandi/lecture-notes-2.pdf.

[48] G. Lindblad, "On the generators of quantum dynamical semigroups," *Communications in Mathematical Physics*, vol. 48, no. 2, pp. 119–130, 1976. DOI: 10.1007/BF01608499.

[49] G. T. Landi, *Lecture notes on statistical mechanics*, 2018. [Online]. Available: http://www.fmt.if.usp.br/~gtlandi/courses/statmech2018.

[50] M. Le Bellac, F. Mortessagne, and G. G. Batrouni, *Equilibrium and Non-Equilibrium Statistical Thermodynamics*. Cambridge University Press, 2004. DOI: 10.1017/CBO9780511606571.

[51] S. Deffner and C. Jarzynski, "Information processing and the second law of thermodynamics: An inclusive, hamiltonian approach," *Phys. Rev. X*, vol. 3, p. 041 003, 4 2013. DOI: 10.1103/PhysRevX.3.041003.

[52] M. Esposito, K. Lindenberg, and C. V. den Broeck, "Entropy production as correlation between system and reservoir," *New Journal of Physics*, vol. 12, no. 1, p. 013 013, 2010. DOI: 10.1088/1367-2630/12/1/013013.

[53] R. Clausius, "Ueber verschiedene für die anwendung bequeme formen der hauptgleichungen der mechanischen wärmetheorie," *Annalen der Physik*, vol. 201, no. 7, pp. 353–400, 1865. DOI: 10.1002/andp.18652010702.

[54] C. Jarzynski, "Nonequilibrium equality for free energy differences," *Phys. Rev. Lett.*, vol. 78, pp. 2690–2693, 14 1997. DOI: 10.1103/PhysRevLett.78.2690.

[55] C. Jarzynski and D. K. Wójcik, "Classical and quantum fluctuation theorems for heat exchange," *Phys. Rev. Lett.*, vol. 92, p. 230 602, 23 2004. DOI: 10.1103/PhysRevLett.92.230602.

[56] J. Santos, A. Timpanaro, and G. Landi, "Joint fluctuation theorems for sequential heat exchange," *Entropy*, vol. 22, no. 7, 2020. DOI: 10.3390/e22070763.

[57] M. Horodecki and J. Oppenheim, "Fundamental limitations for quantum and nanoscale thermodynamics," *Nat Commun*, vol. 4, p. 2059, 2013. DOI: 10.1038/ncomms3059.

[58] F. G. Brandão, M. Horodecki, J. Oppenheim, J. M. Renes, and R. W. Spekkens, "Resource theory of quantum states out of thermal equilibrium," *Physical Review Letters*, vol. 111, no. 25, 2013, ISSN: 00319007. DOI: 10.1103/PhysRevLett.111.250404.

[59] H. Spohn, "Entropy production for quantum dynamical semigroups," *Journal of Mathematical Physics*, vol. 19, no. 5, pp. 1227–1230, 1978. DOI: 10.1063/1.523789.

[60] M. A. Nielsen and I. L. Chuang, *Quantum Computation and Quantum Information: 10th Anniversary Edition*, 10th. USA: Cambridge University Press, 2011, ISBN: 1107002176.

[61] J. M. R. Parrondo, J. M. Horowitz, and T. Sagawa, "Thermodynamics of information," *Nature Phys*, vol. 11, pp. 131–139, 2015. DOI: 10.1038/nphys3230.

[62] J. Goold, M. Huber, A. Riera, L. Del Rio, and P. Skrzypczyk, "The role of quantum information in thermodynamics - A topical review," *Journal of Physics A: Mathematical and Theoretical*, vol. 49, no. 14, p. 143 001, 2016. DOI: 10.1088/1751-8113/49/14/143001.

[63] S. W. Kim, T. Sagawa, S. De Liberato, and M. Ueda, "Quantum szilard engine," *Phys. Rev. Lett.*, vol. 106, no. 7, p. 070 401, 2011. DOI: 10.1103/PhysRevLett.106.070401.

[64] C. Elouard, D. Herrera-Martí, B. Huard, and A. Auffèves, "Extracting work from quantum measurement in maxwell's demon engines," *Phys. Rev. Lett.*, vol. 118, p. 260 603, 26 2017. DOI: 10.1103/PhysRevLett.118.260603.

[65] C. Elouard and A. N. Jordan, "Efficient quantum measurement engines," *Phys. Rev. Lett.*, vol. 120, p. 260 601, 26 2018. DOI: 10.1103/PhysRevLett.120.260601.

[66] J. P. S. Peterson, R. S. Sarthour, and R. Laflamme, "Implementation of a quantum engine fuelled by information," 2020. arXiv: 2006.10136.

[67] M. B. Plenio and V. Vitelli, "The physics of forgetting: Landauer's erasure principle and information theory," *Contemporary Physics*, vol. 42, no. 1, pp. 25–60, 2001. DOI: 10.1080/00107510010018916.

[68] A. M. Timpanaro, J. P. Santos, and G. T. Landi, "Landauer's principle at zero temperature," *Phys. Rev. Lett.*, vol. 124, p. 240 601, 24 2020. DOI: 10.1103/PhysRevLett.124.240601.

[69] S. Toyabe, T. Sagawa, M. Ueda, E. Muneyuki, and M. Sano, "Experimental demonstration of information-to-energy conversion and validation of the generalized Jarzynski equality," *Nature Phys*, vol. 6, pp. 988–992, 2010. DOI: 10.1038/nphys1821.

[70] J. P. S. Peterson, R. S. Sarthour, A. M. Souza, I. S. Oliveira, J. Goold, K. Modi, D. O. Soares-Pinto, and L. C. Céleri, "Experimental demonstration of information to energy conversion in a quantum system at the landauer limit," *Proceedings of the Royal Society A: Mathematical, Physical and Engineering Sciences*, vol. 472, no. 2188, p. 20 150 813, 2016. DOI: 10.1098/rspa.2015.0813.

[71] R. Gaudenzi, E. Burzurí, S. Maegawa, H. S. van der Zant, and F. Luis, "Quantum landauer erasure with a molecular nanomagnet," *Nature Phys*, vol. 14, pp. 565–568, 2018. DOI: 10.1038/s41567-018-0070-7.

[72] L. L. Yan, T. P. Xiong, K. Rehan, F. Zhou, D. F. Liang, L. Chen, J. Q. Zhang, W. L. Yang, Z. H. Ma, and M. Feng, "Single-atom demonstration of the quantum landauer principle," *Phys. Rev. Lett.*, vol. 120, p. 210 601, 21 2018. DOI: 10.1103/PhysRevLett.120.210601.

[73] H. S. Leff and A. F. Rex, *Maxwell's Demon: Entropy, Information, Computing*. Princeton University Press, 1990.

[74] P. D. Smith, *Os homens do fim do mundo: O verdadeiro Dr. Fantástico e o sonho da arma total*, 1st Edition. Companhia das Letras, 2008, ISBN: 9788535913064.

[75] K. Maruyama, F. Nori, and V. Vedral, "Colloquium: The physics of Maxwell's demon and information," *Rev. Mod. Phys.*, vol. 81, pp. 1–23, 1 2009, ISSN: 15390756. DOI: 10.1103/RevModPhys.81.1.

[76] T. Sagawa, *Thermodynamics of Information Processing in Small Systems*. Springer Theses, Springer, New York, 2012, vol. 127. DOI: 10.1007/978-4-431-54168-4.

[77] J. Oppenheim, M. Horodecki, P. Horodecki, and R. Horodecki, "Thermodynamical approach to quantifying quantum correlations," *Phys. Rev. Lett.*, vol. 89, p. 180 402, 18 2002. DOI: 10.1103/PhysRevLett.89.180402.

[78] M. Lostaglio, D. Jennings, and T. Rudolph, "Description of quantum coherence in thermodynamic processes requires constraints beyond free energy," *Nat Commun*, vol. 6, p. 6383, 2015. DOI: 10.1038/ncomms7383.

[79] M. Lostaglio, "The resource theory of quantum thermodynamics," PhD thesis, Imperial College London, 2016.

[80] M. O. Scully, M. S. Zubairy, G. S. Agarwal, and H. Walther, "Extracting work from a single heat bath via vanishing quantum coherence," *Science*, vol. 299, no. 5608, pp. 862–864, 2003. DOI: 10.1126/science.1078955.

[81] R. Dillenschneider and E. Lutz, "Energetics of quantum correlations," *EPL (Europhysics Letters)*, vol. 88, no. 5, p. 50 003, 2009. DOI: 10.1209/0295-5075/88/50003.

[82] O. Abah and E. Lutz, "Efficiency of heat engines coupled to nonequilibrium reservoirs," *EPL*, vol. 106, no. 2, 2014, ISSN: 12864854. DOI: 10.1209/0295-5075/106/20001.

[83] G. Manzano, F. Galve, R. Zambrini, and J. M. R. Parrondo, "Entropy production and thermodynamic power of the squeezed thermal reservoir," *Phys. Rev. E*, vol. 93, p. 052 120, 5 2016. DOI: 10.1103/PhysRevE.93.052120.

[84] W. Niedenzu, V. Mukherjee, A. Ghosh, A. G. Kofman, and G. Kurizki, "Quantum engine efficiency bound beyond the second law of thermodynamics," *Nat Commun*, vol. 9, p. 165, 2018. DOI: 10.1038/s41467-017-01991-6.

[85] C. Marletto, "Constructor Theory of Thermodynamics," arXiv: 1608.02625.

[86] *Constructor theory*, http://constructortheory.org/, Accessed: 2020-08-05.

[87] *Quantum flagship*, https://qt.eu/, Accessed: 2020-08-21.

[88] R. Kosloff and A. Levy, "Quantum Heat Engines and Refrigerators: Continuous Devices," *Annual Review of Physical Chemistry*, vol. 65, no. 1, pp. 365–393, 2014. DOI: 10.1146/annurev-physchem-040513-103724.

[89] N. Brunner, N. Linden, S. Popescu, and P. Skrzypczyk, "Virtual qubits, virtual temperatures, and the foundations of thermodynamics," *Phys. Rev. E*, vol. 85, p. 051 117, 5 2012. DOI: 10.1103/PhysRevE.85.051117.

[90] M. P. Müller, "Correlating Thermal Machines and the Second Law at the Nanoscale," *Phys. Rev. X*, vol. 8, p. 041 051, 4 2018. DOI: 10.1103/PhysRevX.8.041051.

[91] F. Clivaz, R. Silva, G. Haack, J. B. Brask, N. Brunner, and M. Huber, "Unifying paradigms of quantum refrigeration: A universal and attainable bound on cooling," *Phys. Rev. Lett.*, vol. 123, p. 170 605, 17 2019. DOI: 10.1103/PhysRevLett.123.170605.

[92] F. Binder, L. A. Correa, C. Gogolin, J. Anders, and G. Adesso, *Thermodynamics in the Quantum Regime: Fundamental Aspects and New Directions*. Springer, 2018, ISBN: 9783319990453.

[93] F. Tonner and G. Mahler, "Autonomous quantum thermodynamic machines," *Phys. Rev. E*, vol. 72, p. 066 118, 6 2005. DOI: 10.1103/PhysRevE.72.066118.

[94] N. Linden, S. Popescu, and P. Skrzypczyk, "How small can thermal machines be? the smallest possible refrigerator," *Phys. Rev. Lett.*, vol. 105, p. 130 401, 13 2010. DOI: 10.1103/PhysRevLett.105.130401.

[95] M. Youssef, G. Mahler, and A.-S. F. Obada, "Quantum optical thermodynamic machines: Lasing as relaxation," *Phys. Rev. E*, vol. 80, p. 061 129, 6 2009. DOI: 10.1103/PhysRevE.80.061129.

[96] ——, "Quantum heat engine: A fully quantized model," *Physica E: Low-dimensional Systems and Nanostructures*, vol. 42, pp. 454–460, 3 2010. DOI: https://doi.org/10.1016/j.physe.2009.06.032.

[97] M. T. Mitchison, "Quantum thermal absorption machines: refrigerators, engines and clocks," *Contemporary Physics*, vol. 60, no. 2, pp. 164–187, 2019. DOI: 10.1080/00107514.2019.1631555.

[98] H. Häffner, C. Roos, and R. Blatt, "Quantum computing with trapped ions," *Physics Reports*, vol. 469, no. 4, pp. 155–203, 2008. DOI: https://doi.org/10.1016/j.physrep.2008.09.003.

[99] A. Levy, L. Diósi, and R. Kosloff, "Quantum flywheel," *Phys. Rev. A*, vol. 93, p. 052 119, 5 2016. DOI: 10.1103/PhysRevA.93.052119.

[100] T. Feldmann and R. Kosloff, "Characteristics of the limit cycle of a reciprocating quantum heat engine," *Phys. Rev. E*, vol. 70, p. 046 110, 4 2004. DOI: 10.1103/PhysRevE.70.046110.

[101] M. Born and V. Fock, "Beweis des Adiabatensatzes," *Zeitschrift für Physik*, vol. 51, no. 3, pp. 165–180, 1928, ISSN: 0044-3328. DOI: 10.1007/BF01343193.

[102] S. Scopa, G. T. Landi, A. Hammoumi, and D. Karevski, "Exact solution of time-dependent Lindblad equations with closed algebras," *Physical Review A*, vol. 99, no. 2, pp. 1–16, 2019, ISSN: 24699934. DOI: 10.1103/PhysRevA.99.022105.

[103] R. Kosloff and T. Feldmann, "Discrete four-stroke quantum heat engine exploring the origin of friction," *Phys. Rev. E*, vol. 65, p. 055 102, 5 2002. DOI: 10.1103/PhysRevE.65.055102.

[104] Y. Rezek and R. Kosloff, "Irreversible performance of a quantum harmonic heat engine," *New Journal of Physics*, vol. 8, no. 5, pp. 83–83, 2006. DOI: 10.1088/1367-2630/8/5/083.

[105] F. Plastina, A. Alecce, T. J. Apollaro, G. Falcone, G. Francica, F. Galve, N. Lo Gullo, and R. Zambrini, "Irreversible work and inner friction in quantum thermodynamic processes," *Phys. Rev. Lett.*, vol. 113, p. 260 601, 26 2014. DOI: 10.1103/PhysRevLett.113.260601.

[106] "Towards quantum thermodynamics in electronic circuits," *Nature Phys*, vol. 11, pp. 118–123, 2015. DOI: 10.1038/nphys3169.

[107] "A single-atom heat engine," *Science*, vol. 352, no. 6283, pp. 325–330, 2016. DOI: 10.1126/science.aad6320.

[108] G. Maslennikov, S. Ding, R. Hablützel, J. Gan, A. Roulet, S. Nimmrichter, J. Dai, V. Scarani, and D. Matsukevich, "Quantum absorption refrigerator with trapped ions," *Nat Commun*, vol. 10, p. 202, 2019. DOI: 10.1038/s41467-018-08090-0.

[109] M. Rossi, L. Mancino, G. T. Landi, M. Paternostro, A. Schliesser, and A. Belenchia, "Experimental assessment of entropy production in a continuously measured mechanical resonator," *Phys. Rev. Lett.*, vol. 125, p. 080 601, 8 2020, ISSN: 1079-7114. DOI: 10.1103/PhysRevLett.125.080601.

[110] P. Talkner, M. Campisi, and P. Hänggi, "Fluctuation theorems in driven open quantum systems," *Journal of Statistical Mechanics: Theory and Experiment*, vol. 2009, no. 02, P02025, 2009. DOI: 10.1088/1742-5468/2009/02/p02025.

[111] G. Manzano, J. M. Horowitz, and J. M. R. Parrondo, "Quantum fluctuation theorems for arbitrary environments: Adiabatic and nonadiabatic entropy production," *Phys. Rev. X*, vol. 8, p. 031 037, 3 2018. DOI: 10.1103/PhysRevX.8.031037.

[112] A. Levy and R. Kosloff, "The local approach to quantum transport may violate the second law of thermodynamics," *EPL (Europhysics Letters)*, vol. 107, no. 2, p. 20 004, 2014. DOI: 10.1209/0295-5075/107/20004.

[113] S. Elaydi, *An Introduction to Difference Equations*, ser. Undergraduate Texts in Mathematics. Springer New York, 2005, ISBN: 9780387230597.

[114] R. Uzdin, A. Levy, and R. Kosloff, "Equivalence of quantum heat machines, and quantum-thermodynamic signatures," *Phys. Rev. X*, vol. 5, p. 031 044, 3 2015. DOI: 10.1103/PhysRevX.5.031044.

[115] M. V. Berry, "Transitionless quantum driving," *J. Phys. A: Math. Theor*, vol. 42, p. 9, 2009. DOI: 10.1088/1751-8113/42/36/365303.

[116] A. Del Campo, J. Goold, and M. Paternostro, "More bang for your buck: Superadiabatic quantum engines," *Sci Rep*, vol. 4, p. 6208, 2014. DOI: 10.1038/srep06208.

[117] B. Lin and J. Chen, "Performance analysis of an irreversible quantum heat engine working with harmonic oscillators," *Phys. Rev. E*, vol. 67, p. 046 105, 4 2003. DOI: 10.1103/PhysRevE.67.046105.

[118] S. Deffner, O. Abah, and E. Lutz, "Quantum work statistics of linear and nonlinear parametric oscillators," *Chemical Physics*, vol. 375, no. 2, pp. 200–208, 2010. DOI: https://doi.org/10.1016/j.chemphys.2010.04.042.

[119] J. Roßnagel, O. Abah, F. Schmidt-Kaler, K. Singer, and E. Lutz, "Nanoscale heat engine beyond the carnot limit," *Phys. Rev. Lett.*, vol. 112, p. 030 602, 3 2014. DOI: 10.1103/PhysRevLett.112.030602.

[120] E. Torrontegui, S. Ibáñez, S. Martínez-Garaot, M. Modugno, A. del Campo, D. Guéry-Odelin, A. Ruschhaupt, X. Chen, and J. G. Muga, "Chapter 2 - shortcuts to adiabaticity," in *Advances in Atomic, Molecular, and Optical Physics*, ser. Advances In Atomic, Molecular, and Optical Physics, E. Arimondo, P. R. Berman, and C. C. Lin, Eds., vol. 62, Academic Press, 2013, pp. 117–169. DOI: 10.1016/B978-0-12-408090-4.00002-5.

[121] H. Mishima and Y. Izumida, "Transition probability generating function of a transitionless quantum parametric oscillator," *Phys. Rev. E*, vol. 96, p. 012 133, 1 2017. DOI: 10.1103/PhysRevE.96.012133.

[122] S. Deffner, C. Jarzynski, and A. del Campo, "Classical and quantum shortcuts to adiabaticity for scale-invariant driving," *Phys. Rev. X*, vol. 4, p. 021 013, 2 2014. DOI: 10.1103/PhysRevX.4.021013.

[123] M.-D. Choi, "Completely positive linear maps on complex matrices," *Linear Algebra and its Applications*, vol. 10, no. 3, pp. 285–290, 1975. DOI: https://doi.org/10.1016/0024-3795(75)90075-0.

[124] A. Jamiołkowski, "Linear transformations which preserve trace and positive semidefiniteness of operators," *Reports on Mathematical Physics*, vol. 3, no. 4, pp. 275–278, 1972. DOI: https://doi.org/10.1016/0034-4877(72)90011-0.

[125] M. Hartmann, D. Poletti, M. Ivanchenko, S. Denisov, and P. Hänggi, "Asymptotic floquet states of open quantum systems: The role of interaction," *New Journal of Physics*, vol. 19, no. 8, p. 083 011, 2017. DOI: 10.1088/1367-2630/aa7ceb.